4. RESULTS

4.1. Test compounds exhibited good anticholinesterase activity

For preliminary screening of a series of isoalloxazine, triazinoindole-3-thiol, indolequinoxaline, iminoquinazoline-4-one and diarylthiazol-benzylpiperidine derivatives, *in vitro* anticholinesterase (anti-ChE) activity was assessed using Ellman's assay. Current Alzheimer's treatment includes AChE inhibitors which show their beneficial effects by increased functioning of the existing cholinergic neurons, improved general cognitive functions and reduced behavioural disturbances. However, butyrylcholinesterase (BuChE) is also a key degrading enzyme for ACh during the late phase of the disease where BuChE level remains constant or increases while AChE concentration decreases in certain brain regions [78-80]. These reports concluded that balanced inhibition of both AChE and BuChE could be beneficial for the treatment of patients with cognitive deficit observed in AD. Thus, it was decided to check the test compounds for AChE and BuChE inhibitory activities. Among the series, **13, 17** and **70** showed the highest effect by inhibiting AChE with IC_{50} values of 4.72±0.56 μM, 5.22±0.36 μM and 5.40±2.96 μM respectively and inhibiting BuChE with IC_{50} values of 6.98±0.45 μM, 5.29±0.64 μM and 7.28±0.27 μM respectively. The results are summarized in Table 1.

A series of diarylthiazol-benzylpiperidine derivatives were also assessed to determine their anti-ChE potential. Majority of the compounds exhibited good AChE as well as BuChE inhibitory activity. Compounds (**116, 117, 122, 123, 126, 131, 132-135, 137-139** and **146-149**) exhibited higher inhibitory activity of AChE (IC_{50} values: < 1 μM) than the rest of the derivatives. Compounds **(116, 134** and **135)** showed better BuChE inhibitory activity [IC_{50} value (μM): 0.72±0.01, 0.82±0.01 and 0.74±0.01 respectively]. The two test compounds (**131** and **135**) which showed the best AChE inhibitory activities [IC_{50} values (μM): 0.30±0.01 and 0.52±0.01 respectively] also showed reasonably good BuChE inhibitory activities [IC_{50} values (μM): 1.84±0.03 and 0.74±0.01 respectively]. The results are summarized in the Table 1.

4.2. Test compounds attenuated $A\beta_{1-42}$ aggregation

There are evidences indicating that localized AChE and Aβ in senile plaques promoted the assembly of Aβ into fibrils, and accelerated the deposition of Aβ peptide. AChE binds to Aβ directly through its peripheral binding site (PAS) to promote aggregatory effect [81, 82]. On the

basis of the *in vitro* ChE inhibition studies, compounds from the series with potent AChE inhibitory activity were selected for the thioflavin T (ThT) assay [49, 50] (Table 1) to evaluate their ability to inhibit AChE-induced $A\beta_{1-42}$ aggregation. The compounds were also evaluated using Congo red (CR) binding assay to determine their ability to inhibit spontaneous $A\beta_{1-42}$-aggregation.

Results showed that, among the series of isoalloxazine, triazinoindole-3-thiol, indolequinoxaline and iminoquinazoline-4-one derivatives, compounds **(13, 17** and **70)** (at 10 µM) exhibited significant anti-$A\beta_{1-42}$ aggregatory effects in thioflavin-T (ThT) assay (34.59±3.57%, 20.00±2.62% and 23.67±2.98% inhibition respectively) and in CR binding assay (37.86±2.06%, 23.62±1.73% and 26.18±2.16% inhibition respectively).

From the series of diarylthiazol-benzylpiperidine derivatives, three compounds (**131**, **139** and **146**) were found to be the most potent inhibitors of AChE-induced $A\beta_{1-42}$ aggregation with ~27 % inhibition at 10 µM concentration in ThT assay. The results are summarized in Table 1.

Table 1: AChE and BuChE inhibitory activities (IC_{50} values) and inhibition of $A\beta_{1-42}$ aggregation by the test compounds.

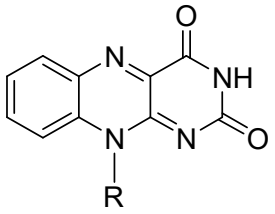

(**1-17**)

Comp.	R	AChE inhibition IC_{50} (µM)	BuChE inhibition IC_{50} (µM)	% $A\beta_{1-42}$ aggregation inhibition (at 10 µM)	
				ThT assay	CR assay
1	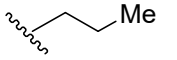	9.32±1.12	40.38±3.42	nd	nd
2	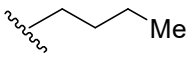	12.2±1.24	43.72±3.25	nd	nd
3	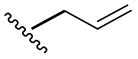	11.22±1.06	27.24±2.65	nd	nd
4	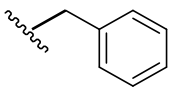	11.53±1.32	31.72±3.36	nd	nd

5	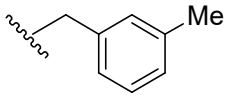	11.63±1.41	42.86±3.54	nd	nd
6	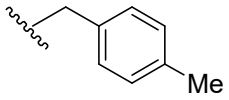	29.39±2.27	7.89±0.57	nd	nd
7	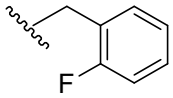	7.28±0.74	21.64±2.51	nd	nd
8	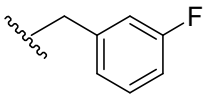	11.46±1.14	8.26±1.01	nd	nd
9	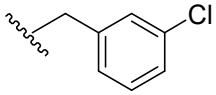	47.26±2.45	10.49±1.20	nd	nd
10	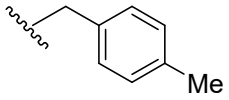	29.95±2.56	7.39±0.84	nd	nd
11	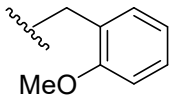	18.82±1.34	8.39±0.58	nd	nd
12	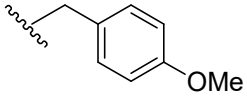	9.34±1.02	47.22±2.59	nd	nd
13	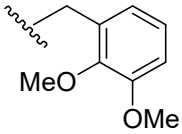	**4.72±0.56**	**6.98±0.45**	**34.59±3.57**	**37.86±2.06**
14	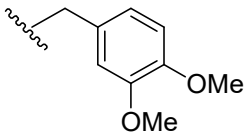	32.55±2.60	8.55±0.94	nd	nd
15	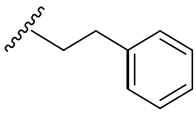	52.75±3.42	23.41±2.41	nd	nd
16	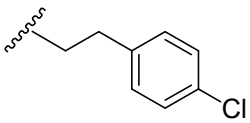	29.5±2.58	7.13±0.74	nd	nd
17	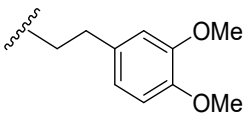	**5.22±0.36**	**5.29±0.64**	**20.00±2.62**	**23.62±1.73**

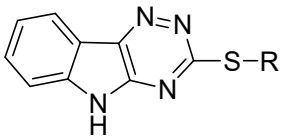

(18-30)

Comp.	R	AChE inhibition IC_{50} (μM)	BuChE inhibition IC_{50} (μM)	% $A\beta_{1-42}$ aggregation inhibition (at 10 μM)	
				ThT assay	CR assay
18	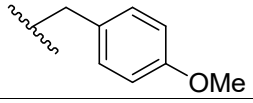	9.64±1.74	46.74±4.67	nd	nd
19	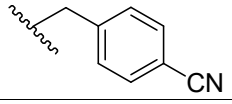	19.02±2.15	75.99±3.888	nd	nd
20	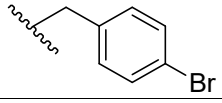	17.49±2.42	51.93±4.71	nd	nd
21	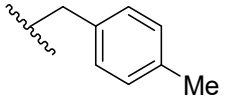	15.52±2.13	49.34±3.69	nd	nd
22	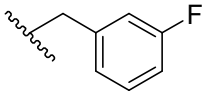	19.16±1.28	5.11±0.71	nd	nd
23	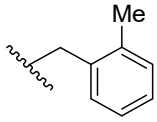	9.88±0.99	6.01±0.77	nd	nd
24	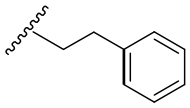	9.93±1.97	6.82±0.83	nd	nd
25	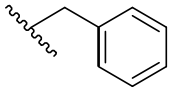	20.33±2.30	42.05±3.62	nd	nd
26	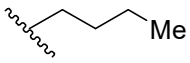	12.28±1.42	40.08±3.60	nd	nd
27	Me	10.03±1.04	33.69±3.53	nd	nd
28	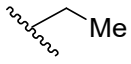	16.01±1.57	48.40±4.68	nd	nd
29	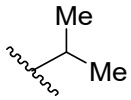	12.62±1.46	55.24±4.74	nd	nd
30	H	11.26±1.26	55.81±4.64	nd	nd

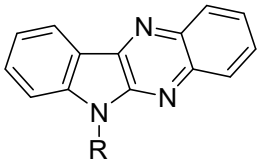

(31-41)

Comp.	R	AChE inhibition IC_{50} (μM)	BuChE inhibition IC_{50} (μM)	% $A\beta_{1-42}$ aggregation inhibition (at 10 μM)	
				ThT assay	CR assay
31		13.37±1.13	15.80±2.19	nd	nd
32		17.47±2.24	22.29±2.35	nd	nd
33	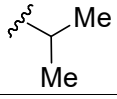	19.14±2.28	18.56±2.27	nd	nd
34	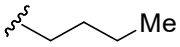	19.98±2.30	21.01±2.32	nd	nd
35	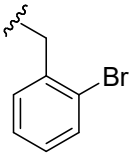	20.28±2.23	35.99±3.55	nd	nd
36	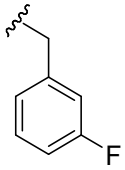	20.92±2.32	16.15±3.20	nd	nd
37	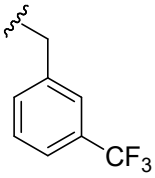	26.63±3.43	93.48±4.97	nd	nd
38	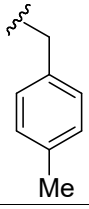	24.19±2.38	33.12±3.52	nd	nd
39	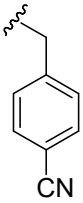	20.59±2.31	24.88±3.39	nd	nd

40	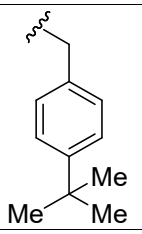	19.08±2.28	11.95±1.07	nd	nd
41	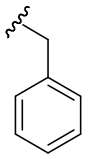	24.09±2.38	13.99±1.47	nd	nd

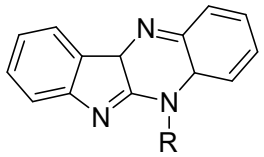

(**42**-**53**)

Comp.	R	AChE inhibition IC_{50} (μM)	BuChE inhibition IC_{50} (μM)	% $A\beta_{1-42}$ aggregation inhibition (at 10 μM)	
				ThT assay	CR assay
42	H	14.96±1.17	13.26±2.12	nd	nd
43	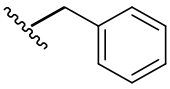	14.78±2.17	16.79±2.22	nd	nd
44	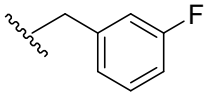	16.39±2.21	15.01±2.17	nd	nd
45	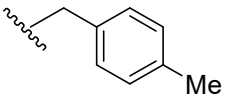	15.81±1.19	32.21±3.50	nd	nd
46	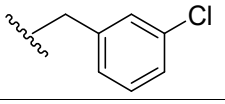	16.88±2.22	30.01±3.47	nd	nd
47	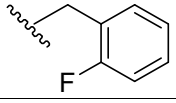	12.07±1.08	21.66±3.33	nd	nd
48	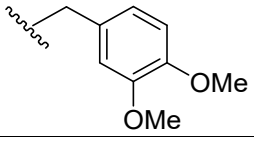	9.421±1.97	13.50±2.13	nd	nd
49	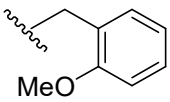	13.70±1.14	24.95±2.39	nd	nd
50	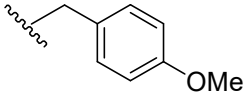	12.18±1.07	25.27±2.40	nd	nd

51	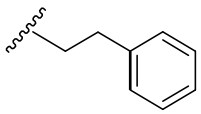	13.07±1.11	20.47±2.31	nd	nd
52	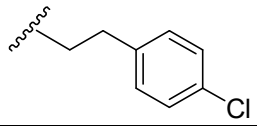	`17.38±2.24	21.74±2.33	nd	nd
53	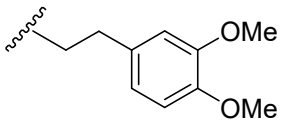	13.75±1.27	18.90±2.27	nd	nd
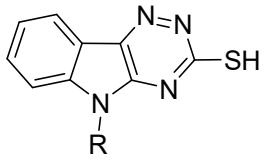 (**54-64**)					
Comp.	**R**	**AChE inhibition IC_{50} (µM)**	**BuChE inhibition IC_{50} (µM)**	**% $A\beta_{1-42}$ aggregation inhibition (at 10 µM)**	
				ThT assay	**CR assay**
54		7.33±0.87	58.61±3.59	nd	nd
55		8.50±0.95	91.62±4.57	nd	nd
56	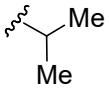	6.16±0.58	35.28±3.42	nd	nd
57	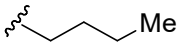	5.36±0.48	14.26±2.17	nd	nd
58	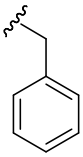	8.05±0.43	75.29±3.72	nd	nd
59	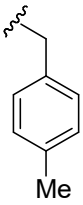	5.73±0.29	97.60±3.48	nd	nd
60	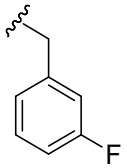	5.52±0.46	70.13±3.29	nd	nd

61	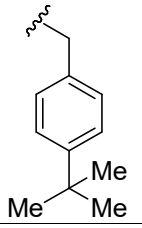	13.97±1.14	18.56±2.27	nd	nd
62	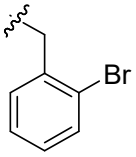	15.35±2.18	22.71±3.35	nd	nd
63	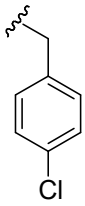	15.73±2.19	23.99±2.38	nd	nd
64	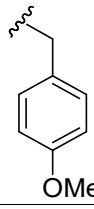	13.21±1.12	19.00±2.28	nd	nd

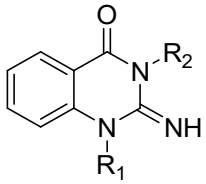

(**65-104**)

Comp.	**R_1**	**R_2**	**AChE inhibition IC_{50} (µM)**	**BuChE inhibition IC_{50} (µM)**	**% $A\beta_{1-42}$ aggregation inhibition (at 10 µM)**	
					ThT assay	**CR assay**
65	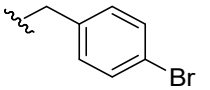	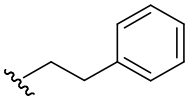	36.23±3.02	11.66±1.20	nd	nd
66	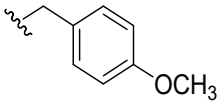	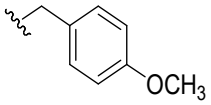	38.27±3.04	53.41±2.25	nd	nd
67	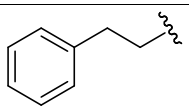	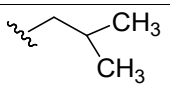	44.45±3.87	86.51±1.82	nd	nd

68	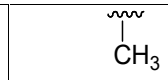	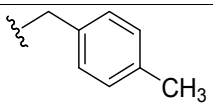	2.44±2.55	27.12±1.63	nd	nd
69	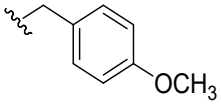	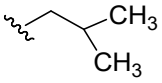	5.92±2.62	8.45±1.12	nd	nd
70	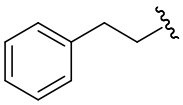	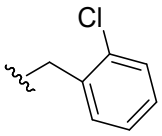	**5.40±2.96**	**7.28±0.27**	**23.67±2.98**	**26.18±2.16**
71	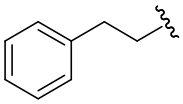	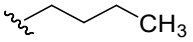	4.73±2.77	15.39±1.39	nd	nd
72	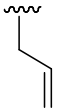	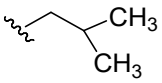	16.83±3.01	32.13±1.15	nd	nd
73	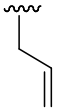	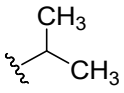	6.88±2.14	24.16±1.22	nd	nd
74	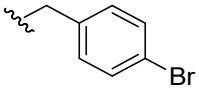		10.55±2.53	101.7±12.9	nd	nd
75	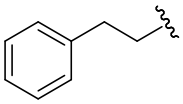	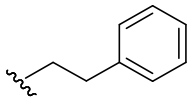	7.72±1.75	150.0±6.21	nd	nd
76	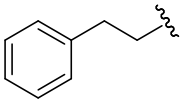	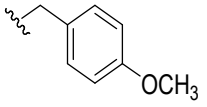	258.9±4.45	106.3±8.50	nd	nd
77	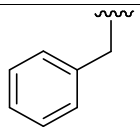	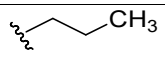	15.77±1.88	7.78±0.23	nd	nd
78	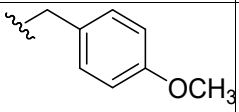	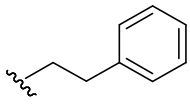	40.99±3.79	24.99±2.15	nd	nd
79	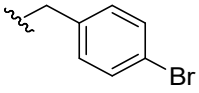	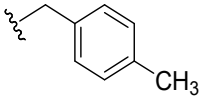	44.76±5.28	55.43±2.71	nd	nd
80	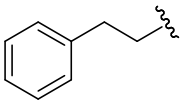	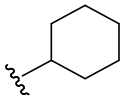	14.82±2.33	9.696±0.76	nd	nd
81		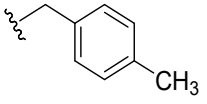	15.73±1.12	40.88±1.61	nd	nd

82	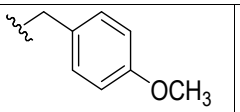	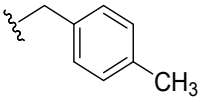	17.34±1.98	3.007±2.06	nd	nd
83	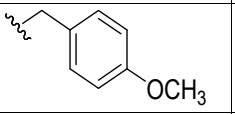	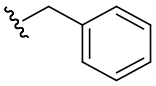	24.66±2.52	8.621±1.74	nd	nd
84	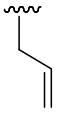	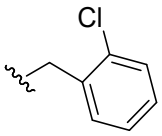	22.07±2.68	18.86±2.61	nd	nd
85	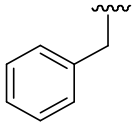	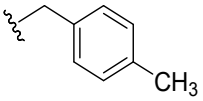	21.93±2.35	1.876±1.48	nd	nd
86	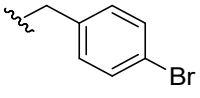	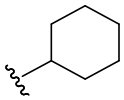	11.93±1.75	5.169±2.11	nd	nd
87	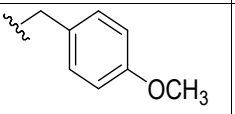	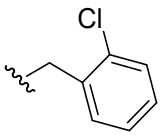	48.53±2.25	2.559±1.14	nd	nd
88	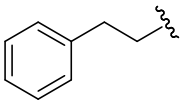	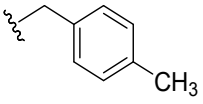	95.21±3.82	6.456±0.77	nd	nd
89	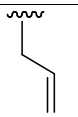	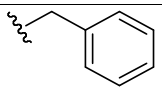	69.85±3.89	9.017±1.30	nd	nd
90	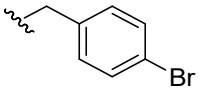	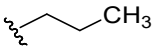	20.88±2.56	560.6±3.84	nd	nd
91	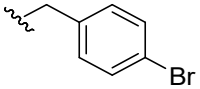	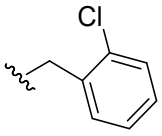	26.37±2.46	106.3±3.73	nd	nd
92	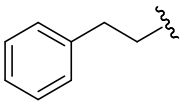	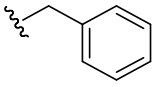	18.42±2.39	77.79±9.88	nd	nd
93	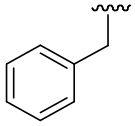	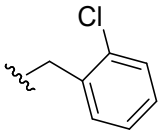	18.23±1.82	8.262±1.71	nd	nd
94		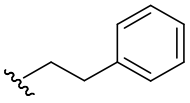	7.03±2.58	54.00±2.13	nd	nd
95	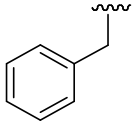	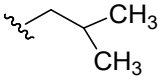	7.14±2.60	7.554±0.70	nd	nd

96	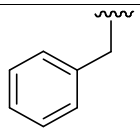	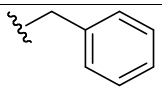	7.36±2.63	2.274±0.31	nd	nd
97	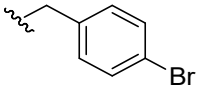	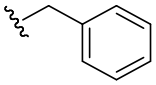	9.56±2.39	40.45±1.28	nd	nd
98		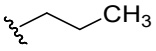	11.53±2.33	119.6±3.43	nd	nd
99		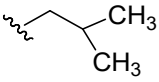	12.67±2.36	49.16±1.26	nd	nd
100		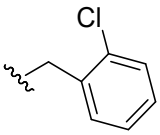	15.44±1.06	6.548±0.49	nd	nd
101	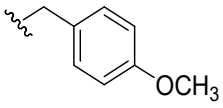	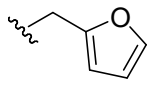	24.82±1.82	43.43±2.18	nd	nd
102	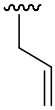		6.96±0.70	6.542±0.35	nd	nd
103	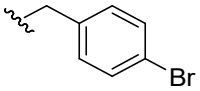	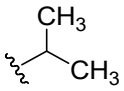	28.22±1.58	18.19±1.33	nd	nd
104	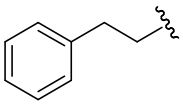	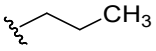	18.87±1.29	11.82±0.89	nd	nd

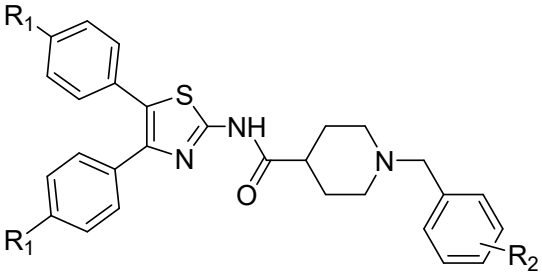

(**105-128**)

Comp.	**R_1**	**R_2**	**AChE inhibition IC_{50} (µM)**	**BuChE inhibition IC_{50} (µM)**	**% $A\beta_{1-42}$ aggregation inhibition (at 10 µM)**	
					ThT assay	**CR assay**
105	Me	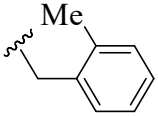	>10	1.50±0.02	nd	nd

106	Me	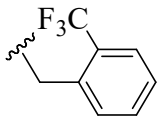	7.57±0.03	1.88±0.03	nd	nd
107	Me	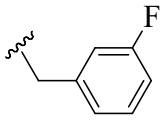	>10	1.97±0.02	nd	nd
108	Me	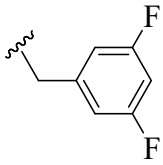	2.50±0.03	3.51±0.03	nd	nd
109	Me	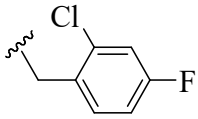	>10	1.60±0.03	nd	nd
110	Me	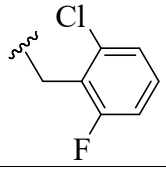	2.88±0.02	2.77±0.03	nd	nd
111	Me	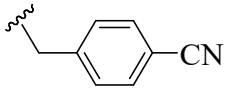	1.28±0.02	5.32±0.04	nd	nd
112	Me	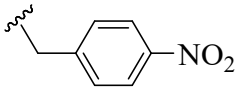	2.32±0.02	>10	nd	nd
113	Me	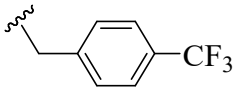	>10	2.78±0.03	nd	nd
114	Cl	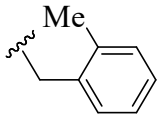	1.10±0.02	1.04±0.02	nd	nd
115	Cl	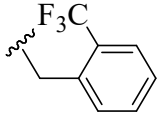	2.77±0.02	3.36±0.03	nd	nd
116	Cl	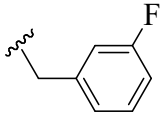	0.65±0.01	0.72±0.01	18.82±2.23	nd
117	Cl	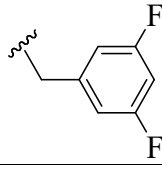	0.64±0.01	3.03±0.04	12.02±2.35	nd
118	Cl	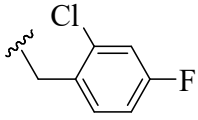	3.70±0.02	>10	nd	nd

119	Cl	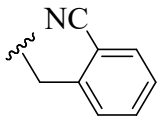	1.77±0.02	1.59±0.03	nd	nd
120	Cl	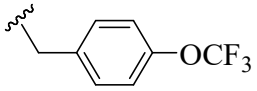	1.38±0.03	2.18±0.03	nd	nd
121	OMe	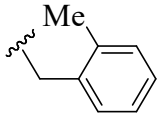	1.34±0.03	1.85±0.03	nd	nd
122	OMe	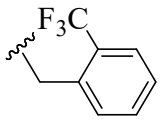	0.68±0.01	1.92±0.02	14.46±2.15	nd
123	OMe	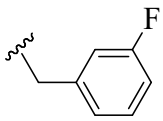	0.57±0.01	1.54±0.03	21.17±1.21	nd
124	OMe	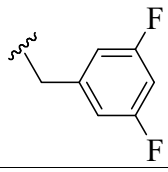	2.45±0.01	>10	nd	nd
125	OMe	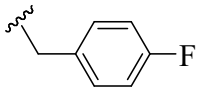	1.16±0.03	1.73±0.03	nd	nd
126	OMe	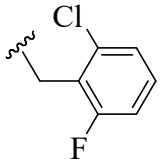	0.41±0.02	1.57±0.04	16.56±1.75	nd
127	OMe	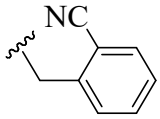	2.80±0.01	3.58±0.01	nd	nd
128	OMe	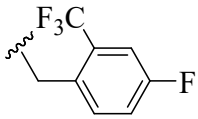	1.23±0.02	1.78±0.03	nd	nd

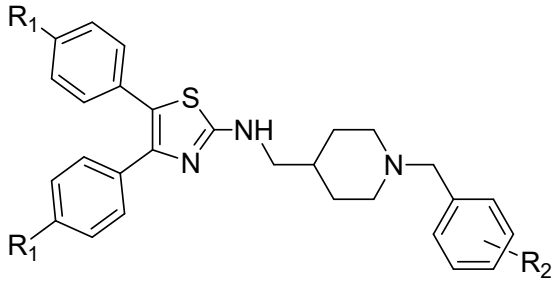

(**129-139**)

Comp.	R_1	R_2	AChE inhibition IC_{50} (μM)	BuChE inhibition IC_{50} (μM)	% $A\beta_{1-42}$ aggregation inhibition (at 10 μM)	
					ThT assay	CR assay
129	Me	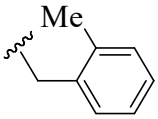	0.50±0.01	2.51±0.01	16.17±1.96	nd
130	Me	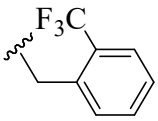	0.40±0.01	2.20±0.03	26.35±2.46	nd
131	Me	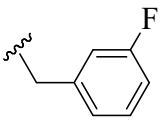	**0.30±0.01**	**1.84±0.03**	**27.65±2.91**	nd
132	Me	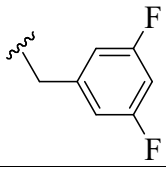	0.37±0.01	1.95±0.03	25.79±3.53	nd
133	Cl	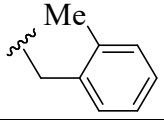	0.87±0.01	1.43±0.02	23.26±2.51	nd
134	Cl	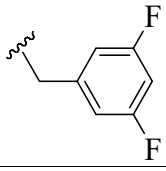	0.63±0.01	0.82±0.01	19.39±2.65	nd
135	Cl	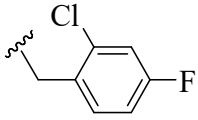	**0.52±0.01**	**0.74±0.01**	15.00±2.13	nd
136	Cl	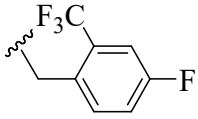	1.24±0.04	3.30±0.02	nd	nd
137	OMe	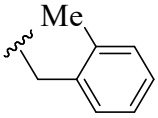	0.59±0.01	2.21±0.03	25.64±2.77	nd
138	OMe	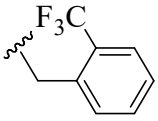	0.69±0.01	8.01±0.02	20.60±2.35	nd
139	OMe	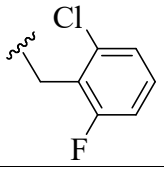	0.36±0.01	2.15±0.01	**27.20±3.15**	nd

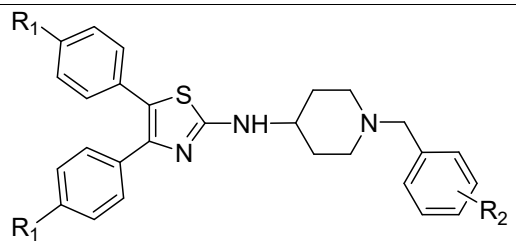

(**140-149**)

Comp.	R_1	R_2	AChE inhibition IC_{50} (μM)	BuChE inhibition IC_{50} (μM)	% $A\beta_{1-42}$ aggregation inhibition (at 10 μM)	
					ThT assay	CR assay
140	Me	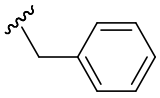	1.28±0.03	3.59±0.01	Nd	nd
141	Me	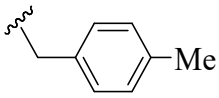	1.09±0.03	6.03±0.04	Nd	nd
142	Cl	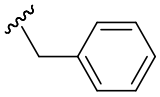	1.38±0.02	3.30±0.03	nd	nd
143	Cl	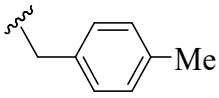	3.19±0.01	>10	nd	nd
144	Cl	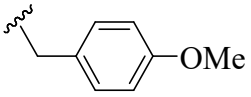	1.12±0.01	1.57±0.02	nd	nd
145	Cl	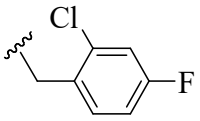	1.02±0.03	1.72±0.03	nd	nd
146	Cl	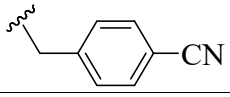	0.37±0.01	1.97±0.02	**27.47±2.85**	nd
147	OMe	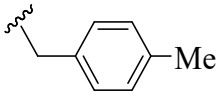	0.83±0.03	2.25±0.03	19.24±2.38	nd
148	OMe	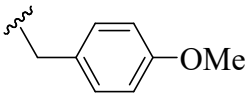	0.77±0.03	2.53±0.03	11.42±1.43	nd
149	OMe	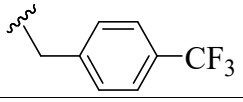	0.75±0.03	1.68±0.03	18.93±2.85	nd
Tacrine	--	--	0.05±0.01	0.01±0.00	10.63±1.28	nd
Donepezil	--	--	0.01±0.00	1.26±0.01	37.26±2.69	nd

Results are the mean ± SEM of at least three determinations. Inhibition of $A\beta_{1-42}$ aggregation produced by the test compounds at 10 μM. nd=Not determined.

4.3. Test compounds showed neuroprotective effect in SH-SY5Y cells

To check therapeutic suitability of the selected test compounds, their effect on cell viability and neuroprotective activity against oxidative stress were evaluated using the human neuroblastoma SH-SY5Y cell line. For assessment of cytotoxicity of the test compounds, cells were exposed to relatively high concentrations of the test compounds (40 μM and 80 μM) for 24 hr followed by determination of the cell viability using 3-(4,5-dimethylthiazol-2-yl)-2,5-diphenyltetrazolium bromide (MTT) assay. In this experimental condition all of the selected test compounds caused negligible cell death even at such a high concentrations (Table 2).

In another set of experiments, neuroprotective potential of the selected test derivatives was assessed. Oxidative stress-like condition in SH-SY5Y cells was induced using H_2O_2 as a toxic insult [53, 54]. In this assay [53], addition of H_2O_2 (100 μM) to the growth medium caused significant cell death as evidenced by reduction in cell viability (52-56 %) compared to the control. To assess the neuroprotective potential of the test compounds against the toxic onslaught of H_2O_2, the cells were pre-treated for 2 hr with the test compounds (5 μM, 10 μM and 20 μM) followed by H_2O_2 treatment for 24 hr. At 5 μM concentration, the compounds showed insignificant protective effect (data not shown). However, as shown in Table 2, the selected derivatives exhibited significant neuroprotective effect at 10 μM and 20 μM concentrations. Amongst all of the test compounds, compound (**131**) showed the highest neuroprotection against the H_2O_2 insult. The results revealed that the tested compounds can protect neuronal cells against oxidative stress-associated cell death.

Table 2: Cell viability, neuroprotection and free radical scavenging activity of some of the test compounds in the human neuroblastoma SH-SY5Y cell line and DPPH assay

Com. No.	Cell viability (%)		Neuroprotection (%)		RP of DPPH (%)	
	40 μM	80 μM	10 μM	20 μM	10 μM	20 μM
13	**94.5±2.2**	**91.6±2.3**	**33.8±3.8**	**52.9±3.7**	**50.3±3.4**	**66.8±3.0**
17	**92.7±2.0**	**90.9±2.2**	**30.3±2.7**	**45.2±3.3**	**47.8±3.7**	**61.6±3.6**
70	**94.4±2.5**	**92.6±2.8**	**27.2±2.5**	**43.8±3.9**	**44.4±3.5**	**60.2±3.4**
116	93.6±2.5	91.1±2.9	29.2±2.4	50.8±3.4	40.6±3.1	61.7±2.8
117	95.6±2.4	92.8±3.1	31.5±3.7	53.4±2.9	43.5±2.4	64.6±2.8
122	92.4±3.7	93.1±2.1	21.9±3.2	38.7±2.7	43.0±2.9	63.6±2.9

123	94.0±2.7	90.3±3.9	33.3±2.3	39.9±3.0	40.5±3.3	62.6±3.1
126	92.9±2.2	91.6±4.3	32.9±2.6	55.7±2.9	46.0±2.7	63.6±2.4
129	91.4±3.1	90.1±3.1	26.9±2.9	52.7±2.8	49.0±2.8	58.9±2.7
130	93.5±2.8	91.7±3.6	29.3±2.8	48.8±3.3	48.9±2.1	59.4±3.1
131	**95.2±2.6**	**91.3±2.9**	**39.6±2.3**	**59.5±2.4**	**54.6±2.7**	**70.5±2.6**
132	91.8±2.0	89.7±3.2	28.8±1.4	42.5±2.6	51.2±2.7	56.5±3.3
133	95.4±1.9	90.9±2.4	23.6±2.8	49.7±3.1	45.4±2.9	63.4±2.4
134	92.4±3.7	91.7±2.8	29.8±2.2	42.9±3.2	44.8±2.2	60.9±2.2
135	92.7±2.6	88.9±3.6	31.5±2.7	53.7±2.6	46.3±3.2	57.4±2.3
137	91.6±3.3	87.2±3.9	34.2±2.1	41.4±2.2	42.5±3.1	63.4±2.7
138	94.2±3.6	90.1±2.5	33.2±3.1	48.4±2.2	51.8±2.8	66.9±2.6
139	94.2±2.2	87.1±3.6	28.8±2.4	41.5±2.9	48.3±2.5	57.1±2.8
146	94.2±3.2	92.5±1.9	32.0±3.3	53.2±2.7	42.2±2.4	63.2±3.2
147	95.4±2.7	89.5±2.7	29.9±2.1	47.4±2.3	47.2±3.1	63.4±2.3
148	92.1±3.6	89.5±3.2	25.5±2.8	40.1±3.4	49.3±2.2	65.5±2.9
149	94.5±2.6	90.4±2.4	30.4±2.4	42.0±2.2	50.0±2.9	66.2±2.4
Tacrine	89.4±2.3	90.0±3.4	44.7±3.3	57.9±2.1	54.9±2.1	68.8±3.7
Donepezil	96.9±1.4	92.3±2.4	48.2±2.4	62.0±2.5	59.9±2.6	75.5±2.9
Ascorbic acid	nd	nd	nd	nd	56.4±2.7	67.7±2.7

Percentage cell viability of SH-SY5Y cells exposed to relatively high concentrations (40 µM and 80 µM) of test compounds. Percentage neuroprotection of SH-SY5Y cells at relatively lower concentrations (10 µM and 20µM) of the test compounds against H_2O_2 (100 µM) insult. RP of DPPH **(%) =** reduction percentage of DPPH. Results are the mean ± SEM of at least three independent experiments. nd = not determined.

4.4. Test compounds showed antioxidant activity in DPPH assay

2,2-Diphenyl-1-picrylhydrazyl (DPPH) is one of the few stable and commercially available organic nitrogen radicals. DPPH assay is commonly used for preliminary screening of compounds capable of scavenging activated oxygen species [56]. The selected test compounds were evaluated for their antioxidant potential using DPPH assay. All of the test compounds exhibited significant free radical scavenging activity. At 10 µM concentration, the test compounds showed free radical scavenging activity in the range of 40-55 % with compound (**131**) showing the highest activity of 55 %. Moreover, at 20 µM concentration, the test

compounds exhibited free radical scavenging activity ranging from 56-70 % with compound (**131**) showing 70 % activity.

4.5. Test compounds showed passive *in vitro* BBB permeability

The very first requirement of a successful CNS drug is its ability to cross BBB and reach its therapeutic target. In this regard, BBB permeation has a great importance. To determine the BBB penetration of the selected test compounds, a parallel artificial membrane permeation assay for blood-brain barrier (PAMPA-BBB) was utilized. This simple and rapid model described by Di *et al* [58], has the advantage to predict passive BBB permeation with high accuracy. The *in vitro* permeability (P_e) of the test compounds through the lipid extract of porcine brain was determined in PBS-ethanol (70:30). For validation of the assay, reported permeability values of

Table 3: Permeability (P_e) results from the PAMPA-BBB assay with their predictive penetration in CNS.

Comp. No.	P_e (10^{-6} cm/s)[a]	Prediction[b]	Compd	P_e (10^{-6} cm/s)	Prediction
13	15.3±0.6	CNS+	132	10.1±0.6	CNS+
17	12.2±0.4	CNS+	133	8.8±0.4	CNS+
70	14.2±0.3	CNS+	134	12.5±1.3	CNS+
116	15.9±1.2	CNS+	135	13.2±1.5	CNS+
117	8.8±0.4	CNS+	137	12.3±0.8	CNS+
122	12.3±0.8	CNS+	138	8.4±0.8	CNS+
123	12.5±0.8	CNS+	139	12.2±0.6	CNS+
126	8.2±0.4	CNS+	146	8.4±0.8	CNS+
129	10.6±1.1	CNS+	147	9.6±1.1	CNS+
130	12.8±0.8	CNS+	148	10.3±0.6	CNS+
131	14.5±1.5	CNS+	149	8.6±0.2	CNS+

Data are expressed as mean ± SEM of three independent experiments. CNS+ indicates good passive CNS permeation.

nine quality standards [58] were compared with their experimental permeability values (see supplementary information, Table S1) which gave a linear relationship, Pe(Exp.)= 1.171Pe(Ref.) + 1.489 (R2 = 0.983) (see supplementary information, Fig. S2). From this equation and

considering limits established by Di. *et al* [58, 59, 83], a molecule with a permeability (Pe) of >6.2×10-6 cm/s (see supplementary information, Table S2) can cross the BBB by passive diffusion. The selected test compounds showed permeability (Pe) values above this limit, suggesting that they could cross the BBB by passive diffusion (Table 3).

4.6. Test compounds (13, 17, 70 and 131) showed protection in scopolamine-induced AD-like phenotype in mice model

4.6.1. Test compounds (13, 17, 70 and 131) showed enhanced spatial learning ability in MWM test

Compounds (**13, 17, 70** and **131)** with already proven *in vitro* ChE inhibition activity were further evaluated using the *in vivo* scopolamine-induced amnesic mice model. Scopolamine-induced amnesia in rodents is an accepted standard model in behavioural pharmacology for evaluation of ChE inhibiting anti-Alzheimer's drug candidates. Scopolamine distinctly blocks muscarinic cholinergic receptors that lead to impairment of cognitive functions. MWM test was adopted for the assessment of spatial learning and memory. As shown in Fig. 1-I-A and 1-II-A, the scopolamine-treated control animals (1.4 mg/kg, i.p.) showed significant rise in ELT as compared to the vehicle-treated control animals in all trial sessions (p<0.001) indicating scopolamine-induced memory impairment. However, treatment with **13, 17, 70** (10 mg/kg, p.o.) (Fig. 1-I-A, p<0.001) and **131** (5 mg/kg, p.o.) (Fig. 1-II-A, p<0.001) significantly reduced the ELT, from third day onward in the probe trial session as compared to the scopolamine-treated control group.

Additionally, spatial learning ability was evaluated by counting the number of crossings over the platform area. Scopolamine-treated control group animals had shown reduced number of platform crossings during all the trial sessions as compared to the vehicle-treated control animals (Fig. 1-I-B, p<0.01 and 1-II-B, p<0.001). **13**, **17**, **70** (10 mg/kg, p.o.) (Fig. 1-I-B, p<0.01) and **131** (5 mg/kg, p.o.) (Fig. 1-II-B, p<0.05) significantly increased the count of platform crossings as compared to the scopolamine-treated control group. Standard drug donepezil (at 5 mg/kg, p.o.) significantly reduced ELT (Fig. 1-I-A, p<0.001 and Fig. 1-II-A, p<0.001) and increased platform area crossings (Fig. 1-I-B, p<0.01 and Fig. 1-II-B, p<0.01) as compared to the scopolamine-treated control group. In brief, **13**, **17**, **70** and **131** significantly reduced the ELT while increased the number of crossings above the platform area in MWM test

demonstrating their potential to improve spatial learning and memory, which were impaired by scopolamine.

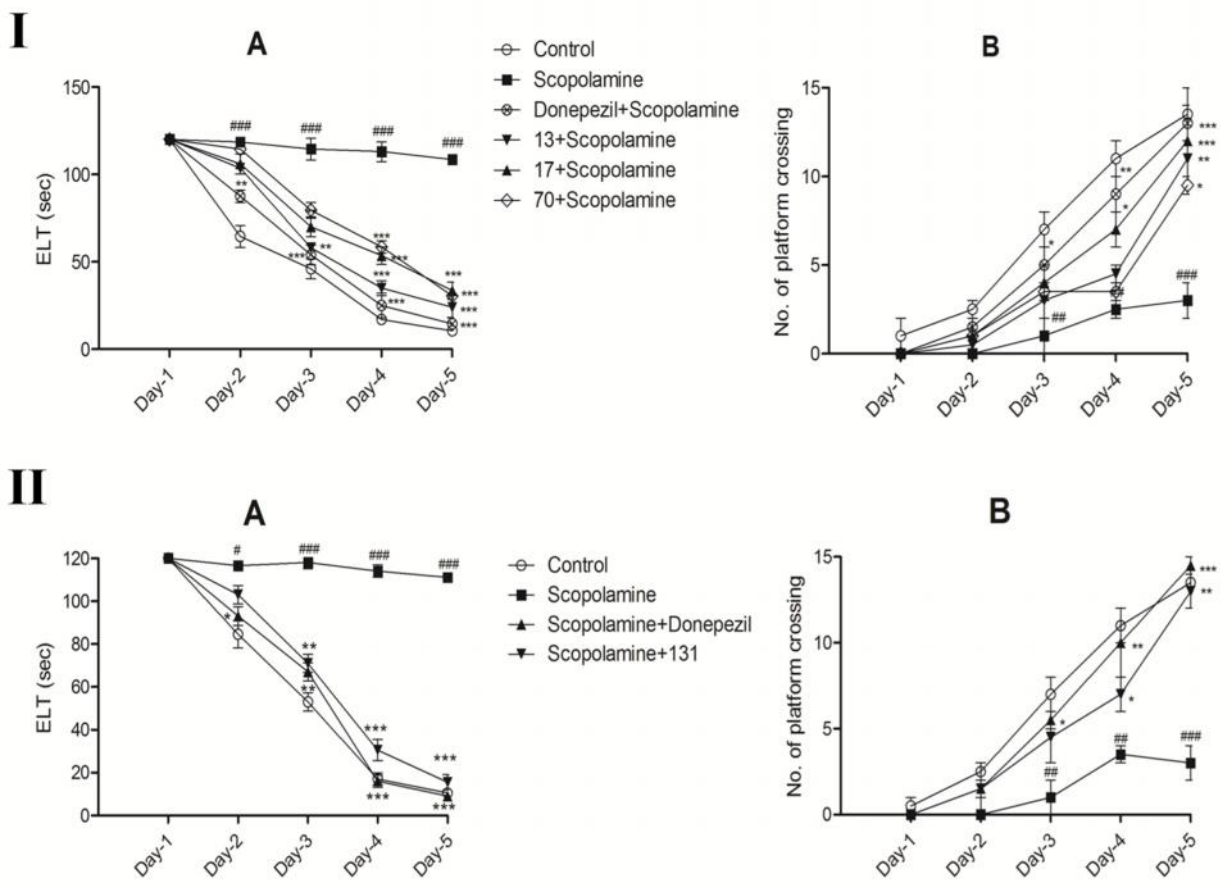

Fig. 1: Test compounds (**13, 17, 70** and **131**) enhanced spatial learning ability of scopolamine-induced amnesic mice in MWM test. Scopolamine treatment (1.4 mg/kg, i.p.) increased the ELT during probe trial sessions (I-A and II-A), and reduced the number of platform area crossings (I-B and II-B) as compared to the vehicle-treated control mice. **13, 17, 70** (10 mg/kg, p.o.) (I-A & B) and **131** (5 mg/kg, p.o.) (II-A and II-B) significantly reversed these alterations similar to donepezil (5 mg/kg, p.o.). Data are expressed as mean ± SEM (n=6). $^{###}p<0.001$, $^{##}p<0.01$ *vs.* vehicle-treated control group. *** $p<0.001$, ** $p<0.01$, * $p<0.05$ *vs.* scopolamine-treated control group.

4.6.2. Test compounds (13, 17, 70 and 131) showed i*n vivo* anti-ChE and antioxidant activities

Scopolamine-induced amnesia in mice is a well-established model to evaluate anti-ChE activity [61]. Ability of **13, 17, 70** and **131** to inhibit AChE and BuChE activities *in vitro* has already been demonstrated. The compounds (**13, 17, 70** and **131**) were further assessed for their effect on ChE activity in the mice brain using Ellman's colorimetric assay. Scopolamine

treatment (1.4 mg/kg, i.p.) significantly increased AChE (Fig. 2-I-A, $p<0.001$ and Fig. 2-II-A, $p<0.001$) as well as BuChE (Fig. 2-I-B, $p<0.001$ and Fig. 2-II-B, $p<0.001$) activities in mice brain as compared to the vehicle-treated control group. While, **13, 17, 70** (10 mg/kg, p.o.) and **131** (5 mg/kg, p.o.) treatment significantly reduced the elevated AChE (Fig. 2-I-A, $p<0.001$ and Fig. 2-II-A, $p<0.001$) and BuChE (Fig. 2-I-B, $p<0.001$ and Fig. 2-II-B, $p<0.001$) activities similar to the standard drug donepezil (5 mg/kg, p.o.). These results validated the *in vitro* findings.

Effect of **13, 17, 70** and **131** on altered oxidative stress parameters was also evaluated. Scopolamine treatment significantly increased brain MDA levels as compared to the vehicle-treated control animals (Fig. 2-I-C, $p<0.001$ and Fig. 2-II-C, $p<0.001$). Similar to donepezil, the test compounds (**13, 17, 70** and **131)** significantly abrogated elevated MDA levels as compared to the scopolamine-treated control group (Fig. 2-I-C, $p<0.001$ and Fig. 2-II-C, $p<0.001$). Further, scopolamine treatment significantly reduced brain CAT levels as compared to the vehicle-treated control animals (Fig. 2-I-D, $p<0.001$ and Fig. 2-II-D, $p<0.001$). **13, 17, 70** and **131** treatment significantly increased the brain CAT levels as compared to the scopolamine-treated control group (Fig. 2-I-D, $p<0.01$ and Fig. 2-II-D, $p<0.001$). These results demonstrated the antioxidant profile of the test compounds (**13, 17, 70** and **131**).

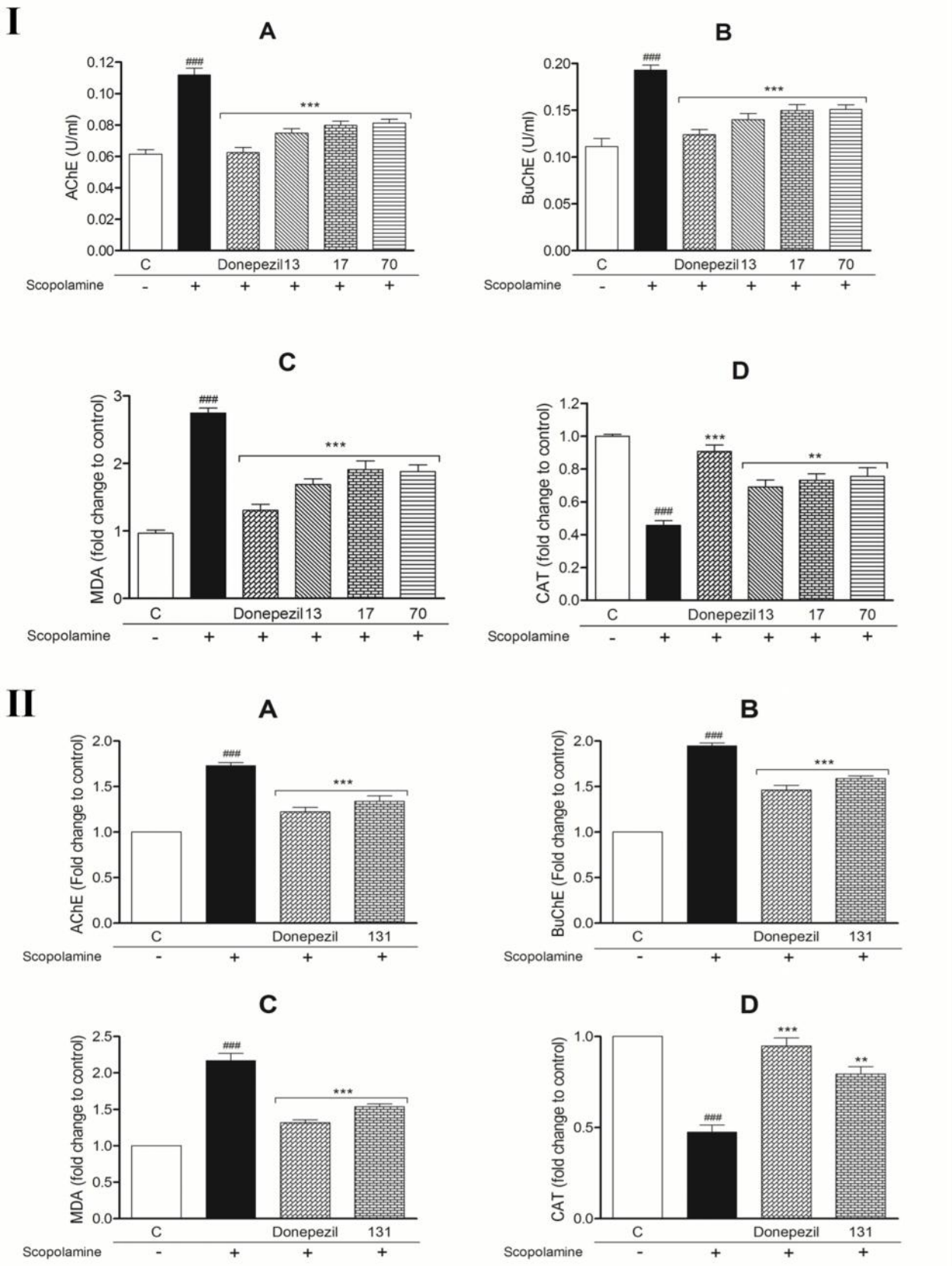
I
A
AChE (U/ml)
0.12
0.10
0.08
0.06
0.04
0.02
0.00
###
***
C
Donepezil 13
17
70
Scopolamine
- + + + + +
B
BuChE (U/ml)
0.20
0.15
0.10
0.05
0.00
###
***
C
Donepezil 13
17
70
Scopolamine
- + + + + +
C
MDA (fold change to control)
3
2
1
0
###
***
C
Donepezil 13
17
70
Scopolamine
- + + + + +
D
CAT (fold change to control)
1.2
1.0
0.8
0.6
0.4
0.2
0.0
***
###
**
C
Donepezil 13
17
70
Scopolamine
- + + + + +
II
A
AChE (Fold change to control)
2.0
1.5
1.0
0.5
0.0
###
***
C
Donepezil
131
Scopolamine
- + + +
B
BuChE (Fold change to control)
2.0
1.5
1.0
0.5
0.0
###
***
C
Donepezil
131
Scopolamine
- + + +
C
MDA (fold change to control)
2.5
2.0
1.5
1.0
0.5
0.0
###
***
C
Donepezil
131
Scopolamine
- + + +
D
CAT (fold change to control)
1.0
0.5
0.0
***
###
**
C
Donepezil
131
Scopolamine
- + + +

Fig. 2: Test compounds (**13, 17, 70** and **131**) demonstrated anti-cholinesterase (anti-ChE) and antioxidant effects in scopolamine-treated amnesic mice brain. (I-A and II-A) AChE and (I-B and II-B) BuChE levels were increased in scopolamine-treated (1.4 mg/kg, i.p.) mice brains which were significantly attenuated by simultaneous treatment with **13, 17, 70** (10 mg/kg, p.o.) and **131** (5 mg/kg, p.o.). Oxidative stress parameters are represented using estimation of (I-C and II-C) MDA and (I-D and II-D) CAT levels. MDA levels were significantly increased while CAT levels were significantly decreased in scopolamine-treated mice brains as compared to vehicle-treated control group. **13, 17, 70** and **131** treatment significantly decreased the brain MDA levels and increased brain CAT levels similar to donepezil (5 mg/kg, p.o.). Data are expressed as mean ± SEM (n=6). $^{###}p<0.001$ *vs.* vehicle-treated control group. *** $p<0.001$, ** $p<0.01$ *vs.* scopolamine-treated control group. C=vehicle-treated control group.

4.7. *In vitro* neuroprotective effect of test compounds (13, 17 and 70) on primary rat hippocampal neurons

Cytoprotective effect of **13, 17** and **70** was assessed on primary rat hippocampal neurons using MTT assay. Hippocampal neurons exposed to different concentrations of **13, 17** and **70** (10-40 μM) did not show any significant cytotoxicity when compared to the control cells (Fig. 3A). Similar results were observed for donepezil (10-40 μM) (Fig. 3A).

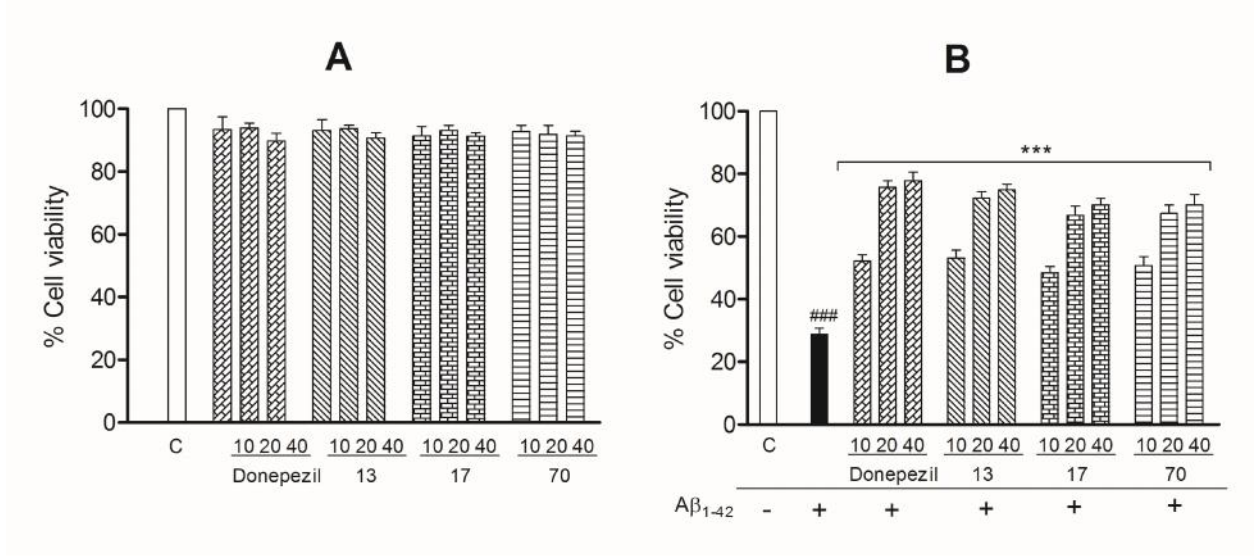

Fig. 3: *In vitro* neuroprotective effects of test compounds **13, 17** and **70**. (A) Primary rat hippocampal neurons exposed to **13, 17** and **70** (10-40 μM) for 24 hr showed percentage cell viability near to the control cells. (B) Neuroprotective potential of **13, 17** and **70** was assessed against $A\beta_{1-42}$ insult. $A\beta_{1-42}$ (10 μM) caused significant toxicity in rat hippocampal neurons as compared to the control cells. However, pre-treatment with **13/17/70** (10-40 μM) significantly reduced $A\beta_{1-42}$ toxicity similar to donepezil (10-40 μM). Data are expressed as mean ± SEM (n=6). $^{###}p<0.001$ *vs.* control cells. *** $p<0.001$ *vs.* $A\beta_{1-42}$-treated control cells. C=control cells.

In another set of experiment, neuroprotective potential of the test compounds (**13**, **17** and **70**) was evaluated in $A\beta_{1-42}$-treated (10 μM) primary hippocampal neurons. $A\beta_{1-42}$ treatment significantly induced cytotoxicity in hippocampal neuronal cells as compared to the control cells

(Fig. 3B, $p<0.001$). As shown in Fig. 3B, pre-treatment with **13**, **17** and **70** significantly reduced $A\beta_{1-42}$ toxicity dose-dependently as evidenced by increased cell viability ($p<0.001$) in the treated groups. These results revealed neuroprotective potential of compounds (**13**, **17** and **70**) against $A\beta_{1-42}$-induced neurotoxicity.

4.8. Antiapoptotic potential of test compounds (13, 17 and 70)

Apoptotic cell death was assessed by quantifying apoptotic (fragmented) nuclei using Hoechst staining in different experimental sets. As shown in Fig. 4A, $A\beta_{1-42}$ (10 μM) treatment

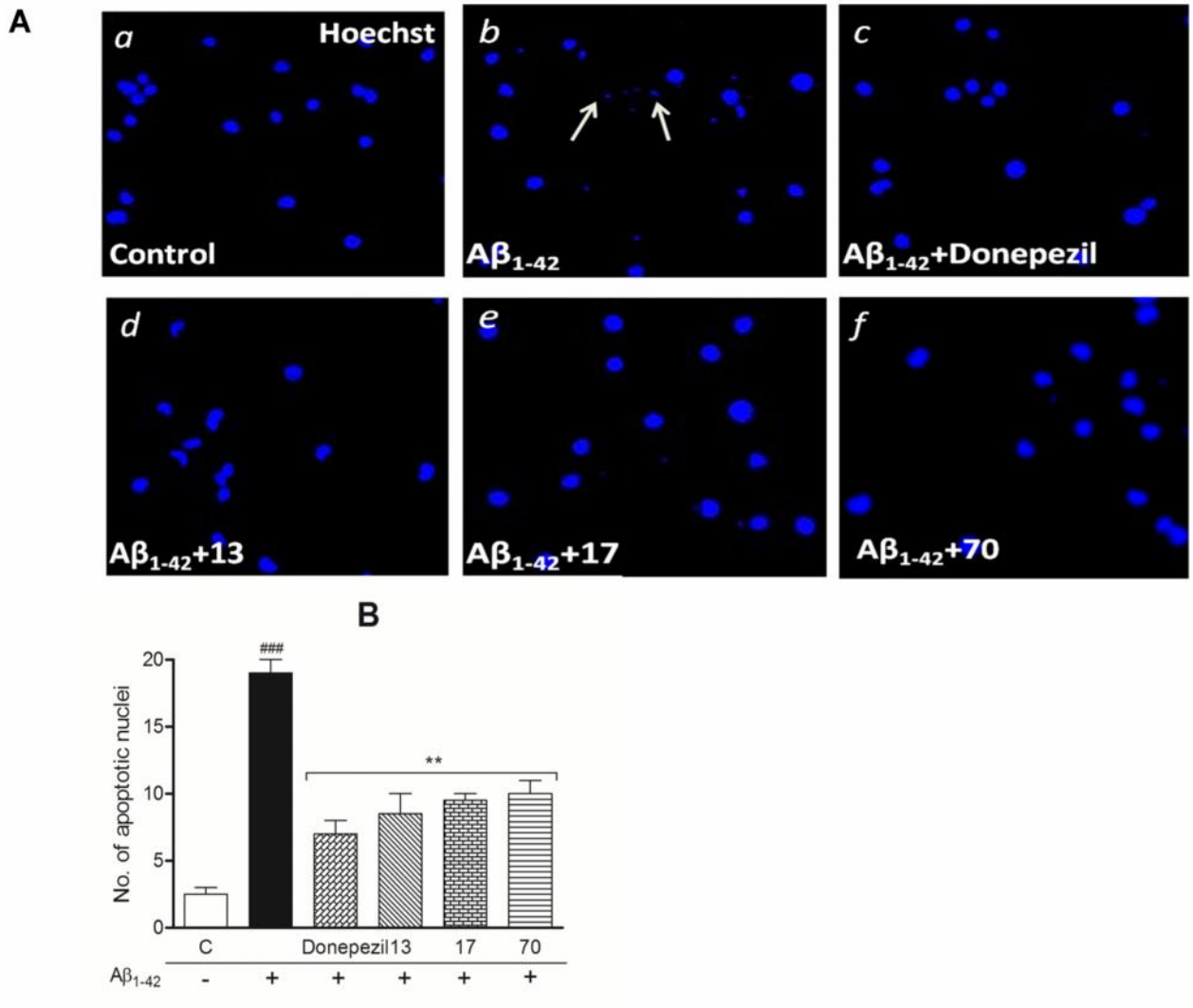

Fig. 4: *In vitro* antiapoptotic effects of test compounds (**13, 17** and **70)** against $A\beta_{1-42}$-induced toxicity of hippocampal neurons. (A) Hoechst-stained hippocampal cell nuclei are represented as: (*a*) control, (*b*) $A\beta_{1-42}$, (*c*) $A\beta_{1-42}$+donepezil, (*d*) $A\beta_{1-42}$+**13**, (*e*) $A\beta_{1-42}$+**17** and (*f*) $A\beta_{1-42}$+**70**-treated cells. $A\beta_{1-42}$ (10 μM) induced nuclei fragmentation (see arrow) [A (*b*)] was abrogated by **13** [A (*d*)], **17** [A (*e*)] and **70** [A (*f*)] (20 μM) similar to

donepezil [A (*c*)] (20 μM). Scale bar = 20 μm. (B) Quantification of apoptotic nuclei was performed by a blind observer by counting 30 cells from each culture group that were randomly selected from three independent cultures (n=3). $A\beta_{1-42}$ treatment significantly increased number of apoptotic nuclei which was significantly reduced by treatment with **13**/**17**/**70**. Data are expressed as mean ± SEM. $^{###}p<0.001$ *vs.* control cells. *** $p<0.001$, ** $p<0.01$ *vs.* $A\beta_{1-42}$-treated control cells. C=control cells.

significantly induced fragmentation of nuclei [Fig.4A (b)] which indicated progression of apoptosis. However, pre-treatment with **13** [Fig. 4A (d)], **17** [Fig. 4A (e)] and **70** [Fig. 4A (f)] significantly suppressed the apoptotic nuclei fragmentation. Quantitative data analysis revealed that $A\beta_{1-42}$ (10 μM) treatment significantly increased number of fragmented nuclei as compared to the control cells (Fig. 4B, $p<0.001$). Pre-treatment with **13**, **17** and **70** (20 μM) significantly reduced the number of apoptotic nuclei as compared to the $A\beta_{1-42}$-treated control cells (Fig. 4B, $p<0.01$).

4.9. Test compounds (13, 17 and 70) attenuated *in vitro* cleaved caspase-3 activation

Caspase-3 activation is a key process during the progression of apoptosis which results in phosphorylation of caspase-3 [84]. In the current study, the expression of activated/cleaved caspase-3 protein was determined to confirm the apoptotic cell death. As shown in Fig. 5A, $A\beta_{1-42}$-treated (10 μM) cells significantly increased the expression of cytoplasmic cleaved capase-3 protein [Fig. 5A (*b*2, *c*2)]. However, **13** [Fig. 5A (*b*4, *c*4)], **17** [Fig. 5A (*b*5, *c*5)] and **70** [Fig. 5A (*b*6, *c*6)] (20 μM) pre-treated cells significantly attenuated the expression of cleaved caspase-3 as compared to the $A\beta_{1-42}$-treated control cells. Counterstaining with dapi was performed to locate the cell nuclei [Fig. 5A (*a*1-*a*5)]. Quantitative analysis revealed increased mean fluorescence intensity of cleaved caspase-3 expression in $A\beta_{1-42}$-treated cells (Fig. 5B, $p<0.001$) as compared to the control cells. Supporting the previous results, pre-treatment with **13, 17** and **70** (Fig. 5B, $p<0.001$) significantly reduced the mean fluorescence intensity of cleaved caspase-3 expression. Percentage of cleaved caspase-3 positive cells was quantified by a blind observer. As shown in Fig. 5C, number of cleaved caspase-3 positive cells was increased by $A\beta_{1-42}$ insult ($p<0.001$) which was significantly suppressed by pre-treatment with **13, 17** and **70** ($p<0.001$). As predicted, donepezil (20 μM) significantly reduced the number of cleaved capase-3 positive cells as compared to the $A\beta_{1-42}$-treated control cells (Fig. 5C, $p<0.001$). These results demonstrated neuroprotective and antiapoptotic effect of **13, 17** and **70** against $A\beta_{1-42}$-induced cytotoxicity.

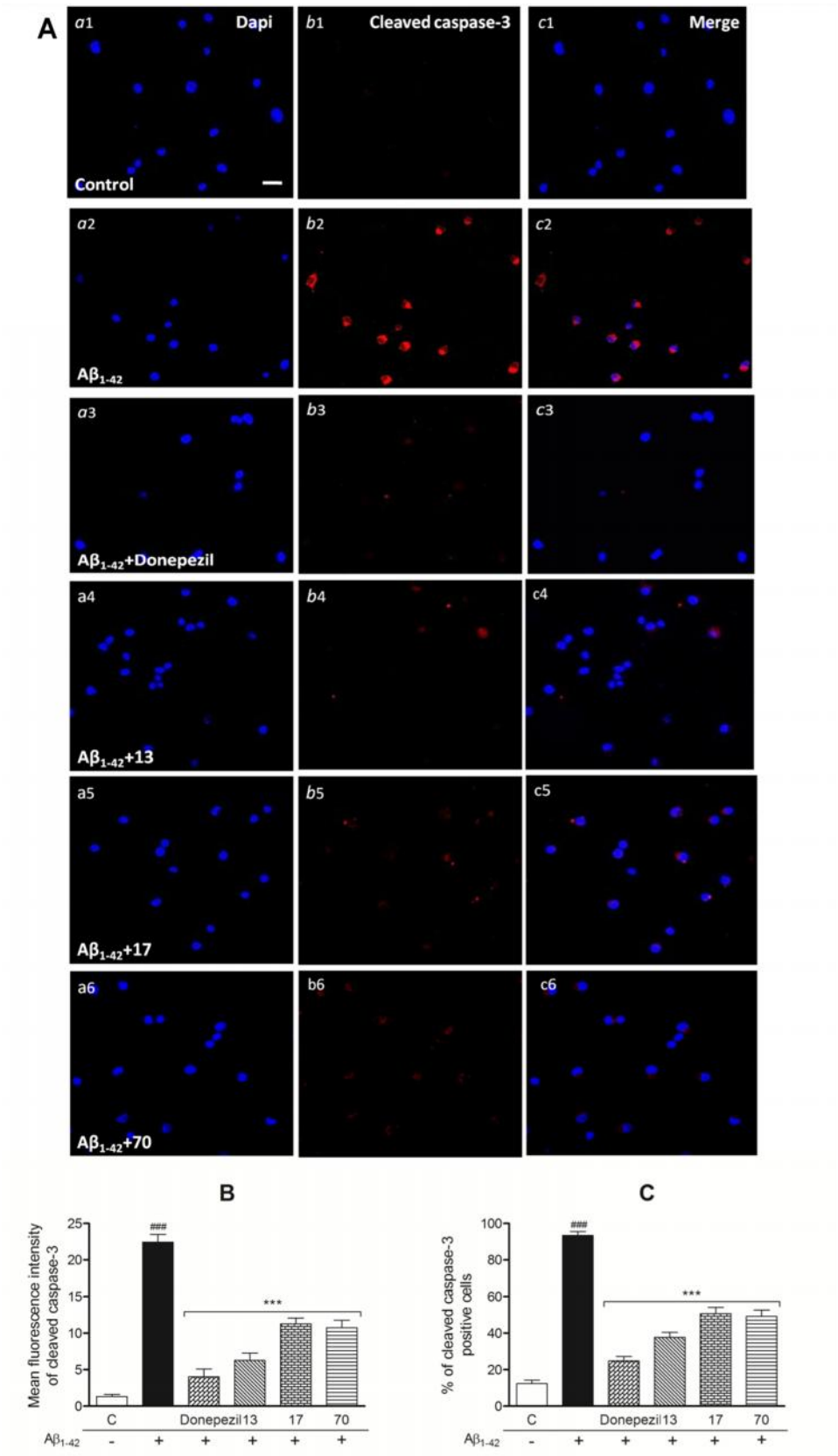
A
a1
Dapi
b1
Cleaved caspase-3
c1
Merge
Control
a2
b2
c2
Aβ1-42
a3
b3
c3
Aβ1-42+Donepezil
a4
b4
c4
Aβ1-42+13
a5
b5
c5
Aβ1-42+17
a6
b6
c6
Aβ1-42+70
B
Mean fluorescence intensity of cleaved caspase-3
###
***
C
Donepezil
13
17
70
Aβ1-42
C
% of cleaved caspase-3 positive cells

Fig. 5: *In vitro* attenuation of caspase-3 activation by test compounds (**13, 17** and **70)**. (A) Primary rat hippocampal neurons were exposed to $A\beta_{1-42}$ (10 μM) to determine antiapoptotic potential of **13, 17** and **70** (20 μM) through assessment of cleaved caspase-3 (active) expression. $A\beta_{1-42}$ treatment significantly increased expression of cleaved caspase-3 protein in the cytoplasm of hippocampal neuronal cells [A (*b*2, *c*2)] which was suppressed by **13** [A (*b*4, *c*4)], **17** [A (*b*5, *c*5)] and **70** [A (*b*6, *c*6)]. Cell nuclei were counterstained with dapi [A (*a*1-*a*5)]. Scale bar=20μm. (B) Mean fluorescence intensity of cleaved caspase-3 protein expression was quantified. $A\beta_{1-42}$-treated cells showed increased mean fluorescence intensity of cleaved caspase-3 protein as compared to the control cells which was significantly attenuated by pre-treatment with **13, 17** and **70**. (C) Quantification of cleaved caspase-3 positive cells was performed by a blind observer by counting 30 cells from each culture group that were randomly selected from three independent cultures (n=3). Percentage of cleaved caspase-3 positive cells was significantly increased following treatment with $A\beta_{1-42}$ which was significantly reduced by pre-treatment with **13, 17** and **70** similar to donepezil (20 μM). Data are expressed as mean ± SEM. $^{###}p<0.001$ *vs.* control cells. *** $p<0.001$ *vs.* $A\beta_{1-42}$-treated control cells. C=control cells.

4.10. Test compounds (13, 17, 70 and 131) possessed ROS scavenging activity

ROS scavenging activity was performed to evaluate antioxidant profile of the test compounds. Elevated level of ROS is a sign of increased oxidative stress in a variety of pathological conditions [85]. $A\beta_{1-42}$ insult is known to induce oxidative stress in AD pathogenesis [86]. Hence, antioxidant potential of the test compounds (**13, 17, 70** and **131**) was further confirmed using DCFH-DA assay. $A\beta_{1-42}$-treated (10 μM) rat hippocampal neurons significantly increased ROS generation (Fig. 6-I-A, $p<0.001$ and Fig. 6-II-A, $p<0.001$). As described earlier, **13, 17, 70** and **131** showed antioxidant activity as evidenced in scopolamine model. Pre-treatment of **13, 17, 70** (10-40 μM) (Fig. 6-I-A, $p<0.001$) and **131** (10 and 20 μM) (Fig. 6-II-A, $p<0.001$) significantly reduced $A\beta_{1-42}$ toxicity by suppressing ROS generation. These results revealed ROS scavenging activity of **13, 17, 70** and **131**. Similar results were observed for the standard drug donepezil (Fig. 6-I-A, $p<0.001$ and Fig. 6-II-A, $p<0.001$).

4.11. Test compounds (13, 17, 70 and 131) attenuated apoptosis rate

Further, to determine antiapoptotic potential of the test compounds (**13, 17, 70** and **131**), cells were stained with Annexin V-FITC and PI. Annexin V can stain the cells in both the early and late apoptosis stages while PI enters the cells in the late apoptosis or necrosis stage. As shown in Fig. 6, $A\beta_{1-42}$ (10 μM) insult significantly increased percentage of early apoptotic cells (Fig. 6-I-B, 39.80% and Fig. 6-II-B, 38.80%) as compared to the control cells (Fig. 6-I-B, 1.89% and Fig. 6-II-B, 1.78%) which was determined by flow cytometry. However, the treatment with **13** (Fig. 6-I-B, 11.60%) **17** (Fig. 6-I-B, 12.60%), **70** (Fig. 6-I-B, 11.30%) and **131** (Fig. 6-II-B, 13.40%) significantly reduced the percentage of $A\beta_{1-42}$-induced early apoptotic cells.

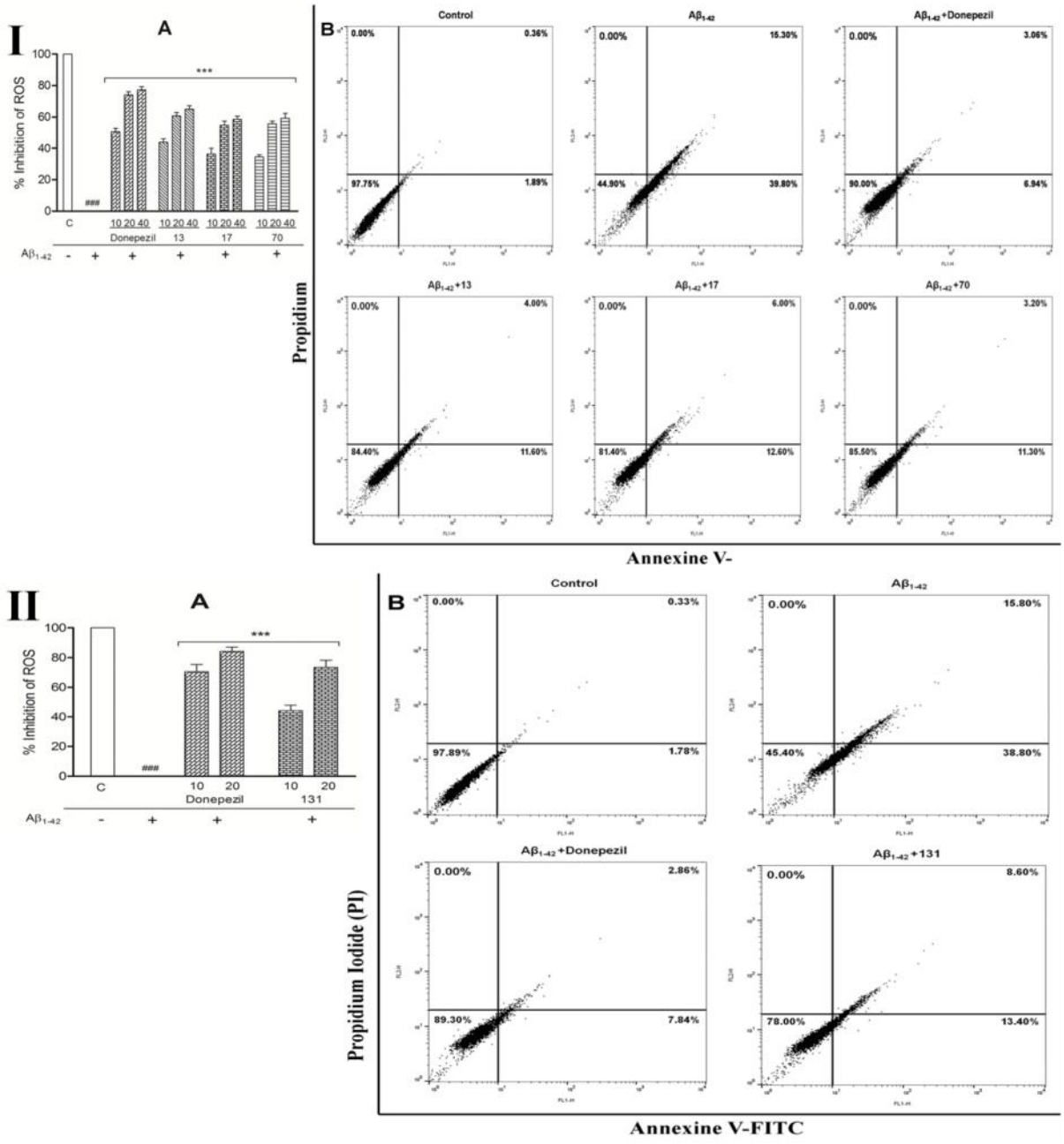

Fig. 6: *In vitro* ROS scavenging and antiapoptotic effects of test compounds (**13, 17, 70** and **131)** against $A\beta_{1-42}$-induced toxicity of hippocampal neurons. (I-A and II-A) $A\beta_{1-42}$ (10 µM) significantly increased ROS generation as compared to the control cells which was significantly reduced by **13, 17** and **70** (10-40 µM) (I-A) and **131** (10 and 20 µM) (II-A). (I-B and II-B) In another set of experiments, the test compounds (**13, 17, 70** and **131**) attenuated apoptosis rate in primary rat hippocampal neurons as assessed by flow cytometry using Annexin V-FITC and PI staining. Cells in the lower left quadrant are viable (Annexine V-FITC-/PI-). Cells in the lower right quadrant are early apoptotic (Annexine V-FITC+/PI-) and those in the upper right quadrant are late apoptotic or nacrotic (Annexine V-FITC+/PI+). Treatment with $A\beta_{1-42}$ (10 µM) significantly increased percentage of early apoptotic cells which was attenuated by pre-treatment with **13, 17, 70** (I-B) and **131 (**II-B) **(**20 µM) similar to donepezil. Data are expressed as mean ± SEM. $^{###}p<0.001$ *vs.* control cells. *** $p<0.001$, ** $p<0.01$ *vs.* $A\beta_{1-42}$-treated control cells. C=control cells.

4.12. Beneficial effects of the test compounds in Aβ1-42-induced Alzheimer's rat model

4.12.1. Test compounds (13, 17, 70 and 131) improved "spontaneous alteration" behaviour in Y maze test

Protection against the damage caused by ICV injection of $A\beta_{1-42}$ in the hippocampal region of rat brain is a promising model to evaluate the neuroprotective potential of a drug

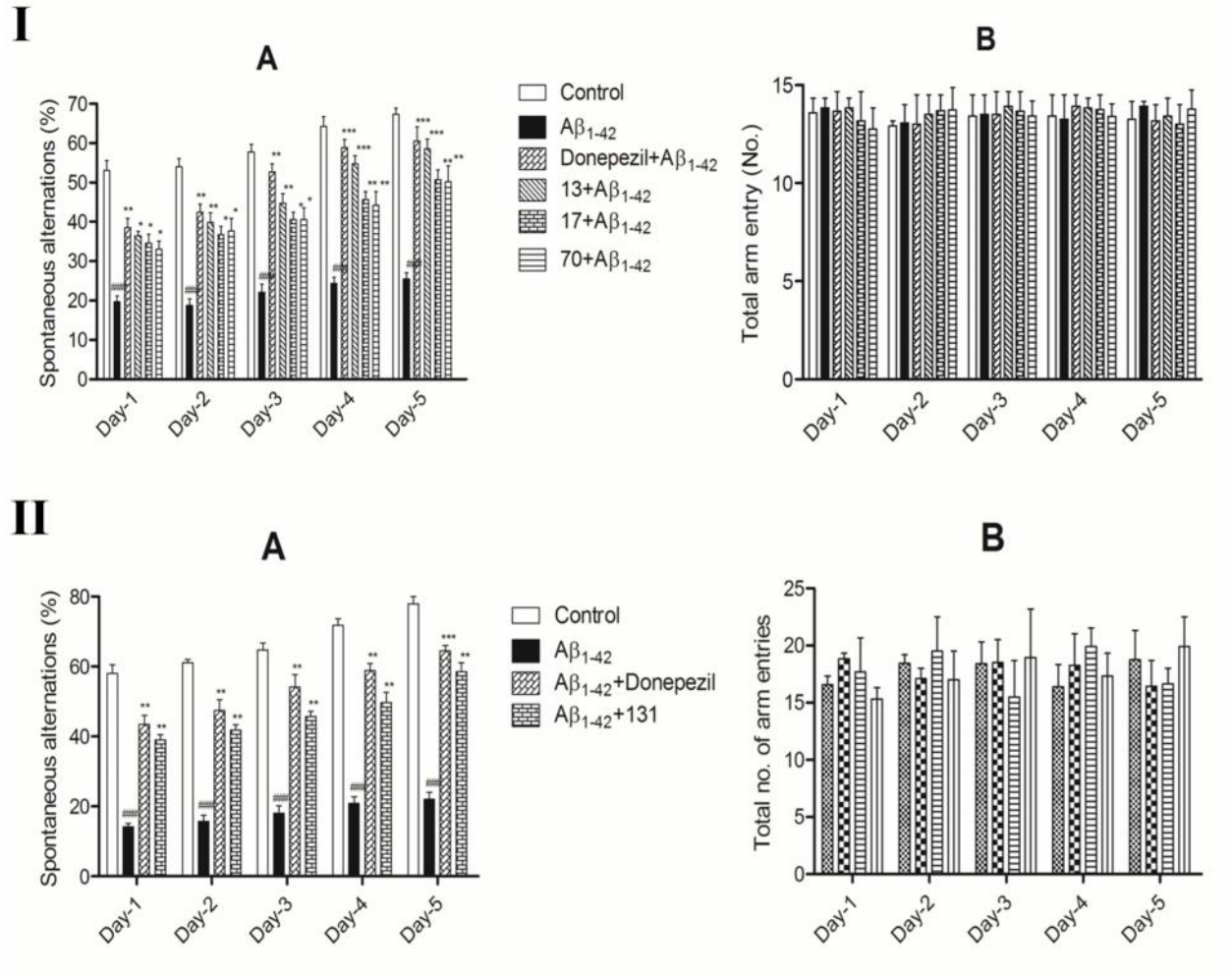

Fig.7: Test compounds (**13, 17, 70** and **131**) restored immediate working memory impairment induced by ICV injection of $A\beta_{1-42}$ in hippocampal region of rat brains as observed in Y maze test. The Y maze test was performed during the last five days of treatment period. Donepezil (5 mg/kg, p.o.), **13, 17, 70** (10 mg/kg, p.o.) and **131** (5 mg/kg, p.o.) were administered to the rats 1 hr prior to the Y-maze task of 5 min duration. (I-A and II-A) $A\beta_{1-42}$ treatment reduced "spontaneous alteration" behaviour which was significantly improved by **13, 17, 70** and **131**. (I-B and II-B) Mean number of the arm entries remained similar across all animal groups suggesting that locomotor activity was not altered with $A\beta_{1-42}$. Data are expressed as mean ± SEM (n=6). $^{###}p<0.001$ *vs.* vehicle-treated control group. *** $p<0.001$, ** $p<0.01$, * $p<0.05$ *vs.* $A\beta_{1-42}$-treated control group.

candidate in AD-like condition [59, 87]. Y maze test was performed to determine the effect of compounds (**13**, **17**, **70** and **131**) on "spontaneous alteration" behaviour which is an indicator of immediate working memory. The percentage of "spontaneous alterations" in the $A\beta_{1-42}$-treated control rats got significantly reduced throughout the training session as compared to the vehicle-treated control animals (Fig. 7-I-A, $p<0.001$ and Fig. 7-II-A, $p<0.001$). $A\beta_{1-42}$ attenuated "spontaneous alterations" were significantly increased by pre-treatment of the animals with **13**, **17**, **70** (10 mg/kg, p.o.) (Fig. 7-I-A, $p<0.01$) and **131** (5 mg/kg, p.o.) (Fig. 7-II-A, $p<0.01$). However, the observed mean number of arm entries was similar across all animal groups suggesting that general locomotor activity was not altered by $A\beta_{1-42}$ treatment (Fig. 7-I-B and Fig. 7-II-B). In brief, treatment with the test compounds (**13**, **17**, **70** and **131**) significantly increased "spontaneous alterations" in $A\beta_{1-42}$-treated rats suggesting their ability to improve hippocampal dependant immediate working memory.

4.12.2. Test compounds (13, 17, 70 and 131) reduced $A\beta_{1-42}$, *p*-tau, cleaved caspase-3 and cleaved PARP burden

According to the earlier reports, AD is mainly characterised by the presence of elevated levels of two key pathological biomarkers, i.e. $A\beta_{1-42}$ and *p*-tau [88]. In the current study, levels of these proteins were determined using Western blot analysis in the $A\beta_{1-42}$ Alzheimer's rat model. Significant elevation in $A\beta_{1-42}$ and *p*-tau protein levels was observed in the hippocampal region of $A\beta_{1-42}$-treated control animal brains (Fig. 8-I-A and Fig. 8-II-A). **13, 17, 70** (Fig. 8-I-A) and **131** (Fig. 8-II-A) treatment significantly reduced the levels of $A\beta_{1-42}$ and *p*-tau proteins in the hippocampal region of $A\beta_{1-42}$-treated Alzheimer's rat brain. Densitometric analysis revealed significant increase in the levels of $A\beta_{1-42}$ (Fig. 8-I-B, $p<0.001$ and Fig. 8-II-B, $p<0.001$) and *p*-tau (Fig. 8-I-C, $p<0.05$ and Fig. 8-II-C, $p<0.01$) proteins in $A\beta_{1-42}$-treated control animal brains. However, levels of $A\beta_{1-42}$ (Fig. 8-I-B, $p<0.001$ and Fig. 8-II-B, $p<0.01$) and *p*-tau (Fig. 8-I-C, $p<0.01$ and Fig. 8-II-C, $p<0.05$) proteins were significantly reduced by **13, 17, 70** (10 mg/kg, p.o.) and **131** (5 mg/kg, p.o.). Thus the ability of **13, 17, 70** and **131** to normalize the key proteins in AD rats revealed anti-AD potential of the test compounds. In addition, antiapoptotic potential of **13, 17, 70** and **131** was evaluated by determining the levels of cleaved caspase-3 (active) and cleaved PARP proteins in the hippocampal region of $A\beta_{1-42}$-treated rat brains. The levels of cleaved caspase-3 and cleaved PARP were increased in the $A\beta_{1-42}$-treated control rat brains as

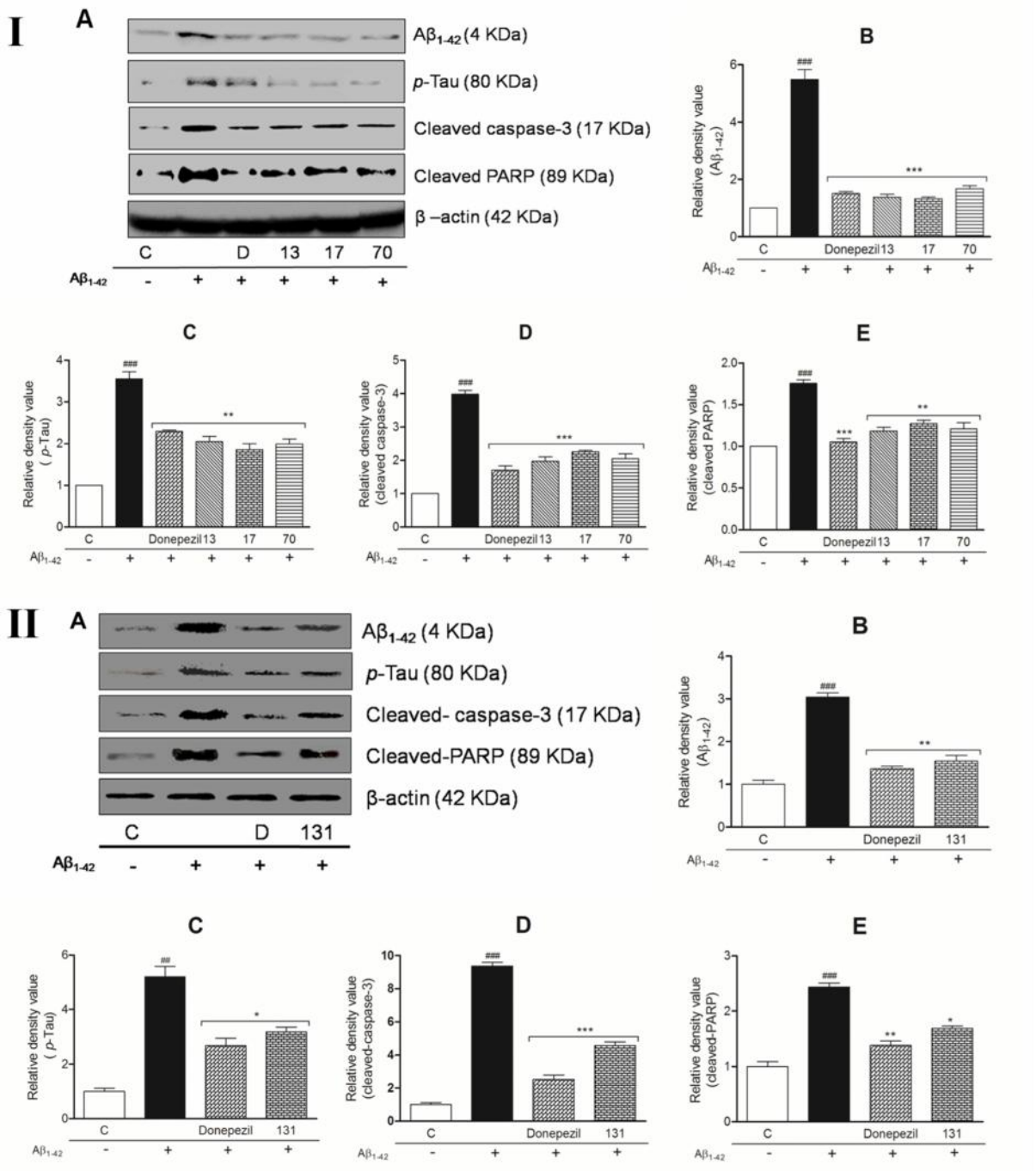

Fig. 8: Test compounds (**13, 17, 70** and **131**) attenuated $A\beta_{1-42}$, *p*-tau, cleaved caspase-3 and cleaved PARP burden *in vivo*. (I & II-A) The expression of $A\beta_{1-42}$, *p*-tau, cleaved caspase-3 and cleaved PARP proteins in the hippocampal region of $A\beta_{1-42}$-induced Alzheimer's rat brain from different treatment groups was determined by Western blot analysis. Densitometry analysis revealed increased expression of $A\beta_{1-42}$ (I & II-B), *p*-tau (I & II-C), cleaved caspase-3 (I & II-D) and cleaved PARP (I & II-E) in $A\beta_{1-42}$-treated animals which was significantly reduced by **13, 17, 70** (10 mg/kg, p.o.) and **131** (5 mg/kg, p.o.) similar to donepezil. Data are expressed as mean ± SEM (n=4). $^{###}p<0.001$ *vs.* vehicle-treated control group. *** $p<0.001$, ** $p<0.01$ *vs.* $A\beta_{1-42}$-treated control group. C=vehicle-treated control group. D=donepezil+$A\beta_{1-42}$ treatment group.

compared to the vehicle-treated control animals (Fig. 8-I-A and Fig. 8-II-A). Densitometric analysis revealed significant decrease in cleaved caspase-3 (Fig. 8-I-D, $p<0.001$ and Fig. 8-II-D, $p<0.001$) and cleaved PARP (Fig. 8-I-E, $p<0.01$ and Fig. 8-II-E, $p<0.05$) protein levels in $A\beta_{1-42}$-treated rat brains after **13**, **17**, **70** and **131** treatment. These results further revealed antiapoptotic potential of the test compounds.

4.12.3. Test compounds (13, 17 and 70) activated the canonical Wnt/β-catenin pathway

There are evidences which demonstrated alterations in the two key components of the canonical Wnt signalling pathway i.e. GSK-3 and β-catenin in AD rat brain [89, 90]. $A\beta_{1-42}$ mediated neurotoxicity is associated with reduced levels of *p*-GSK-3α and *p*-GSK-3β, and loss of the cytoplasmic β-catenin in the hippocampal neurons [87, 91]. Reports also showed reduced levels of β-catenin target gene-neuroD1 in different rodent models of AD [92, 93]. **13, 17** and **70** (10 mg/kg, p.o.) treatment significantly elevated the levels of *p*-GSK-3α and *p*-GSK-3β proteins abrogated by $A\beta_{1-42}$ toxicity (Fig. 9A). Densitometric analysis revealed that $A\beta_{1-42}$ toxicity significantly reduced the levels of *p*-GSK-3α (Fig. 9B, $p<0.01$) and *p*-GSK-3β (Fig. 9C, $p<0.01$) proteins. However, **13, 17** and **70** treatment significantly reversed this attenuation (Fig. 9B, $p<0.05$ and Fig. 9C, $p<0.001$). Subsequently, the β-catenin and neuroD1 levels were also analysed. Immunoblot analysis revealed that **13, 17** and **70** treatment significantly increased the levels of β-catenin and neuroD1 in the hippocampal region of rat brain as compared to the $A\beta_{1-42}$-treated control group (Fig. 9A). Quantification of protein levels showed significant reduction in β-catenin (Fig. 9D, $p<0.01$) and neuroD1 (Fig. 9E, $p<0.01$) levels following $A\beta_{1-42}$ treatment which were significantly increased by **13, 17** and **70**. The findings pointed towards the beneficial role of **13, 17** and **70** against $A\beta_{1-42}$-induced Alzheimer's-like condition in rat through activation of canonical Wnt/β-catenin pathway.

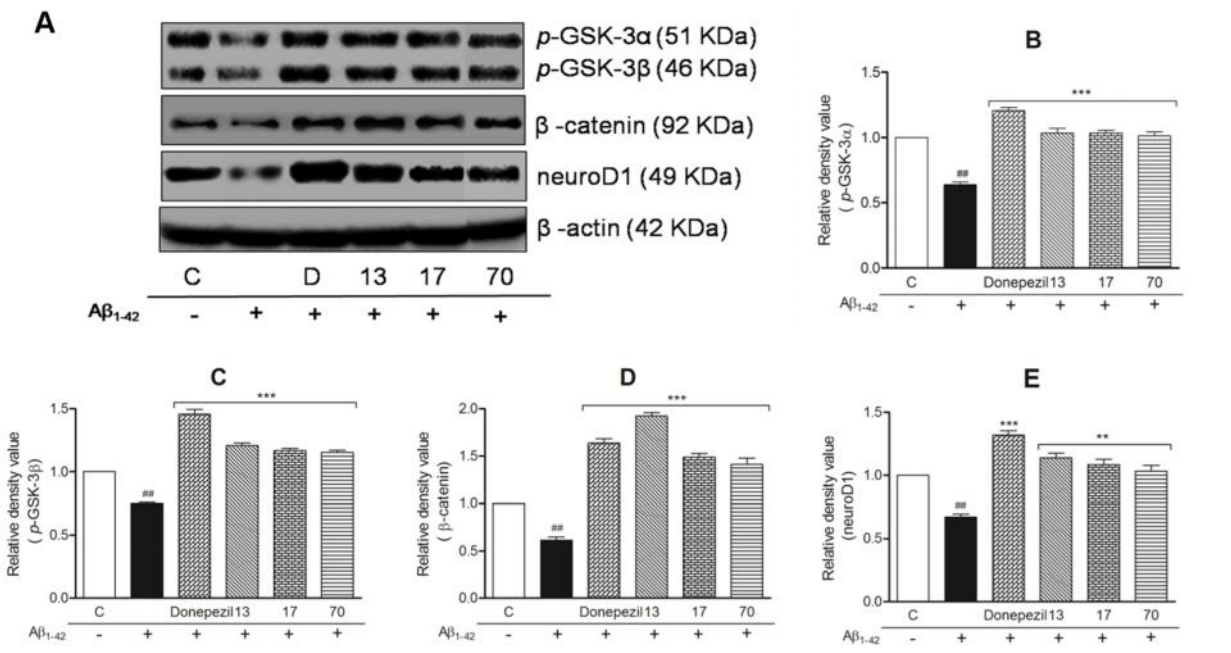

Fig. 9: Test compounds (**13, 17** and **70**) activated the canonical Wnt/β-catenin pathway *in vivo*. (A) Expression of the key components of Wnt signalling pathway (*p*-GSK-3, β-catenin and neuroD1) was determined by Western blot analysis (B-E). Densitometric analysis revealed that **13, 17** and **70** (10 mg/kg, p.o.) up-regulated *p*-GSK-3α/3β, β-catenin and neuroD1levels in $A\beta_{1-42}$-induced Alzheimer's rat brain similar to donepezil (5 mg/kg, p.o.). Data are expressed as mean ± SEM (n=6). $^{\#\#}$ $p<0.01$ *vs.* vehicle-treated control group. *** $p<0.001$, ** $p<0.01$ *vs.* $A\beta_{1-42}$-treated control group. C=vehicle-treated control group. D=donepezil+$A\beta_{1-42}$ treatment group (A).

4.13. Test compound (131) was found safe in acute toxicity study

For the development of a compound as a new drug, acute toxicity profile of the compound is considered to be an important criterion. The most promising anti-Alzheimer's candidates arising out of the current study are compounds **13, 17, 70** and **131**. To investigate the safety profile, acute toxicity of compounds **(13, 17, 70** and **131)** was determined in male Swiss Albino mice at doses of 0, 677, 1333 and 2000 mg/kg (n = 5 per group) by oral administration. Mice were regularly observed for 14 days after treatment. After the observation period of 14 days, all the animals remained alive and appeared healthy in terms of fur sleekness, water and food consumption and body weight. On the 15th day, all the animals were sacrificed for macroscopic examination to evaluate possible damage to the heart, liver and kidneys. The results indicated that mice treated with test compounds **(13, 17, 70** and **131)** did not show any acute toxicity or mortality immediately or during the post-treatment period. Therefore, compounds **(13, 17, 70** and **131)** were found to be non-toxic and well tolerated at doses up to 2000 mg/kg.

4.14. Test compound (131) exhibited good Pharmacokinetic profile

The preliminary pharmacokinetic analysis of the most promising test compound **(131)** was performed in male Wistar rats. Animals were administered with compound **(131)** at a dose of 5 mg/kg orally followed by blood sampling at the indicated time points (see experimental section). Pharmacokinetic parameters summarized in Table 4 were calculated from the conc-

Table 4. Pharmacokinetic parameters of compound (**131**) after single oral dose (5 mg/kg) administration.

Pharmacokinetic parameters	Values
C_{max} (ng/ml)	21.20±1.99
t_{max} (hr)	3.66±0.57
$AUC_{(0-8)}$ (ng.hr/ml)	587.16±62.09
$t_{1/2}$ (hr)	19.42±4.69

Date are expressed as mean±SD (n=4).

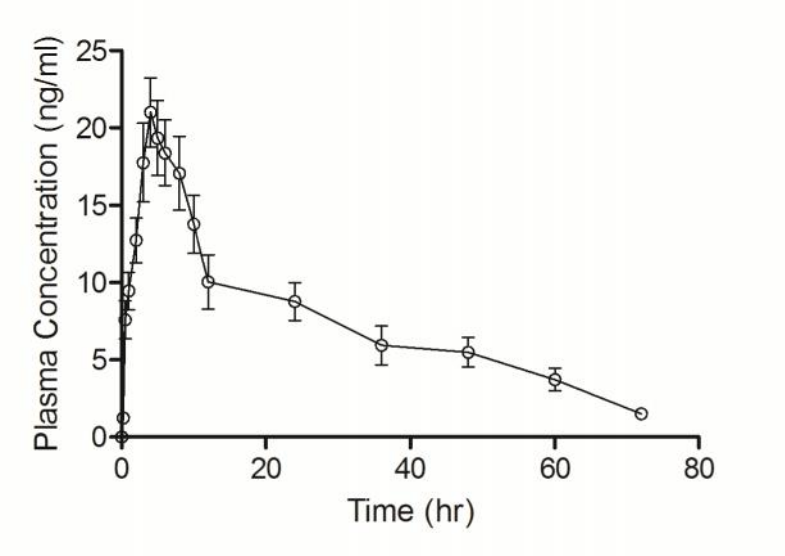

Fig. 10: Mean plasma concentration vs. time curve of single oral dose (5 mg/kg) of compound **(131)** in rats. Error bars represents the standard deviation of the mean (n=4).

entration-time profile using noncompartmental extravascular analysis. The mean concentration time course of compound (**131**) after single oral administration is shown in Figure 10. An asymmetric curve of the compound (**131**) deviating from the Guaussian distribution curve suggested a prolonged elimination phase as compared to the absorption phase. Peak plasma

concentration (C_{max}) of the compound (**131**) was achieved approximately at 3.66±0.57 hr after single dose oral administration. In addition, the terminal elimination half-life ($t_{1/2}$) was observed to be 19.42±4.69 hr. Overall, the results suggested that the compound (**131**) exhibited good oral absorption and was eliminated at a rate which is moderate as compared to the absorption phase. However, further *in vivo* human clinical trials are required to prove actual usability of the developed test compound (**131**).

4. RESULTS

4.1. Effect of the test compounds on 5-HT$_{2A}$ and 5-HT$_{2B}$ receptors as assessed using rat thoracic aorta and rat fundus preparations *in vitro*

All of the synthesized compounds were evaluated *in vitro* for 5-HT$_{2A}$ and 5-HT$_{2B}$ sensitivity on rat thoracic aorta and rat fundus preparations to establish the binding affinities of the compounds for 5-HT$_{2A}$ and 5-HT$_{2B}$ receptors respectively (Table 1). All the test compounds were initially evaluated at 2×10^{-5} M concentration in both the *in vitro* experiments to determine their 5-HT$_{2A}$/5-HT$_{2B}$ agonist or antagonist activity. In case a compound was found to be agonist or antagonist in either preparation, the receptor selectivity was evidenced by pD_2 or pA_2 values respectively. pD_2 value is the negative logarithm of the EC_{50} of an agonist which indicates its potency while pA_2 depicts the negative logarithm of the molar concentration of the antagonist that makes it necessary to double the concentration of the agonist needed to produce the original response. None of the compounds showed special affinity for 5-HT$_{2A}$ receptor on rat thoracic aorta preparation. However, compounds (**10, 12-16, 19-21, 27-29, 35** and **37**) were found to be 5-HT$_{2B}$ receptor agonists which was evident by their pD_2 values while compounds (**9** and **34**) were found to possess 5-HT$_{2B}$ receptor antagonistic property showing pA_2 values greater than 6 (Table 1)**.** Only those compounds which did not show 5-HT$_{2A}$ and 5-HT$_{2B}$ affinities *in vitro* were selected for further *in vivo* 5-HT$_{2C}$ receptor selectivity study.

Table 1: *In vitro* assessment of the test compounds for 5-HT$_{2A}$ and 5-HT$_{2B}$ receptors' actions using isolated rat thoracic aorta and rat fundus preparations respectively.

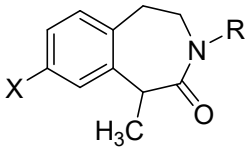

Comp.	X	R	5-HT$_{2A}$		5-HT$_{2B}$	
			Agonist (pD_2 value)	**Antagonist** (pA_2 value)	**Agonist** (pD_2 value)	**Antagonist** (pA_2 value)
1	H	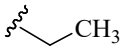	*	*	*	*
2	H	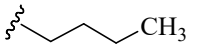	*	*	*	*
3	H	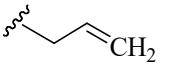	*	*	*	*

4	H	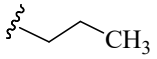	*	*	*	*
5	H	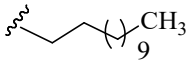	*	*	*	*
6	H	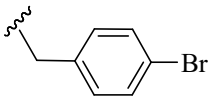	*	*	*	*
7	H	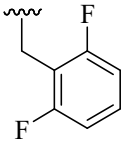	*	*	*	*
8	H	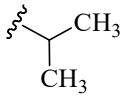	*	*	*	*
9	H	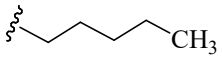	*	*	-	6.95±0.25
10	H	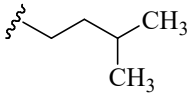	*	*	8.46±0.39	-
11	H	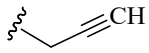	*	*	*	*
12	H	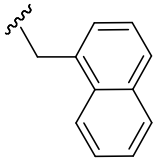	*	*	7.21±0.24	-
13	H	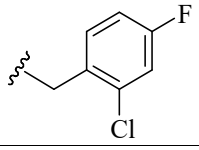	*	*	7.76±0.22	-
14	H	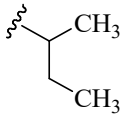	*	*	6.73±0.41	-
15	H	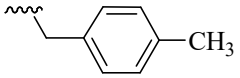	*	*	7.84±0.34	-
16	H	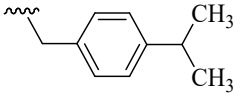	*	*	8.39±0.28	-
17	H	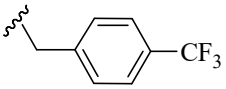	*	*	*	*
18	H	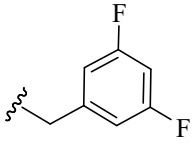	*	*	*	*

19	H	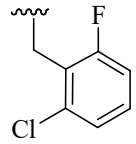	*	*	7.03±0.10	-
20	H	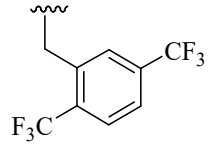	*	*	6.48±0.29	-
21	H	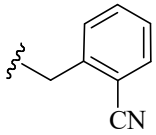	*	*	6.99±0.36	-
22	H	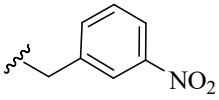	*	*	*	*
23	H	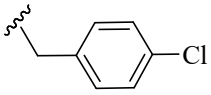	*	*	*	*
24	H	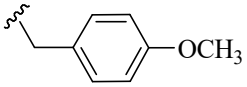	*	*	*	*
25	H	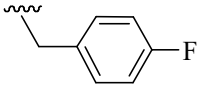	*	*	*	*
26	H	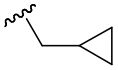	*	*	*	*
27	H	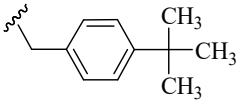	*	*	6.81±0.13	-
28	H	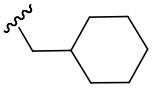	*	*	8.47±0.19	-
29	H	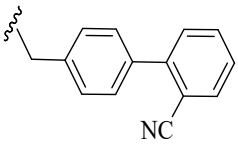	*	*	7.70±0.33	-
30	H	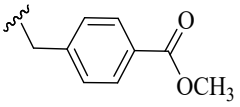	*	*	*	*
31	H	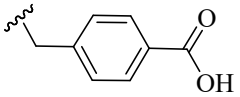	*	*	*	*

32	Cl	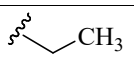	*	*	*	*
33	Cl	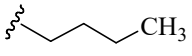	*	*	*	*
34	Cl	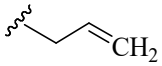	*	*	-	8.38±0.19
35	Cl	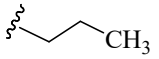	*	*	8.59±0.20	-
36	Cl	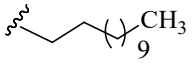	*	*	*	*
37	Cl	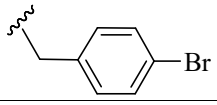	*	*	7.44±0.14	-
38	Cl	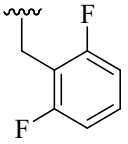	*	*	*	*
39	H	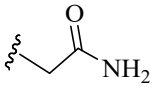	*	*	*	*

Results are expressed as mean±SEM *compounds were found inactive at 2 × 10^{-5} M concentration. Those compounds which showed activity at this concentration were later proceeded for determining their pD_2/pA_2values.

Thus, compounds (**1-8, 11, 17, 18, 22-26, 30-33, 36, 38** and **39**) were selected for 5-HT$_{2C}$ receptor affinity studies since all these compounds were found to be inactive in the *in vitro* studies on both the tissues, suggesting their lack of affinity for the 5-HT$_{2A}$ and 5-HT$_{2B}$ receptors. Hence, these compounds could be either selective 5-HT$_{2C}$ receptor modulators or inactives.

4.2. Test compounds exhibited depressogenic effects in despair swim test

There are evidences demonstrating that overactivation of 5-HT$_{2C}$ receptor may develop depressive and anxiety symptoms in a certain population of patients. 5-HT mediated activation of 5-HT$_{2C}$ receptor is responsible for the development of many of the negative side effects associated with selective serotonin re-uptake inhibitor (SSRI) medications [60]. Despair swim test model was adopted for the assessment of depression. Rajkumar *et al* [39] have demonstrated the ability of *m*-CPP to induce depressogenic behaviour in rodents due to its 5-HT$_{2C}$ receptor agonist activity. Compounds (**1-8, 11, 17, 18, 22-26, 30-33, 36, 38** and **39**) were screened for the despair swim test. As expected for a positive control, *m*-CPP showed significant increase in the immobility time indicative of the depressive effect (Fig 1, $p<0.001$). Compounds (**1, 6-8, 18, 24,** and **30**) showed significant increase in the immobility time as compared to the saline control (Fig 1, $p<0.001$) which was possibly due to their 5-HT$_{2C}$ receptor agonist activity. These compounds

showed 5-HT$_{2C}$ agonist mediated depressogenic response similar to the standard *m-CCP*. The rest of compounds did not show a significant effect in this test suggesting their inactivity for 5-HT$_{2C}$ receptor. Compounds (**1, 6-8, 18, 24,** and **30**) demonstrating activity in this test were proceeded for further evaluation.

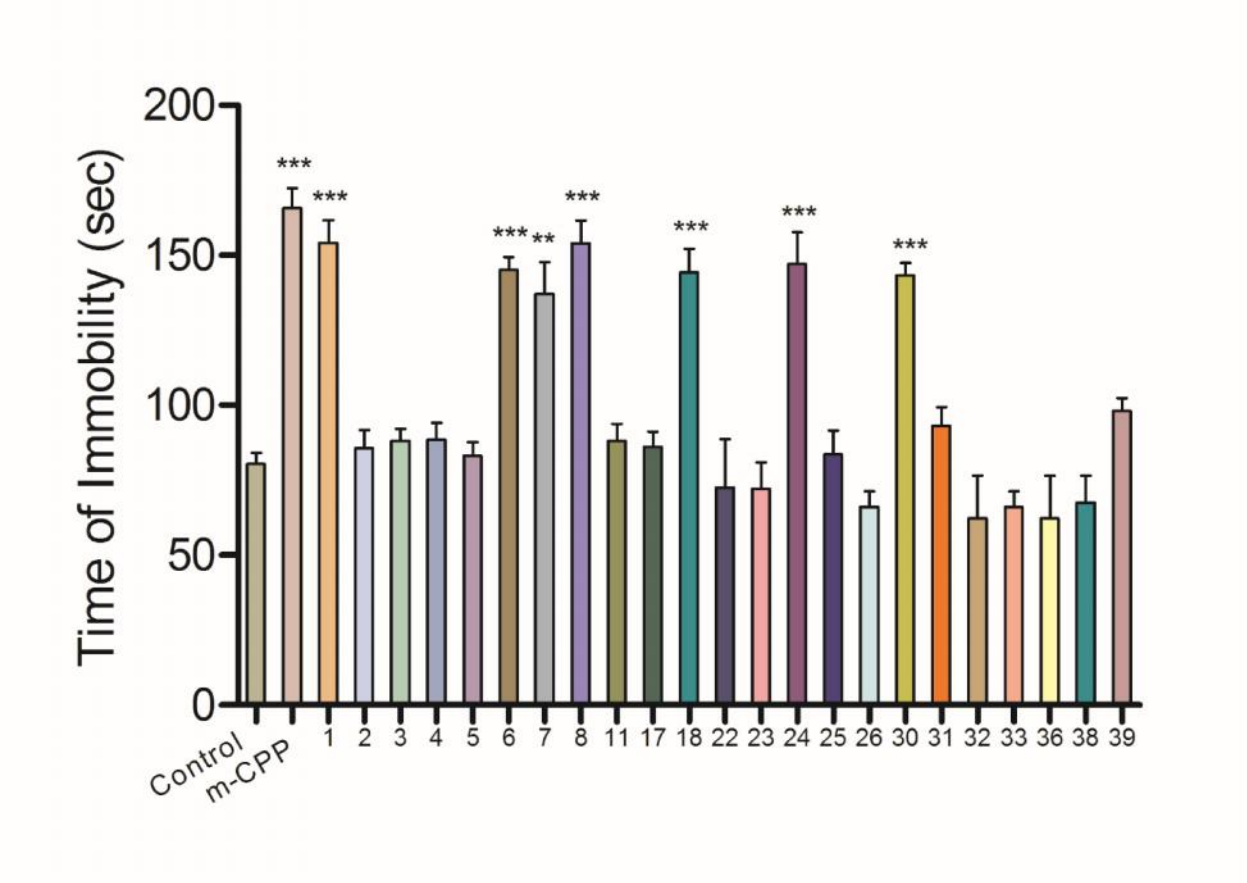

Fig 1: Effect of *m*-CPP (2 mg/kg, p.o.) and the test compounds (10 mg/kg, p.o.) in despair swim test. Values represent the immobility time. Data are expressed as mean ± SEM. $^{***}p<0.001$, $^{**}P<0.01$ indicate level of significance *vs* vehicle-treated control group (N=6).

4.3. Test compounds showed anxiogenic affects in elevated plus maze test

Anxiety is regulated mainly by the amygdala region of the brain with high levels of 5-HT$_{2C}$ receptor expression. Previous report [61] demonstrated that activation of amygdale by some 5-HT$_{2C}$ receptor agonist is strongly associated with the anxiety state. Thus antagonism of 5-HT$_{2C}$ receptor might be beneficial for the treatment of anxiety [52, 62]. Thus, the chosen compounds (**1, 6-8, 18, 24,** and **30**) were evaluated on the anxiety model. Elevated plus maze test was adopted to assess the anxiety-like condition. In the elevated plus maze test, *m*-CPP showed

significant anxiogenic response in mice (Fig 2A, p<0.001). Compounds (**1, 6-8, 18, 24,** and **30**) showed significant decrease in the exploration (Fig. 2A, p<0.001) as well as time spent (Fig. 2B, p<0.001) in the open arm, demonstrating their anxiogenic effect like the one showed by *m*-CPP, that substantiated their 5-HT$_{2C}$ receptor selectivity.

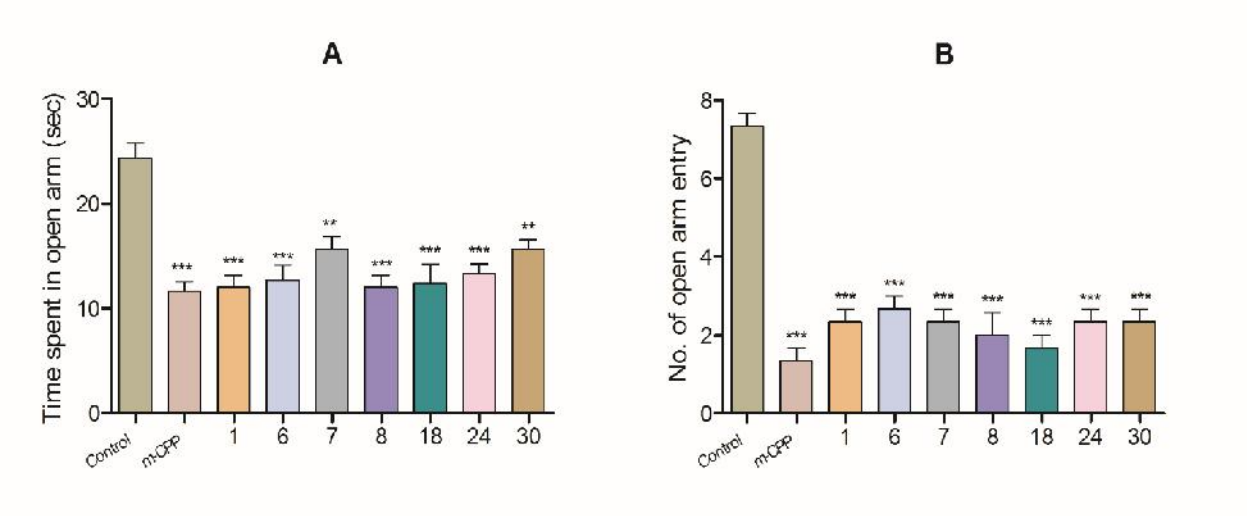

Fig 2: Effect of *m*-CPP (2 mg/kg, p.o.) and the test compounds (10 mg/kg, p.o.) on the elevated plus maze test. (A) Time spent in open arm and (B) number of open arm entries are represented. Data are expressed as mean ± SEM. $^{***}p$<0.001, $^{**}P$<0.01 indicate level of significance *vs* vehicle-treated control group (N=6).

4.4. Test compounds showed hypophagic effects

Tecott *et.al* [63] demonstrated that 5-HT$_{2C}$ receptor knockout mice developed obesity and remained hyperphagic throughout their life. Pro-opiomelanocortin (POMC) neurons express predominantly 5-HT$_{2C}$ receptor mRNA wherein 5-HT$_{2C}$ agonism leads to increased production of α-melanocyte stimulating hormone (α-MSH) which ultimately enhances MC4 receptor signalling [63-66] resulting in reduced food intake. 5-HT$_{2C}$ receptor agonists also increase satiety resulting in reduced food intake [65, 67]. Compounds (**1, 6-8, 18, 24,** and **30**) were assessed for the 5-HT$_{2C}$ receptor mediated hypophagic response. In accord with the above cited findings, compounds (**1, 6-8, 18, 24,** and **30**) significantly decreased the amount of food intake (Fig 3A, p<0.001). Their hypophagic effects were significantly reversed by pre-treatment of the animals with RS-102221, a selective 5-HT$_{2C}$ receptor antagonist, (Fig 3A, p<0.001) confirming their 5-HT$_{2C}$ receptor agonistic activity. *m*-CPP also showed significant hypophagic effect (Fig 3A, p<0.001) in this model.

4.5. Test compounds induced penile erection

Compounds (**1, 6-8, 18, 24,** and **30**) were also evaluated for the 5-HT$_{2C}$ receptor mediated penile erection in absence and presence of RS-102221, a 5-HT$_{2C}$ antagonist. *m*-CPP induces penile erection, excessive grooming and increased levels of oxytocin, prolactin and corticosterone in rats. Paraventricular nucleus is believed to control sexual behaviour and neuroendocrine responses [68]. *m*-CPP significantly induced penile erection and engorged penis (Fig 3B, $p<0.001$) in the test. Compounds (**1, 6-8, 18, 24,** and **30**) also showed similar effects (Fig 3B, $p<0.001$) which were significantly suppressed by pre-treatment of the animals with RS-102221 (Fig 3B, $p<0.001$). These results substantiated selective antagonism of the test compounds towards 5-HT$_{2C}$ receptors.

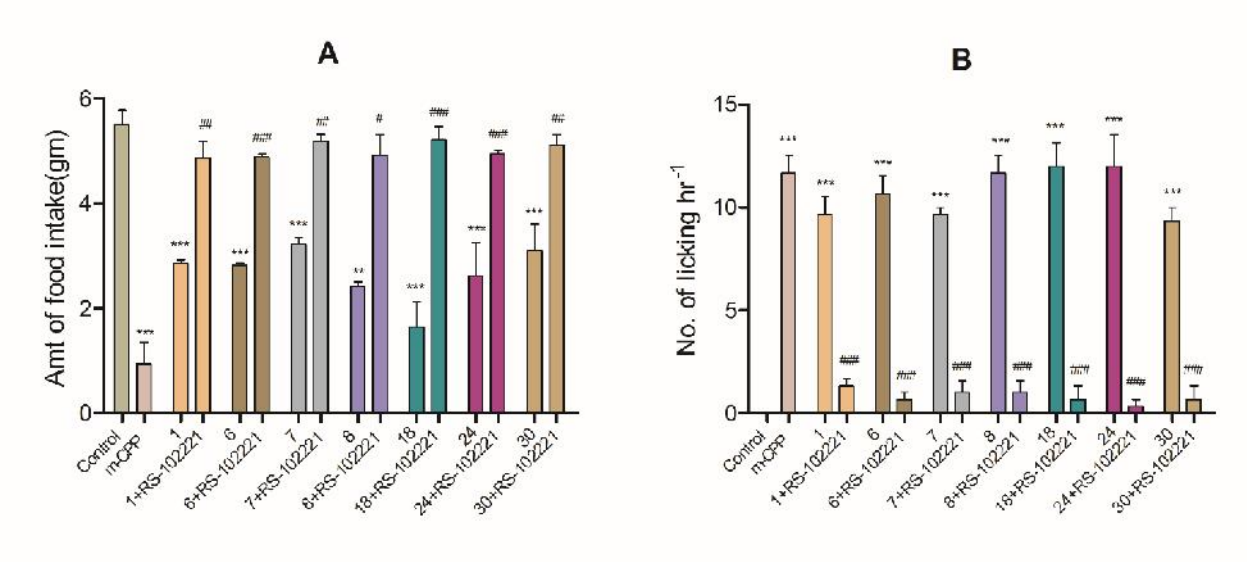

Fig 3: Effect of *m*-CPP (2 mg/kg, p.o.) and the test compounds (10 mg/kg, p.o.) on hypophagic and penile erection models. (A) Amount of food intake upon test compound administration alone and with pretreatment of RS-102221 (2 mg/kg, i.p.). (B) Number of penile lickings upon test compound administration alone and with pretreatment of RS-102221 (2 mg/kg, i.p.). Data are expressed as mean ± SEM. $^{***}p<0.001$, $^{**}P<0.01$ indicate level of significance *vs* vehicle-treated control group (N=6). $^{###}p<0.001$, $^{##}p<0.01$, $^{##}p<0.05$ indicates significant difference from respective test compound-treated group (only compound) (N=6).

4.6. Test compounds reduced DA and 5-HT levels in the rat brain

Previous studies [37, 38, 56, 69] revealed that 5-HT$_{2C}$ receptors have influence on the firing of monoamine neurotransmitters. 5-HT$_{2C}$ agonists negatively regulate firing of dopamine (DA) and 5-HT neurons in the dorsal raphe nucleus (DRN) and ventral tegmental area (VTA), respectively [54, 55]. There was observed a significant decrease in the brain concentrations of

DA (Fig 4A, p<0.001) and 5-HT (Fig 4B, p<0.001) in the animals exposed to the compounds (**1, 6-8, 18, 24,** and **30**). Pre-treatment of the animals with RS-102221 at a dose of 2 mg/kg, p.o. significantly reversed the decreased levels of DA (Fig 4A, p<0.001) and 5-HT (Fig 4A, p<0.001) which further supported the above described finding. This study revealed that the test compounds, which were found to be 5-HT$_{2C}$ agonists in different *in vivo* models as described above, significantly decreased the DA and 5-HT levels in the brain similar to those caused by *m*-CPP.

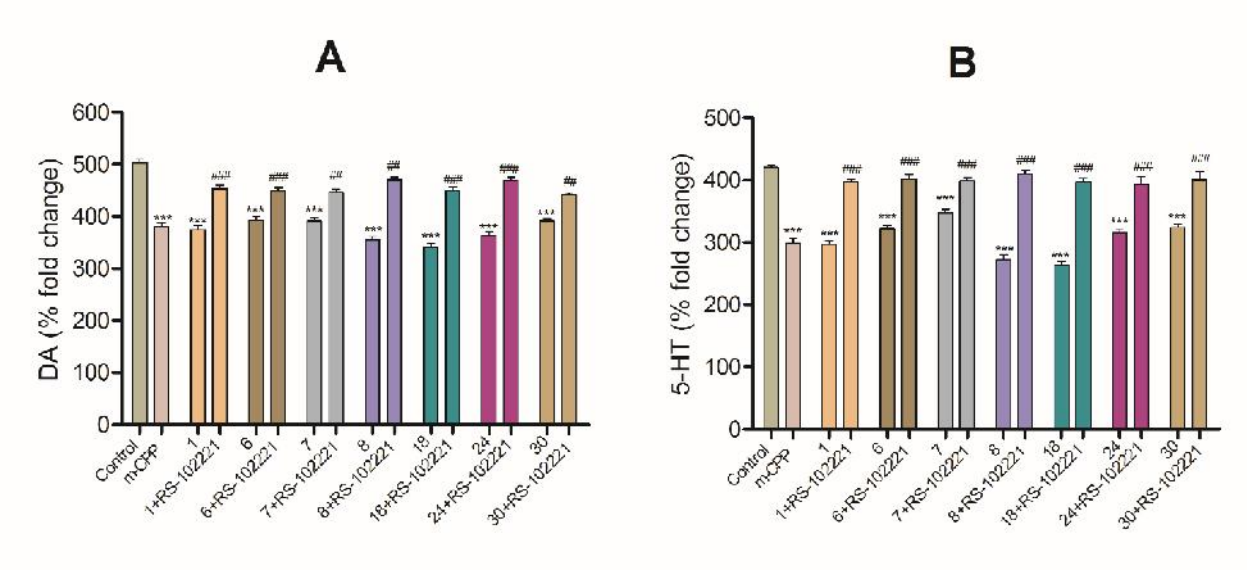

Fig 4: Effect of *m-CPP* (2 mg/kg, p.o.) and the test compounds (10 mg/kg, p.o.) on DA and 5-HT levels in the rat brain. Values represent the % fold change of in (A) DA and (B) 5-HT levels in the rat brain after treatment of test compounds alone and in presence of RS-102221. Data are expressed as mean ± SEM. $^{***}p$<0.001 indicates level of significance *vs* vehicle-treated control group (N=6). $^{###}p$<0.001, $^{##}p$<0.01 indicates significant difference from respective test compound treated group (only compound) (N=6).

Thus, these results have demonstrated that the evaluated compounds (**1, 6-8, 18, 24,** and **30**) are selective 5-HT$_{2C}$ receptor agonists.

4. RESULTS

The newly synthesized benzazepine derivatives were assessed as potential NMDAR antagonists using cell-based MTT assay. Two of the test compounds (**3** and **10**) identified as potent NMDAR antagonists from the *in vitro* experiments (4.1), were further evaluated for $A\beta_{1-42}$ aggregation inhibitory, neuroprotective, free radical scavenging, antioxidant and antiapoptotic activities in different *in vitro* and *in vivo* experiments.

4.1. Test compounds (3 and 10) protected SH-SY5Y cells against NMDA-induced excitotoxicity

Neuroprotective potential due to NMDAR antagonism of the synthesized benzazepine derivatives was assessed by MTT assay. SH-SY5Y cells were given NMDA (5 mM) treatment in absence and presence of the test compounds. NMDA-treated cells showed significant excitotoxic neuronal cell death (55-60 %). All the benzazepine derivatives were evaluated at 10 μM concentration. As shown in Table 1, majority of the compounds showed protection against NMDA-induced excitotoxicity. Amongst them, compounds (**3** and **10**) showed the highest effects as evidenced by 83.55 ± 3.74 % and 90.42 ± 3.51 % neuroprotection respectively against NMDA-induced excitotoxic damage. The results demonstrated NMDAR antagonist potential of the test compounds as they efficiently attenuated NMDA-induced excitotoxicty which is solely mediated through NMDAR [51-53].

4.2. Test compounds (3 and 10) attenuated $A\beta_{1-42}$ aggregation

Aβ, a pathological hallmark of AD, imparts toxicity at least in part through overactivation of NMDAR [54]. In pathological conditions, the amyloid precursor proteins (APP) get cleaved by different secretase enzymes to form Aβ fragments which aggregate subsequently. These aggregated Aβ peptides prove very toxic and cause AD pathogenesis [55]. Thus, any ligand capable of inhibiting/attenuating the aggregation of Aβ peptides can protect the cells against excitotoxicity. In the current study, benzazepine derivatives with the most promising NMDAR antagonist activity were assessed for $A\beta_{1-42}$ aggregation inhibitory activity using ThT and CR binding assays. As shown in Table 1, the two test compounds (**3** and **10**) efficiently attenuated $A\beta_{1-42}$ aggregation in both the assays. Compounds (**3** and **10**)-mediated anti-$A\beta_{1-42}$ aggregatory

effects were evidenced by 23.80 ± 2.74 % and 34.86 ± 1.54 % inhibition respectively in ThT assay while 28.79 ± 1.33 % and 38.10 ± 1.54 % inhibition respectively in CR binding assay.

Table 1: Neuroprotive and $A\beta_{1-42}$ aggregation inhibitory effects of the synthesized benzazepine derivatives.

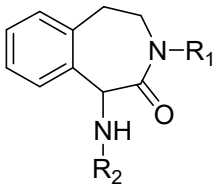

(**1-42**)

Comp.	R_1	R_2	% Neuroprotection[a] (Assessed by MTT assay)	% Inhibition of $A\beta_{1-42}$ aggregation[b] (at 10μM)	
				ThT assay	CR binding assay
1		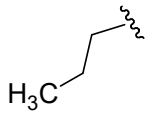	30.36 ± 1.16	nd	nd
2		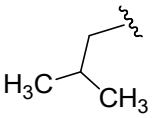	45.24 ± 4.29	nd	nd
3		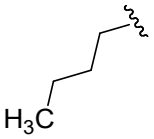	**83.55 ± 3.74**	**23.80 ± 2.74**	**28.79 ± 1.33**
4			36.90 ± 3.90	nd	nd
5		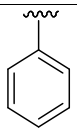	51.79 ± 2.76	nd	nd
6		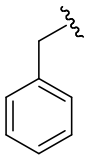	55.23 ± 2.25	nd	nd
7		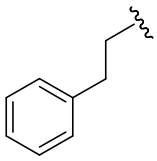	57.76 ± 3.08	nd	nd

8		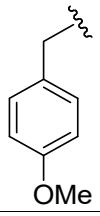	47.65 ± 6.88	nd	nd
9		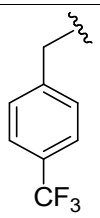	68.45 ± 1.68	nd	nd
10		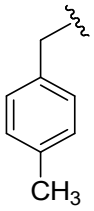	**90.42 ± 3.51**	**34.86 ± 1.54**	**38.10 ± 1.54**
11		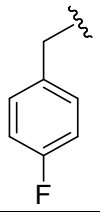	53.43 ± 3.82	nd	nd
12		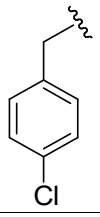	62.28 ± 1.58	nd	nd
13		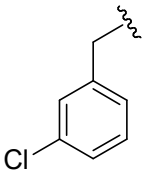	80.86 ± 3.42	nd	nd
14		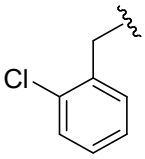	51.19 ± 4.87	nd	nd
15		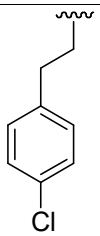	63.69 ± 4.87	nd	nd

16		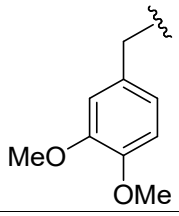	70.62 ± 2.34	nd	nd
17		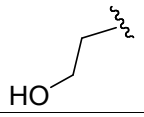	61.31 ± 3.90	nd	nd
18		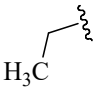	53.57 ± 1.03	nd	nd
19			47.02 ± 5.67	nd	nd
20			57.74 ± 4.64	nd	nd
21		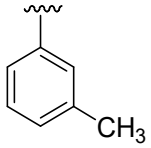	48.96 ± 2.42	nd	nd
22		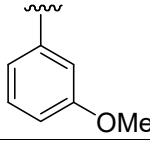	42.72 ± 2.97	nd	nd
23		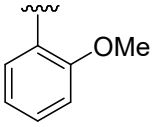	46.43 ± 3.17	nd	nd
24		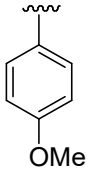	30.56 ±2.38	nd	nd
25		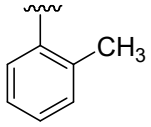	36.35 ± 2.15	nd	nd
26		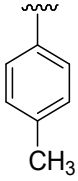	45.99 ± 3.07	nd	nd
27		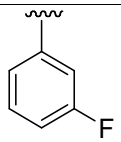	55.86 ± 3.07	nd	nd

28		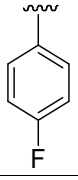	59.31 ± 3.34	nd	nd
29		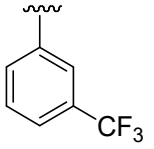	60.68 ± 2.66	nd	nd
30		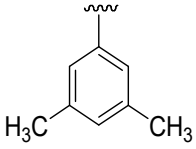	50.34 ± 2.83	nd	nd
31			65.51 ± 3.24	nd	nd
32	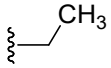	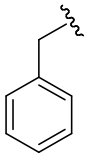	80.34 ± 2.98	nd	nd
33	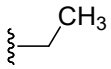	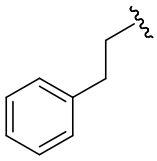	66.83 ± 3.47	nd	nd
34	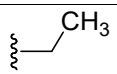	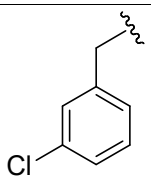	90.17 ± 2.99	nd	nd
35	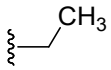	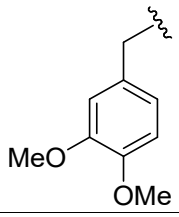	81.57 ± 3.48	nd	nd
36	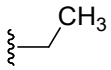	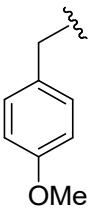	66.83 ± 3.44	nd	nd

37			54.54 ± 3.45	nd	nd
38			71.74 ± 4.47	nd	nd
39	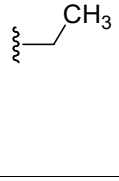		71.70 ± 3.53	nd	nd
40	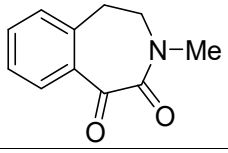		40.07 ± 4.69	nd	nd
41	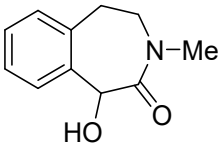		44.40 ± 3.61	nd	nd
42	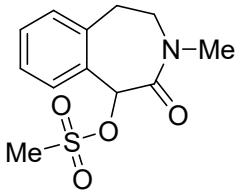		57.04 ± 1.88	nd	nd
Memantine	---		96.51 ± 2.55	43.74 ± 2.13	45.86 ± 2.67

[a]The neuroprotective effect of the test derivatives (10 μM) was assessed against NMDA-induced (5 mM) excitotoxicity in SH-SY5Y cells using MTT assay. [b]$A\beta_{1-42}$ aggregation inhibitory effect of the most potent benzazepine derivatives (10 μM) was assessed using thioflavin-T (ThT) and Congo red (CR) binding assays. Results are the mean ± SEM of at least three independent experiments. nd= Not determined.

4.3. Test compounds (3 and 10) protected primary rat hippocampal neurons against Aβ$_{1-42}$-induced excitotoxicity

Before determining the neuroprotective potential of the test compounds (**3** and **10**), their cytotoxicity was assessed on primary rat hippocampal neurons using MTT assay. They (**3** and **10**) did not cause any sign of significant cytotoxicity up to a concentration of 40 µM (Fig. 2A). Similar results were observed for the standard drug memantine (Fig. 2A).

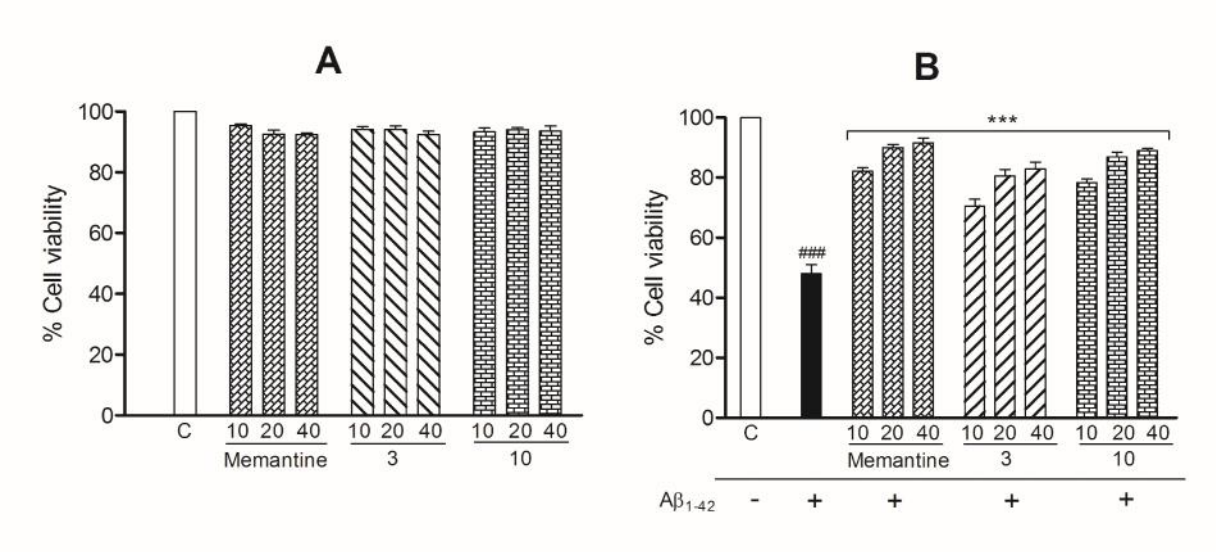

Fig. 2: *In vitro* neuroprotective potential of the test compounds (**3** and **10**) against Aβ$_{1-42}$-induced toxicity. (A) Exposure of **3** or **10** (10-40 µM) to the primary rat hippocampal neurons for 24 hr did not cause any significant toxicity. (B) Assessment of neuroprotective potential of **3** and **10** against Aβ$_{1-42}$ insult. Significant toxicity was caused by Aβ$_{1-42}$ (10 µM) in rat hippocampal neurons as compared to the control cells. Pre-treatment with **3** and **10** (10-40 µM) significantly attenuated Aβ$_{1-42}$-induced toxicity like memantine (10-40 µM). Data are expressed as mean ± SEM (n=6). $^{###}p$<0.001 *vs.* control cells. *** p<0.001 *vs.* Aβ$_{1-42}$-treated control cells. C=control cells.

The neuroprotective potential of compounds (**3** and **10**) was evaluated against Aβ$_{1-42}$-induced toxicity. Previous reports have demonstrated that direct treatment of the cultured hippocampus neurons to Aβ caused excitotoxic damage through NMDAR overactivation which was reversed by NMDAR antagonists [49, 56, 57]. In the present study, the hippocampal neuronal cells exposed to Aβ$_{1-42}$ (10 µM) showed significant toxicity as compared to the control cells (Fig. 2B, p<0.001). However, pre-treatment of the cells with **3** or **10** significantly attenuated Aβ$_{1-42}$-induced toxicity, which was evidenced by increased cell viability (Fig. 2B, p<0.001). These results revealed neuroprotective potential of the test compounds (**3** and **10**) against Aβ$_{1-42}$-induced excitotoxic damage in the primary rat hippocampal neurons.

4.4. Test compounds (3 and 10) showed ROS scavenging activity

ROS scavenging activity was performed to evaluate the antioxidant potential of the test benzazepines. Elevated level of ROS is an indication of increased oxidative stress in various pathological conditions [58]. In AD, at least a part of the Aβ-mediated neurotoxicity is attributed to the elevated oxidative stress. Aβ promotes ROS formation, protein oxidation, lipid peroxidation and ultimately neuronal cell death. Aβ-mediated oxidative damage can be attenuated by free radical scavengers such as vitamine E [18, 59, 60]. In the current study, ROS scavenging ability of the test compounds (**3** and **10**) was assessed using DCFH-DA assay. A significant rise in ROS generation was observed in the hippocampal neurons which were exposed to $A\beta_{1\text{-}42}$ (10 μM) as compared to the control cells (Fig. 3A, $p<0.001$). Pre-treatment with **3** and **10** (10-40 μM) significantly attenuated $A\beta_{1\text{-}42}$-induced elevated ROS levels (Fig. 3A, $p<0.001$). The results revealed ROS scavenging ability of the test compounds (**3** and **10**) against $A\beta_{1\text{-}42}$-induced oxidative stress. The standard drug memantine also showed similar results (10-40 μM) (Fig. 3A, $p<0.001$).

4.5. Test compounds (3 and 10) attenuated *in vitro* cleaved caspase-3 activation

It has been reported previously that exposure of Aβ to the primary rat hippocampal neurons caused NMDAR-dependant inward calcium flow leading to mitochondrial calcium overload and membrane depolarization which together caused apoptotic cell death [61, 62]. Apoptotic cell death was evaluated by quantifying apoptotic (fragmented) nuclei using Hoechst staining in different experimental sets. Supporting the previous reports [33, 61], $A\beta_{1\text{-}42}$ (10 μM) insult caused significant nuclei fragmentation [Fig. 3B (*b*)] indicating progression of apoptosis. However, pre-treatment of the cells with **3** [Fig. 3B (*d*)] or **10** [Fig. 3B (*e*)] significantly attenuated apoptotic nuclei fragmentation. Quantitative data analysis revealed that $A\beta_{1\text{-}42}$ (10 μM) insult significantly increased the number of fragmented nuclei as compared to the control cells (Fig. 3C, $p<0.001$). Pre-treatment with **3** or **10** (20 μM) significantly reduced the number of apoptotic nuclei as compared to the $A\beta_{1\text{-}42}$-treated control cells (Fig. 3C, $p<0.001$) similar to the standard drug memantine (Fig. 3C, $p<0.001$).

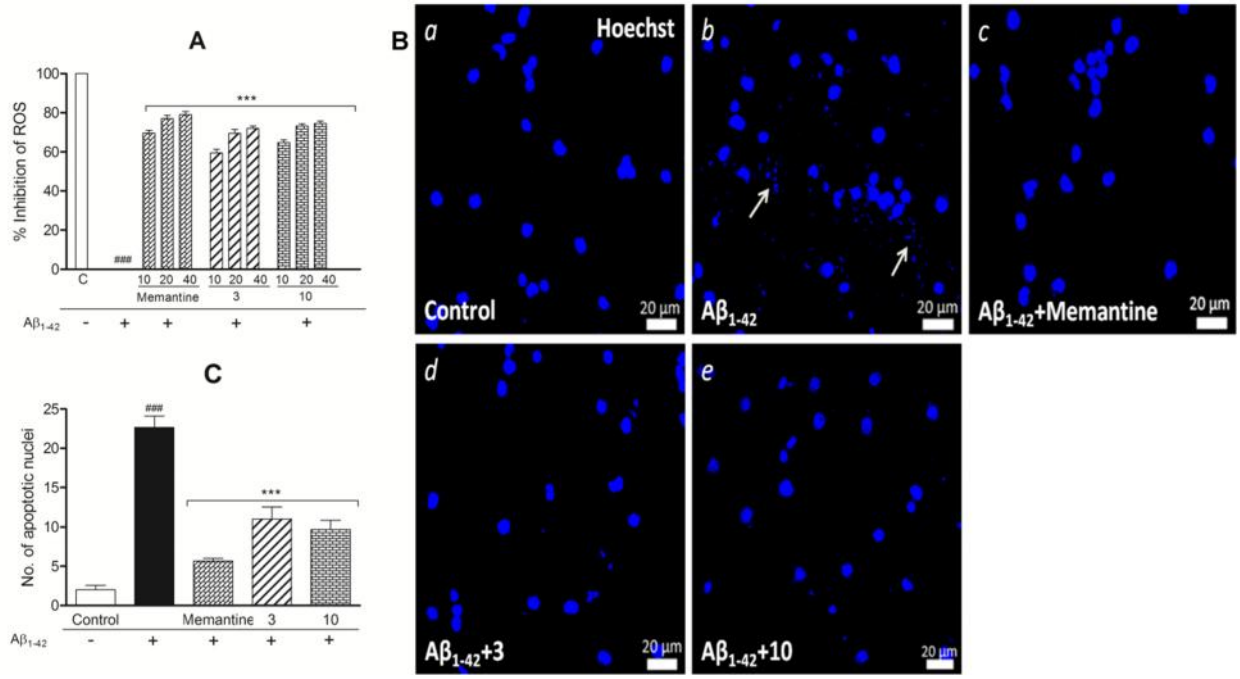

Fig. 3: Compounds (**3** and **10**) demonstrated *in vitro* ROS scavenging and antiapoptotic effects against $A\beta_{1-42}$-induced toxicity in primary rat hippocampal neurons. (A) $A\beta_{1-42}$ (10 µM)-induced elevated ROS level was significantly attenuated by pre-treatment of the cells with **3** and **10** (10-40 µM). (B) Hoechst-stained hippocampal cell nuclei are represented as: (*a*) control, (*b*) $A\beta_{1-42}$, (*c*) $A\beta_{1-42}$+memantine, (*d*) $A\beta_{1-42}$+**3** and (*e*) $A\beta_{1-42}$+**10**-treated cells. $A\beta_{1-42}$ (10 µM)-induced nuclei fragmentation (see arrow) [B (*b*)] was abrogated by **3** [B (*d*)] and **10** [B (*e*)] (20 µM) like memantine [B (*c*)] (20 µM). Scale bar=20µm. (C) Apoptotic nuclei were quantified by a blind observer by counting 30 cells from each culture group that were selected randomly from three independent cultures (n=3). $A\beta_{1-42}$-induced toxicity significantly elevated the number of apoptotic nuclei which were significantly reduced by **3** and **10**. Data are expressed as mean ± SEM. $^{###}p<0.001$ *vs.* control cells. *** $p<0.001$ *vs.* $A\beta_{1-42}$-treated control cells. C=control cells.

4.6. Test compounds (3 and 10) attenuated rate of apoptosis

Antiapoptotic potential of the test compounds (**3** and **10**) was further assessed using flow cytometry. The primary rat hippocampal neuronal cells were stained with Annexin V-FITC and PI. Annexin V enters the cells in the early and late stages of apoptosis while PI staining is observed in the late apoptosis stage or necrosis stage. $A\beta_{1-42}$ (10 µM) insult significantly elevated the percentage of apoptotic cells at a faster rate (Fig. 4, 27.20%) as compared to the control cells (Fig. 4, 1.89%). However, pre-treatment with **3** (Fig. 4, 12.15%) or **10** (Fig. 4, 7.92%) significantly attenuated the percentage of $A\beta_{1-42}$-induced early apoptotic cells.

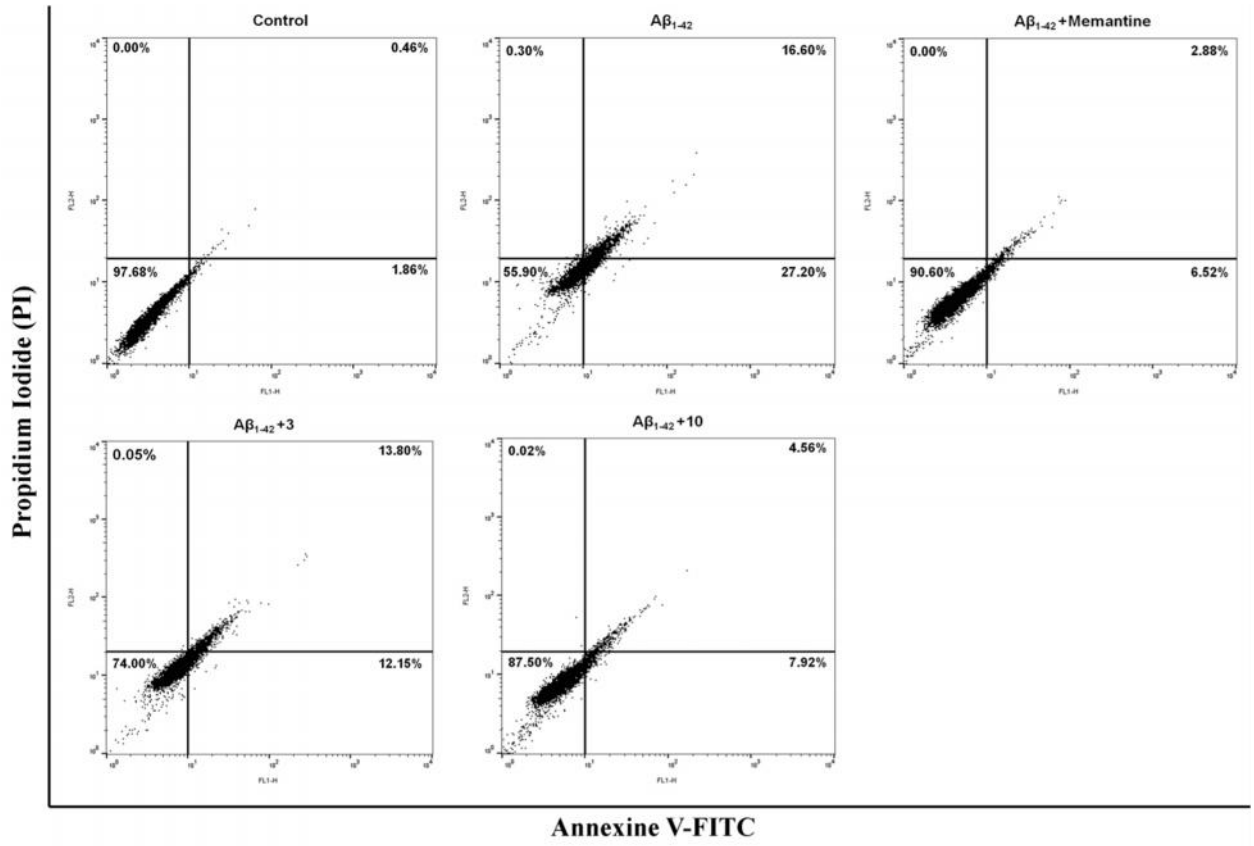

Fig. 4: Test compounds (**3** and **10**) attenuated the rate of apoptosis in primary rat hippocampal neurons which was assessed by flow cytometry using Annexin V-FITC and PI staining. Cells in the lower left quadrant are viable (Annexine V-FITC-/PI-). Cells in the lower right quadrant are early apoptotic (Annexine V-FITC+/PI-) and those in the upper right quadrant are late apoptotic or necrotic (Annexine V-FITC+/PI+). $A\beta_{1-42}$ (10 μM) induced early apoptosis was attenuated by **3** and **10** (20 μM) like memantine (20 μM).

4.7. Test compounds (3 and 10) attenuated caspase-3 activation *in vitro*

Caspase-3 activation is a key event during the progression of apoptosis as evidenced by phosphorylation of caspase-3 protein [63]. In the present study, $A\beta_{1-42}$-induced apoptotic cell death was confirmed by determining the expression of activated/cleaved caspase-3 protein. As shown in Fig. 5A, the expression of cytoplasmic cleaved capase-3 protein was increased in the hippocampal neurons after $A\beta_{1-42}$ (10μM) insult [Fig. 5A (*b*2, *c*2)]. Pre-treatment with **3** [Fig. 5A (*b*4, *c*4)] or **10** [Fig. 5A (*b*5, *c*5)] (20 μM) significantly attenuated the expression of cleaved caspase-3 as compared to the $A\beta_{1-42}$-treated control cells, which supported the earlier results. Cell nuclei were located using dapi counterstaining [Fig. 5A (*a*1-*a*5)]. Quantitative analysis revealed that mean fluorescence intensity of cleaved caspase-3 expression increased significantly in $A\beta_{1-42}$-treated cells (Fig. 5B, $p<0.001$) as compared to the control cells. Pre-treatment of the cells with the test compounds (**3** or **10**) (Fig. 5B, $p<0.001$) significantly reduced the mean

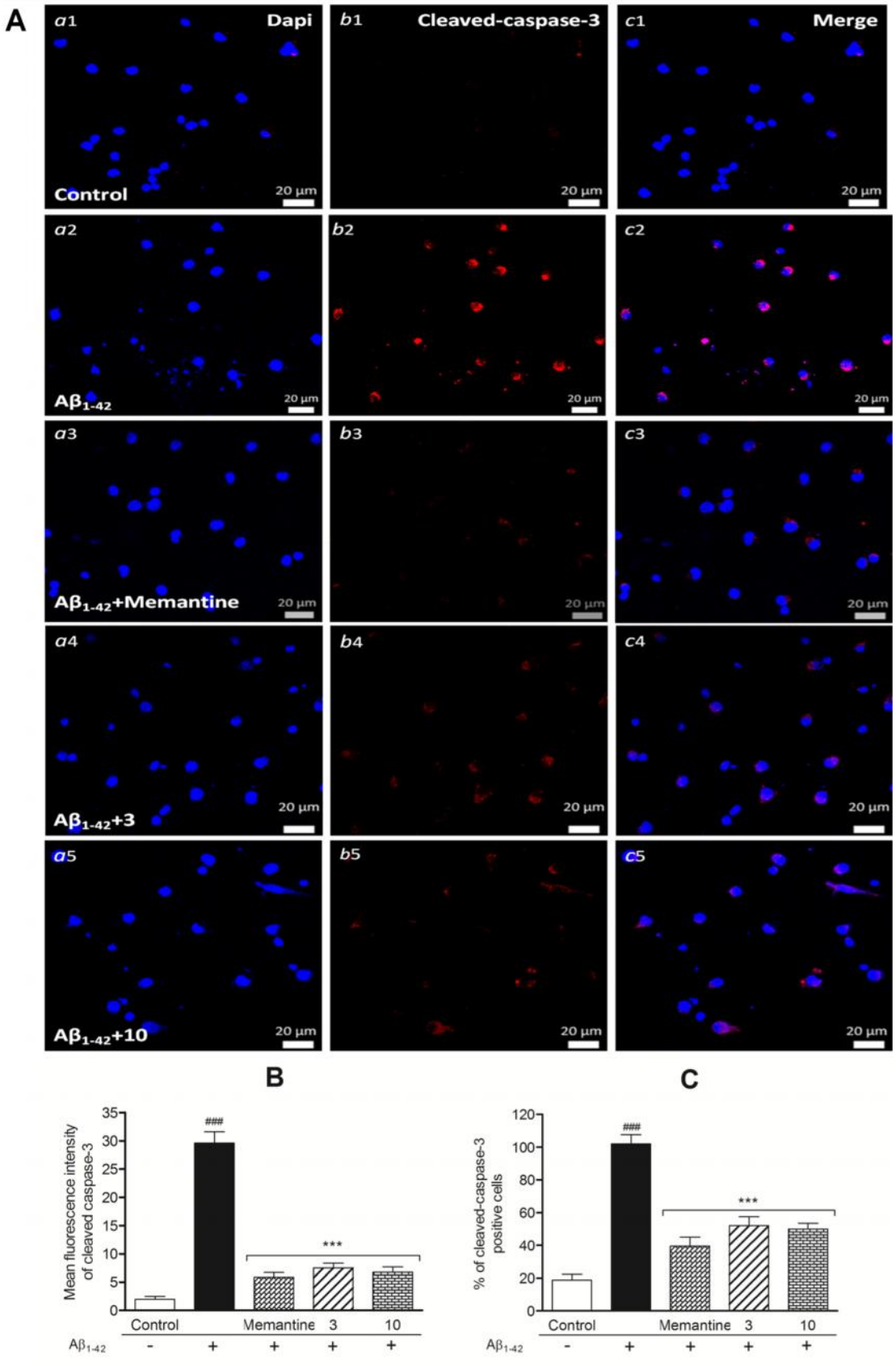
A
a1
Dapi
b1
Cleaved-caspase-3
c1
Merge
Control
Aβ1-42
Aβ1-42+Memantine
Aβ1-42+3
Aβ1-42+10
20 μm
B
Mean fluorescence intensity of cleaved caspase-3
###
***
Control
Memantine
3
10
Aβ1-42
C
% of cleaved-caspase-3 positive cells

Fig. 5: Test compounds (**3** and **10**) attenuated $A\beta_{1-42}$-induced caspase-3 activation *in vitro*. (A) Antiapoptotic potential of **3** and **10** (20 μM) was assessed by estimating the cleaved caspase-3 (active) expression in the primary rat hippocampal neurons after $A\beta_{1-42}$ (10 μM) intoxication. $A\beta_{1-42}$ treatment significantly elevated the cleaved caspase-3 expression in the cytoplasm of hippocampal neuronal cells [A (*b*2, *c*2)] which was abrogated by **3** [A (*b*4, *c*4)] and **10** [A (*b*5, *c*5)]. Cell nuclei were counterstained with dapi [A (*a*1-*a*5)]. Scale bar=20 μm. (B) Mean fluorescence intensity of cleaved caspase-3 protein expression was quantified. $A\beta_{1-42}$-treated cells exhibited increased mean fluorescence intensity of cleaved caspase-3 expression as compared to the control cells which was significantly attenuated by **3** and **10**. (C) Quantification of cleaved caspase-3 positive cells was done by a blind observer by counting 30 cells from each culture group that were selected randomly from three independent cultures (n=3). Enhanced percentage of cleaved caspase-3 positive cells after $A\beta_{1-42}$ toxicity was significantly reduced by pretreatment with **3** and **10,** like the standard drug memantine (20 μM). Data are expressed as mean ± SEM. $^{###}p<0.001$ *vs.* control cells. *** $p<0.001$ *vs.* $A\beta_{1-42}$-treated control cells.

fluorescence intensity of cleaved caspase-3 expression. The cleaved caspase-3 positive cells were quantified by a blind observer. $A\beta_{1-42}$ toxicity significantly increased the number of cleaved caspase-3 positive cells (Fig. 5C, $p<0.001$) which was significantly reduced by **3** and **10** (Fig. 5C, $p<0.001$). Memantine (20 μM) significantly reduced the number of cleaved capase-3 positive cells as compared to the $A\beta_{1-42}$-treated control cells (Fig. 5C, $p<0.001$). All the above findings supported the neuroprotective, free radical scavenging, antioxidant and antiapoptotic potentials of **3** and **10** against $A\beta_{1-42}$-induced excitotoxic damage.

4.8. Test compounds (3 and 10) showed good passive BBB permeability

A successful CNS drug must have the ability to cross BBB to reach its therapeutic target. Thus, BBB permeation has a great importance in the development of efficient CNS therapeutics. To determine the BBB penetration of the test compounds (**3** and **10**), a parallel artificial membrane permeation assay for blood-brain barrier (PAMPA-BBB) was performed. This simple and rapid model described by Di *et al*, [42, 43] has the advantage to predict passive BBB permeation with high accuracy. The *in vitro* permerability (P_e) of **3** and **10** through the lipid extract of porcine brain was determined in PBS/ethanol (70:30). Validation of the assay was done by comparing the experimental permeability values of nine commercial drugs with the reported permeability values [43] (see supplementary information, Table S1) that gave a linear relationship [P_e(Exp.)= 1.171P_e(Ref.) + 1.489 (R^2 = 0.983)] (see supplementary information, Fig. S1). From this equation and considering the limits established by Di. *et al* [42], a molecule with a permeability value (P_e) of >6.2 × 10^{-6} cm/s (see supplementary information, Table S2) was considered capable of crossing the BBB by passive diffusion. Compounds (**3** and **10**) showed P_e

values much above this limit, suggesting that they could cross the BBB by passive diffusion (Table 2).

Table 2: Permeability (P_e) of the test compounds determined by PAMPA-BBB assay.

Compound	P_e (10^{-6} cm/s)[a]	Prediction
3	10.61 ± 0.47	CNS+
10	12.38 ± 0.38	CNS+

[a]Data are expressed as mean ± SEM of three independent experiments. CNS+ indicates good passive CNS permeation.

4.9. Test compounds showed neuroprotective effects in Aβ$_{1-42}$-induced excitotoxicity rat model

4.9.1. Test compounds (3 and 10) enhanced learning and memory

Hippocampal region of brain is considered as the centre of origin for learning and memory. Therefore, degradation of hippocampal neurons through direct toxicity of Aβ may obstruct learning and memory [64, 65]. Spatial learning and memory was assessed using MWM test during the last five days of the treatment period in rats which underwent intrahippocampal injection of Aβ$_{1-42}$. Aβ$_{1-42}$-treated rats showed significantly increased ELT (Fig. 6A, p<0.001) and reduced the number of platform area crossings (Fig. 6B, p<0.001) as compared to the vehicle-treated control animals in all trial sessions indicating alteration in spatial learning and memory. However, treatment with the test compounds (**3** and **10**) (5 mg/kg, p.o.) exhibited significantly reduced ELT (Fig. 6A, p<0.001) and increased the platform area crossings (Fig. 6B, p<0.01) as compared to the Aβ$_{1-42}$-treated control group. Thus, the reduced ELT and increased platform area crossings by animals treated with **3** and **10** revealed their potential to improve spatial learning and memory, impaired by direct Aβ$_{1-42}$ toxicity.

Furthermore, Y maze test was performed to assess the "spontaneous alteration" behaviour in animals which was indicative of immediate working memory. Aβ$_{1-42}$-treated rats showed significantly reduced "spontaneous alterations" throughout the training session as compared to the vehicle-treated control animals (Fig. 6C, p<0.001). A significant rise in "spontaneous alterations" was observed after treatment of the animals with **3** and **10** (5 mg/kg, p.o.) (Fig. 6C,

p<0.05) which was attenuated by Aβ$_{1-42}$ insult. However, the mean number of arm entries was found to remain unchanged in all experimental groups suggesting that general locomotor activity was not hampered by Aβ$_{1-42}$-induced toxicity (Fig. 6D). The results revealed the potential of **3** and **10** to improve hippocampal dependant immediate working memory which was altered by Aβ$_{1-42}$ treatment.

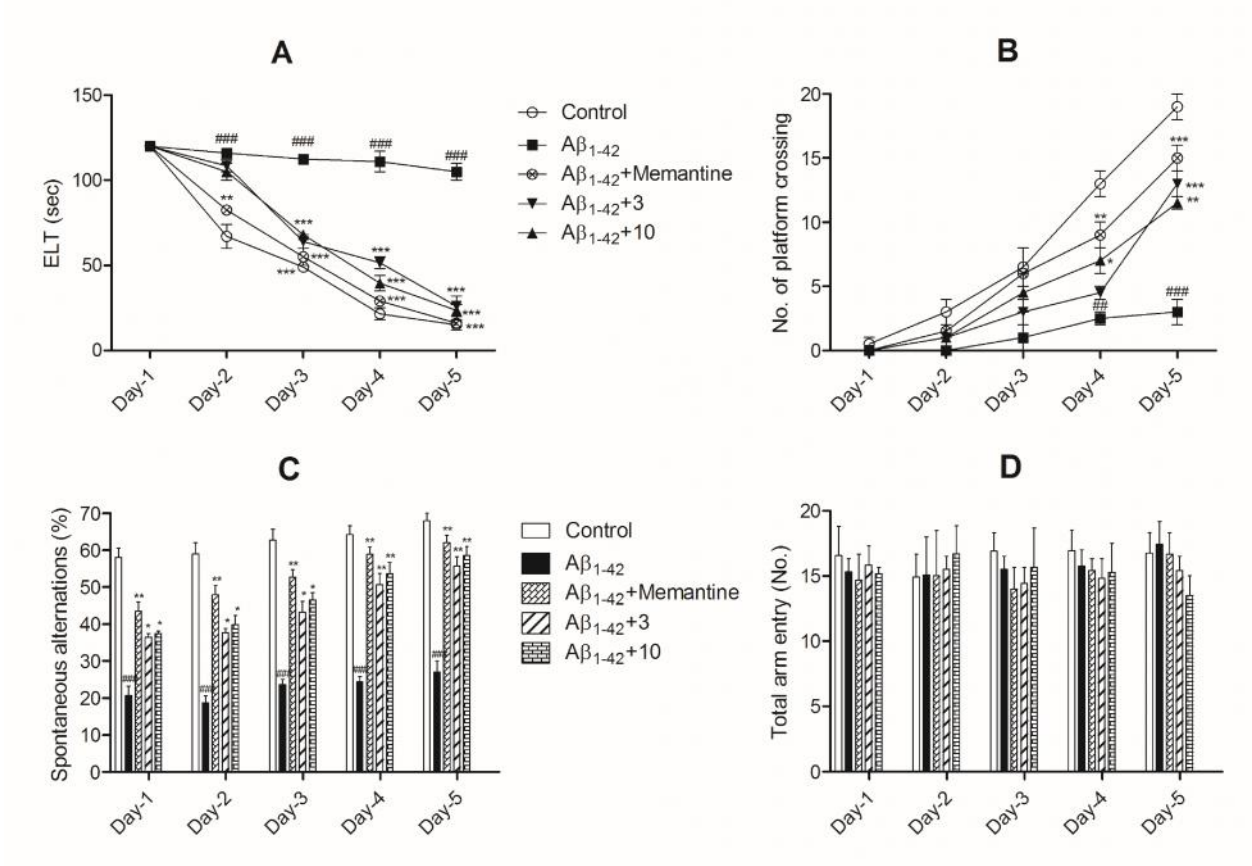

Fig. 6: Test compounds (**3** and **10**) improved learning and memory impaired by ICV injection of Aβ$_{1-42}$ in the hippocampal region of rat brain as assessed by MWM and Y maze tests. In the MWM test, Aβ$_{1-42}$-treated control group exhibited significant rise in the ELT during probe trial sessions (A), and reduced the number of platform area crossings (B) as compared to the vehicle-treated control group. **3** and **10** (5 mg/kg, p.o.) significantly reversed these alterations (A, B) as was the case with memantine (5 mg/kg, p.o.). In the Y maze test, (C) Aβ$_{1-42}$ toxicity significantly abrogated "spontaneous alteration" behaviour which was improved significantly by **3** and **10**. (D) Mean number of the arm entries was observed to be unchanged across all the experimental groups suggesting that the locomotor activity remained unaltered by Aβ$_{1-42}$. Data are expressed as mean ± SEM (n=12). $^{###}$ p<0.001, $^{##}$ p<0.01 *vs.* vehicle-treated control group. *** p<0.001, ** p<0.01, * p<0.05 *vs.* Aβ$_{1-42}$-treated control group.

4.9.2. Test compounds (3 and 10) showed *in vivo* antioxidant activity

Antioxidant activity of the test compounds (**3** and **10**) was evaluated following learning and memory assessment. $A\beta_{1-42}$-treated animals showed significantly increased MDA levels (Fig. 7A, $p<0.001$) and reduced CAT levels (Fig. 7B, $p<0.001$) in the hippocampal region of rat brain as compared to the vehicle-treated control group. However, treatment with compounds (**3** and **10**) significantly abrogated the elevated MDA levels (Fig. 7A, $p<0.001$) and elevated the CAT levels (Fig. 7B, $p<0.001$) as compared to the $A\beta_{1-42}$-treated control group. Thus, the results further support therapeutic potential of **3** and **10** against $A\beta_{1-42}$-induced excitotoxic damage through antioxidant mechanism.

4.9.3. Test compounds (3 and 10) attenuated glutamate and glycine levels

The NMDAR overactivation is a key event in the pathogenesis of excitotoxicity, strongly associated with the elevated levels of excitatory neurotransmitters viz. glutamate and glycine in the brain [44]. Previous reports also demonstrated elevated levels of glutamate and glycine after ICV injection of Aβ in rodent brains which were attenuated by NMDAR antagonists [44, 49]. In the present study, glutamate and glycine levels were estimated in the hippocampal region of rat brain from different experimental groups. Supporting the previous reports [44, 49], glutamate (Fig. 7C, $p<0.01$) and glycine (Fig. 7D, $p<0.001$) levels were significantly increased in the hippocampal region of $A\beta_{1-42}$-treated animal brains as compared to the brains of vehicle-treated control group. However, treatment of the animals with **3** and **10** significantly attenuated the levels of glutamate (Fig. 7C, $p<0.05$) and glycine (Fig. 7D, $p<0.01$) which were elevated by $A\beta_{1-42}$ treatment.

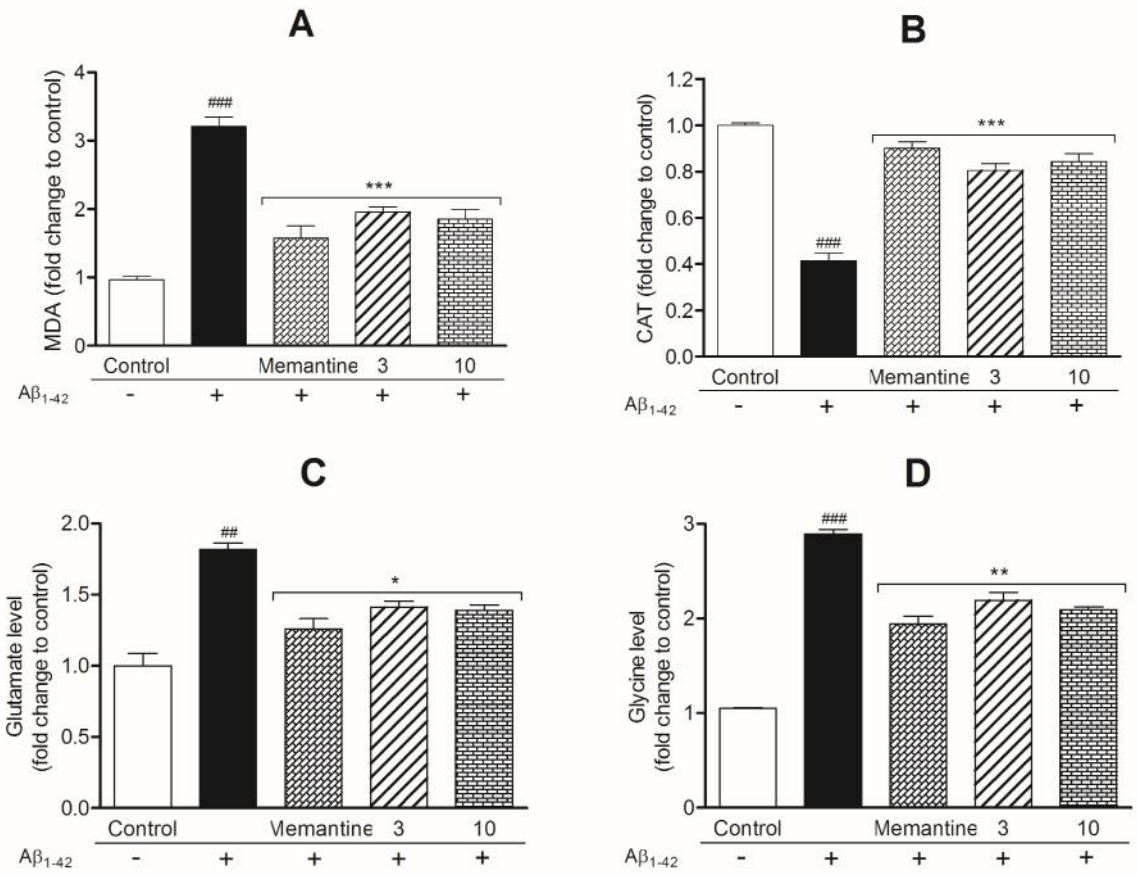

Fig. 7: Test compounds (**3** and **10**) normalized the altered oxidative stress parameters and reduced the elevated levels of excitatory neurotransmitters in the hippocampal region of $A\beta_{1\text{-}42}$-treated rat brains. Oxidative stress was assessed by determining the levels of (A) MDA and (B) CAT. MDA levels were significantly raised while CAT levels were significantly reduced in the $A\beta_{1\text{-}42}$-treated control group as compared to the vehicle-treated control group which were significantly reversed by treatment with **3** and **10** (5 mg/kg, p.o.). Levels of excitatory neurotransmitters viz. (C) glutamate and (D) glycine elevated by $A\beta_{1\text{-}42}$ toxicity were significantly attenuated by treatment with **3** and **10**, similar to memantine (5 mg/kg, p.o.). Data are expressed as mean ± SEM (n=4). $^{###}p<0.001$, $^{##}p<0.01$ *vs.* vehicle-treated control group. *** $p<0.001$, ** $p<0.01$, * $p<0.05$ *vs.* $A\beta_{1\text{-}42}$-treated control group. C=vehicle-treated control group.

4.10. Test compounds (3 and 10) reduced Aβ1-42, *p*-tau, cleaved caspase-3 and cleaved PARP burden in rat brain

Excitotoxicity, mediated through NMDAR overactivation, is one of the major causes for the development of AD which is mainly characterized by the presence of two key pathological biomarkers, i.e. Aβ and *p*-tau [66]. A number of studies have demonstrated that Aβ toxicity is mediated via increased phosphorylation of tau protein which affects multiple signaling cascades including MAPK, PI3K/AKT, NF-*k*B and Wnt pathways [67, 68]. In the present study, levels of

$A\beta_{1-42}$ and *p*-tau were determined in the hippocampal region of $A\beta_{1-42}$-treated rat brains using Western blot analysis. $A\beta_{1-42}$ and *p*-tau levels were significantly increased in the $A\beta_{1-42}$-treated animals (Fig. 8A) as compared to the vehicle-treated control group. Compounds (**3** and **10**) significantly abrogated $A\beta_{1-42}$ and *p*-tau burden in the hippocampal region of $A\beta_{1-42}$-injected rat brains (Fig. 8A). Densitometric analysis showed significant rise in the levels of $A\beta_{1-42}$ (Fig. 8B, $p<0.001$) and *p*-tau (Fig. 8C, $p<0.001$) in the $A\beta_{1-42}$-treated control group which were significantly attenuated by treatment with **3** (Fig. 8B and 8C, $p<0.01$) and **10** (Fig. 8B and 8C, $p<0.001$). Thus, the test compounds (**3** and **10**) have the potential to normalize altered levels of

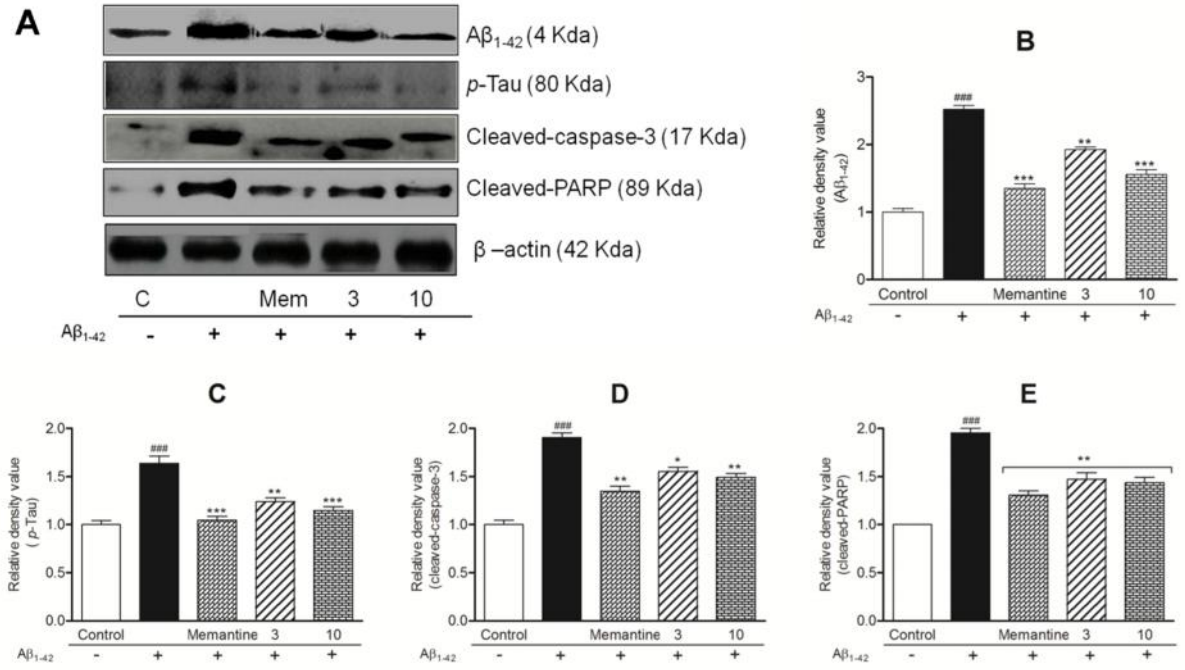

Fig. 8: Test compounds (**3** and **10**) attenuated $A\beta_{1-42}$, *p*-tau, cleaved caspase-3 and cleaved PARP levels in the hippocampal region of $A\beta_{1-42}$-treated rat brains. (A) The expression of $A\beta_{1-42}$, *p*-tau, cleaved caspase-3 and cleaved PARP proteins was determined by Western blot analysis. Densitometry analysis showed increased expression of $A\beta_{1-42}$ (B), *p*-tau (C), cleaved caspase-3 (D) and cleaved PARP (E) in the $A\beta_{1-42}$-treated animals which were significantly abrogated by **3** and **10** similar to memantine (5 mg/kg, p.o.) (B-D). Data are expressed as mean ± SEM (n=4). $^{###}p<0.001$ *vs.* vehicle-treated control group. $^{***}p<0.001$, $^{**}p<0.01$, $^{*}p<0.05$ *vs.* $A\beta_{1-42}$-treated control group. C=vehicle-treated control group. Mem=$A\beta_{1-42}$+memantine-treated group.

$A\beta_{1-42}$ and *p*-tau proteins in the $A\beta_{1-42}$-injected rat brains. Moreover, *in vivo* antiapoptotic potential of **3** and **10** was assessed by determining the levels of cleaved caspase-3 (active) and cleaved PARP proteins in the hippocampal region of $A\beta_{1-42}$-injected rat brains. The levels of cleaved caspase-3 and cleaved PARP were significantly increased in the $A\beta_{1-42}$-treated control

group as compared to the vehicle-treated control group (Fig. 8A) which were significantly reduced after treatment of the animals with **3** and **10** (Fig. 8A). Densitometric analysis showed that **3** (Fig. 8D, $p<0.05$ and 8E, $p<0.01$) and **10** (Fig. 8D and 8E, $p<0.01$) significantly attenuated the cleaved caspase-3 and cleaved PARP levels which were raised by $A\beta_{1-42}$ toxicity. These results further revealed the antiapoptotic potential of the test compounds.

4.11. Test compounds (3 and 10) attenuated activation of tau kinases

Studies have indicated that Aβ-induced tau phosphorylation is mediated through activation of various tau kinases, including mitogen-activated protein kinase (MAPK) and glycogen synthase kinase 3β (GSK-3β) [49, 69-71]. To determine the effects of compounds (**3** and **10**) on tau kinases which are activated during Aβ-induced tau phosphorylation, immunoblot

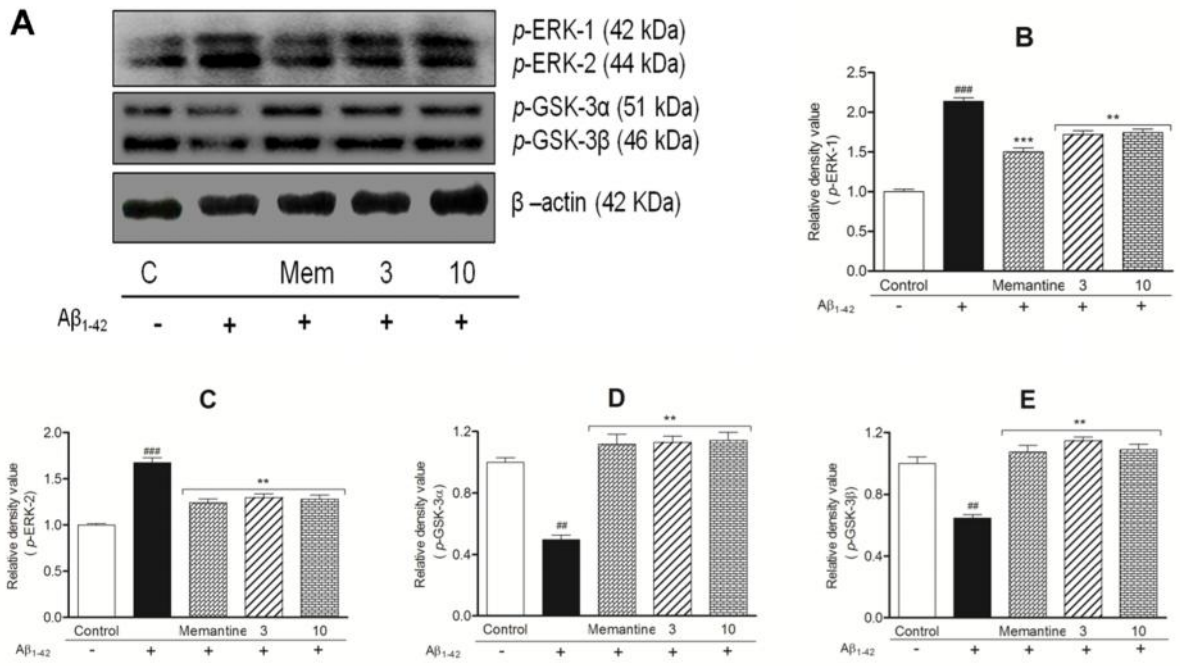

Fig. 9: Test compounds (**3** and **10**) attenuated activation of tau kinases in the hippocampal region of $A\beta_{1-42}$-intoxicated rat brains. (A) Expression of the tau kinases i.e. *p*-ERK-1/2 and *p*-GSK-3β was determined by Western blot analysis. Densitometric analysis revealed that $A\beta_{1-42}$ toxicity significantly elevated *p*-ERK-1/2 (B, C) levels while reduced *p*-GSK-3α/3β (D, E) levels as compared to the vehicle-treated control group. Treatment with **3** and **10** modified the *p*-ERK-1/2 (B, C) and *p*-GSK-3α/3β (D, E) levels in the $A\beta_{1-42}$-treated rat brains like memantine (5 mg/kg, p.o.) (B-E). Data are expressed as mean ± SEM (n=4). $^{###}$ $p<0.001$, $^{##}$ $p<0.01$ *vs.* vehicle-treated control group. *** $p<0.001$, ** $p<0.01$ *vs.* $A\beta_{1-42}$-treated control group. C=vehicle-treated control group. Mem=$A\beta_{1-42}$+memantine-treated group

analysis was performed in the hippocampal region of rat brains which received ICV injection of $A\beta_{1-42}$. A significant induction of the MAPK, i.e. phospho-extracellular receptor kinase-1/2 (*p*-ERK-1/2) was observed in the $A\beta_{1-42}$-treated control group as compared to the vehicle-treated control group (Fig. 9A). However, treatment with **3** and **10** significantly attenuated *p*-ERK-1/2 induction in the $A\beta_{1-42}$ injected rat brains (Fig. 9A). Densitometric analysis showed significant rise in *p*-ERK-1/2 levels following $A\beta_{1-42}$ toxicity (Fig. 9B and 9C, $p<0.001$) which was significantly attenuated by treatment with **3** and **10** (Fig. 9B and 9C, $p<0.01$). Subsequently, the *p*-GSK-3 levels were determined. The levels of *p*-GSK-3α and *p*-GSK-3β were significantly reduced in the hippocampal region of $A\beta_{1-42}$-treated animal brains as compared to the vehicle-treated control group (Fig. 9A). Compounds (**3** and **10**) (5 mg/kg, p.o.) significantly elevated *p*-GSK-3α (Fig. 9A) and *p*-GSK-3β (Fig. 9A) levels which were reduced by $A\beta_{1-42}$ insult. Densitometric analysis showed that $A\beta_{1-42}$ toxicity significantly reduceid the levels of *p*-GSK-3α (Fig. 9D, $p<0.01$) and *p*-GSK-3β (Fig. 9E, $p<0.01$). However, **3** and **10** treatment significantly reversed this attenuation (Fig. 9D and 9E, $p<0.01$).

4.12. Test compound (10) showed relatively higher affinity towards glycine binding site of NMDAR

NMDA at higher concentrations induces excitotoxicity through binding to the glutamate binding site of the NMDAR [52, 72]. Another endogenous agonist, i.e. glycine binds to the glycine binding site of the NMDAR. For complete activation of NMDAR, both glutamate as well as glycine sites must be occupied by the respective agonists. Thus a ligand capable of blocking either of the two binding sites of NMDAR can protect the cells against NMDA-induced excitotoxicity [7, 53, 73, 74]. The most potent test compound (**10**) was evaluated further for its affinity towards glutamate or glycine binding sites of NMDAR. In the molecular modeling study the compound (**10**) showed relatively higher affinity for the glycine binding site as compared to the glutamate binding site of the NMDAR.

Molecular dynamics is a powerful technique to understand mechanism and dynamics of ligand-protein complexes. The Molecular Mechanics Generalized Born (GB) Surface Area (MM-GBSA) and Molecular Mechanics Poisson Boltzmann (PB) Surface Area (MM-PBSA) are the two popular binding affinity analysis techniques. Although the PB is a more popular technique, the GB technique is considered to be more proficient for protein-drug systems. MM-

GBSA technique is widely applied for ligand-receptor binding interactions for many targets. Here, the most active compound (**10**) was considered for the study and MD simulations and MM-GBSA studies were performed to evaluate probable affinity of the compound (**10**) for the NMDAR activation sites i.e. glutamate and glycine binding sites. Both *R* and *S* configurations of the test compound (**10**) were generated and docked into the glutamate (PDB Code: 2A5S) and glycine (PDB Code: 1PB7) binding sites of NMDAR. The generated receptor-ligand complexes were subjected to molecular dynamics simulations using AMBER 10 by a procedure mentioned above and the relative binding affinity was determined using MM-GBSA method described in the AMBER10 package, for *R* and *S* configurations on both the binding sites. The ΔG_{MMGBSA} values for the receptor-ligand complexes are mentioned in Table 3.

Table 3: ΔG_{MMGBSA} values of the NMDAR-**10** (*R* and *S*) complexes in the glutamate and glycine sites.

Name	Complex	Receptor	Ligand	ΔG_{MMGBSA}
Glu_*R*	-3645.89±(110.62)	-3661.73±(110.11)	49.64±(4.43)	-33.80±(3.10)
Glu_*S*	-3699.09±(106.71)	-3713.08±(106.42)	49.11±(4.59)	-35.12±(3.15)
Gly_*R*	-3481.03±(106.56)	-3485.46±(106.06)	50.14±(4.65)	-45.70±(2.82)
Gly_*S*	-3391.33±(111.92)	-3400.96±(111.28)	49.31±(4.63)	-39.67±(2.86)

The resultant data showed that the compound (**10**) has relatively higher affinity for the glycine binding site as compared to the glutamate binding site of the NMDAR. The *R* and *S* enantiomers have nearly the same binding affinity for the glutamate site while the *R*- isomer showed slightly higher binding affinity for the glycine site than the *S*- isomer. The receptor-ligand interactions are shown in Fig. 10.

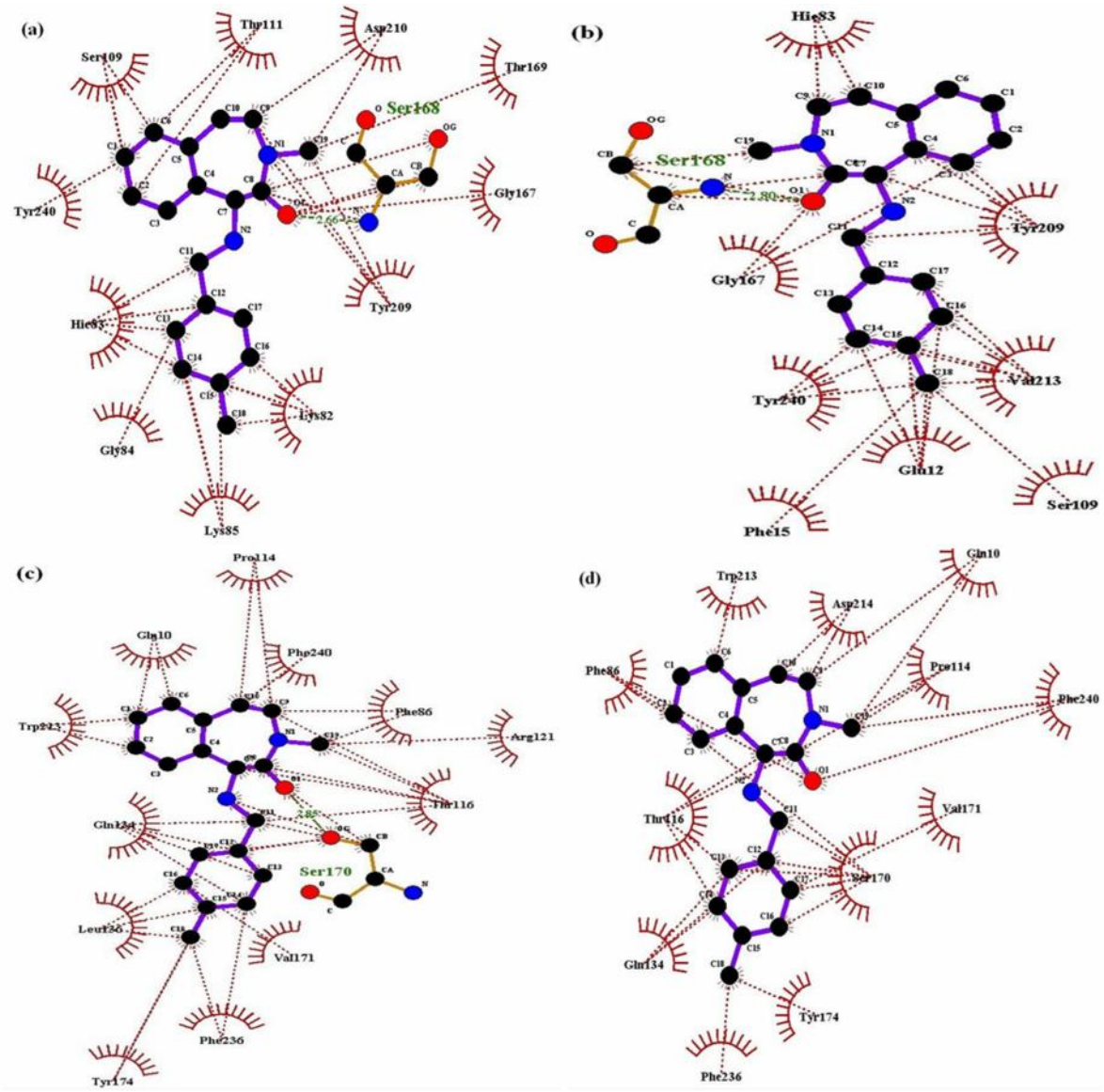

Fig. 10: Interactions of (a) **10*R*** with the glutamate site; (b) **10*S*** with the glutamate site; (c) **10*R*** with the glycine site; (d) **10*S*** with the glycine site of the NMDAR.

4. RESULTS

4.1. Test compounds exhibited good DA receptor modulatory effects *in vitro* assessed by rat superior mesenteric artery

As shown in Table 1, the compounds **(4**, **16** and **19)** were found to be D_1 receptor agonists. Compounds (**4**, **16** and **19**) showed selectivity for D_1 receptor as evidenced by their pD_2 values (7.00 ± 0.23, 7.78 ± 0.41 and 7.53 ± 0.57, respectively). Rest of the compounds were excluded from the current study as they were found to be either antagonist or inactive on dopamine (DA) receptors. Compound (**16**) was evaluated further using different *in vitro* and *in vivo* experiments as it showed the highest agonist potency among the series of compounds.

Table 1: Effects of a series of benzazepine derivatives on isolated rat superior mesenteric artery strip.

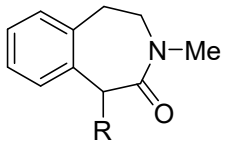

(**1-13**)

Comp.	R	pD_2 value			pA_2 value		
		D_1 receptor	**D_2 receptor**	**D_3 receptor**	**D_1 receptor**	**D_2 receptor**	**D_3 receptor**
1	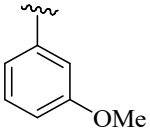	--	--	--	5.17±0.12	5.68±0.16	5.72±0.05
2	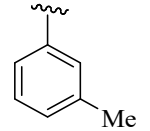	--	--	--	5.57±0.14	5.60±0.11	5.63±0.13
3	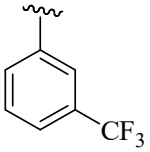	3.72±0.05	3.55±0.13	3.58±0.14	--	--	--

4	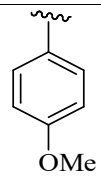	**7.00±0.23**	4.28±0.12	3.92±0.17	--	--	--
5	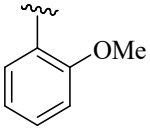	3.98±0.15	4.06±0.16	3.69±0.07	--	--	--
6	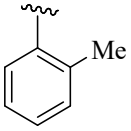	--	--	--	5.72±0.14	5.68±0.12	5.74±0.14
7	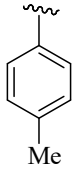	--	--	--	5.73±0.14	5.67±0.07	5.74±0.18
8	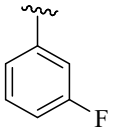	--	--	--	5.64±0.09	5.34±0.10	**7.68±0.15**
9	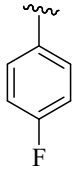	3.71±0.12	3.71±0.11	2.35±0.09	--	--	--
10	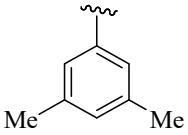	--	--	--	5.48±0.10	5.51±0.14	5.53±0.13
11	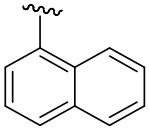	4.68±0.07	4.71±0.08	4.73±0.15	--	--	--
12	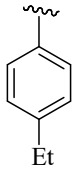	--	--	--	5.74±0.07	5.83±0.10	5.86±0.14

13	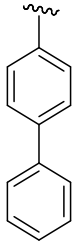	--	--	--	5.71±0.08	5.67±0.16	5.69±0.10

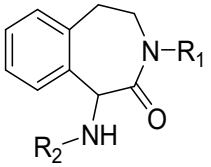

(**14-25**)

Comp.	R_1	R_2	pD_2 value			pA_2 value		
			D_1 receptor	D_2 receptor	D_3 receptor	D_1 receptor	D_2 receptor	D_3 receptor
14		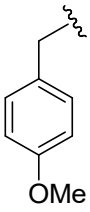	6.25 ± 0.21	4.54 ± 0.25	3.78 ± 0.19	--	--	--
15		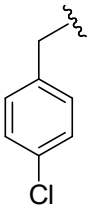	--	--	--	5.41 ± 0.26	5.54 ± 0.19	**8.12 ± 0.34**
16		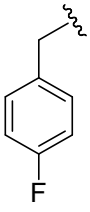	**7.78 ± 0.41**	4.28 ± 0.26	4.25 ± 0.54	--	--	--
17		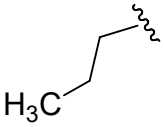	--	--	--	5.15 ± 0.28	5.68 ± 0.12	5.74 ± 0.14
18		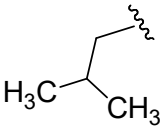	4.32 ± 0.35	4.43 ± 0.24	4.08 ± 0.16	--	--	--

19		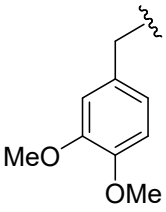	**7.53 ± 0.57**	3.84 ± 0.62	4.21 ± 0.15	--	--	--
20			--	--	--	5.35 ± 0.24	5.27 ± 0.27	5.40 ± 0.23
21		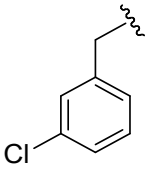	--	--	--	5.38 ± 0.21	5.26 ± 0.17	5.21 ± 0.14
22		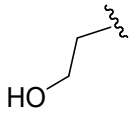	--	--	--	5.02 ± 0.14	5.26 ± 0.14	**7.48 ± 0.37**
23		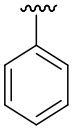	6.03 ± 0.25	4.05 ± 0.27	4.28 ± 0.24	--	--	--
24			--	--	--	4.98 ± 0.24	5.84 ± 0.14	4.57 ± 0.28
25			4.34 ± 0.52	4.52 ± 0.34	3.89 ± 0.13	--	--	--
26	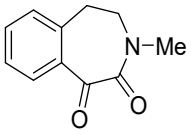		--	--	5.32 ± 0.24	5.12 ± 0.10	5.72 ± 0.05	
27	**A-77363**		**7.42± 0.19**	4.07± 0.20	3.79± 0.14	**--**	**--**	**--**

Data are expressed as mean±SEM.

4.2. Compound (16) offered protection against 6-OHDA-induced injury in human SH-SY5Y neuroblastoma cell culture through D_1 agonism

MTT assay was performed using human SH-SY5Y neuroblastoma cell line to see the cytoprotective effect of compound (**16**). In a set of experiments human SH-SY5Y neuroblastoma cells were incubated with 6-OHDA (100 µM) for 24 h, with or without different concentrations of compound (**16**) and A-77636 (selective D_1 agonist) (5-20 µM). In other set of experiments, cells were incubated with R-SCH-23390 (selective D_1 antagonist) (10 µM) for 2 h followed by treatment with compound (**16**) or A-77636 (5-20 µM) for 3 h before 6-OHDA intoxication. MTT assay was then performed to assess 6-OHDA-induced cytotoxicity, and to assess the neuroprotective role of the test compound (**16**).

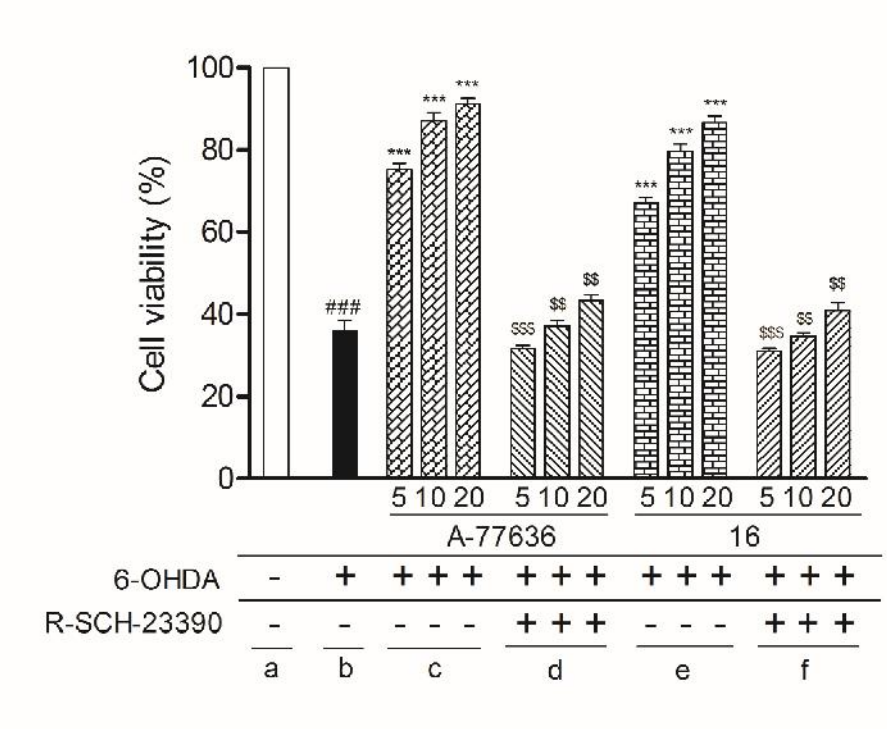

Fig. 1: Effect of compound (**16**) on the injury induced by 6-OHDA in human SH-SY5Y neuroblastoma culture. SH-SY5Y cells were divided into following groups: (a) control, (b) 6-OHDA (100 µM), (c) A-77636 (5-20 µM) + 6-OHDA and (d) R-SCH-23390 (10 µM) + A-77636 (5-20 µM) + 6-OHDA, (e) **16** (5-20 µM) + 6-OHDA, (f) R-SCH-23390 (10 µM) + **16** (5-20 µM) + 6-OHDA. The percentage cell viability was determined by MTT assay after incubation period. Significant values were compared with $^{###}p<0.001$ *vs* control cells; ***$p<0.001$ *vs* 6-OHDA-treated cells; $^{\$\$\$}p<0.001$ *vs* **16**/A-77636 + 6-OHDA-treated cells and $^{\$\$}p<0.01$ *vs* **16**/A-77636 + 6-OHDA-treated cells.

As shown in Figure 1, 6-OHDA significantly decreased the cell viability (p<0.001). On the other hand, the cytotoxic effects of 6-OHDA were reduced significantly by pre-treatment of the cells with the compound (**16**) (5-20 µM) (Fig. 1, p<0.001). Furthermore, the protective effect of compound (**16**) was significantly attenuated by R-SCH-23390 (Fig. 1, p<0.01). This study established that the compound (**16**)**,** which was found to be a potent D_1 agonist in previous (isolated rat superior mesenteric artery preparation) studies, showed protection in 6-OHDA injured human SH-SY5Y neuroblastoma cells through D_1 agonism, dose dependently. The results of MTT assay showed that the compound (**16**) (5-20 µM) significantly protected human SH-SY5Y neuroblastoma cells from 6-OHDA toxicity through D_1 agonism.

4.3. Test compound (16) induced ipsilateral rotations

The rotational (circling) behaviour in rodents with unilateral nigrostriatal damage has been broadly utilized to explore nigrostriatal activity of dopaminergic compounds [35]. Microinjection of the catecholaminergic neurotoxin 6-OHDA, was given unilaterally in rats. The lesioned rats impulsively display minor ipsilateral (towards the lesioned side) rotation. Treatment with a DA receptor agonist provokes active contralateral rotation [36, 37]. In accordance to the above notion, compound (**16**) showed significant contralateral rotations (Fig. 2, p<0.001). This observation revalidated that compound (**16**) is a selective D_1 agonist.

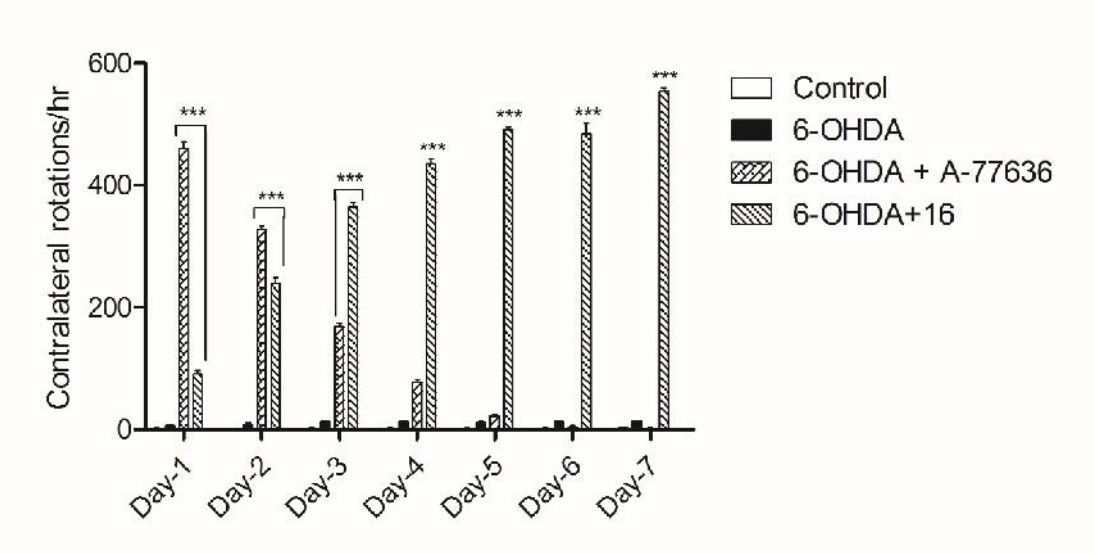

Fig. 2: Cumulative rotations produced by daily dosing with A-77636 and the compound (**16**) over 1 h period for 7 consecutive days of the animals which were microinjected unilaterally with 6-OHDA. Results are expressed as mean ± SEM (n=6). Significant values were compared with ***p<0.001 *vs* 6-OHDA-treated group.

4.4. Test compound (16) exhibited antioxidative effects in 6-OHDA-treated rat brain

A previous report demonstrated that thymoquinone (a bioactive constituent of volatile oil of *Nigella sativa* seed) significantly decreased MDA levels and increased SOD levels in 6-OHDA-induced Parkinson's rat model at a dose of 5 mg/kg [38]. Compound (**16**) in the same dose i.e. 5 mg/kg p.o., significantly improved the oxidative parameters in the 6-OHDA-induced Parkinson's rat model. To evaluate whether compound (**16**) exerts antioxidative effect, brain tissues of rats treated with compound (**16**) were subjected to colorimetric estimation to establish its antioxidative properties in the brain. The results showed that 6-OHDA treatment significantly decreased the brain GSH levels compared to the vehicle-treated control group (Fig. 3A, $p<0.001$). Treatment with the standard drug (A-77636) (Fig. 3A, $p<0.001$) and the test compound (**16**) (Fig. 3A, $p<0.001$) significantly increased brain GSH levels compared to the corresponding 6-OHDA-treated group. Further, 6-OHDA treatment significantly increased the brain MDA level compared to the control group (Fig. 3B, $p<0.001$). Treatment with the standard drug (A-77636) (Fig. 3B, $p<0.001$) and the test compound (**16**) (Fig. 3B, $p<0.001$) significantly decreased brain MDA levels compared to the corresponding 6-OHDA-treated group. Additionally, 6-OHDA treatment significantly decreased the brain SOD level compared to the control group (Fig. 3C, $p<0.001$). Treatment with the standard drug (A-77636) (Fig. 3C, $p<0.001$) and the test compound (**16**) (Fig. 3C, $p<0.001$) significantly increased brain SOD levels compared to the corresponding 6-OHDA-treated group. 6-OHDA treatment also decreased significantly the brain catalase level compared to the control group (Fig. 3D, $p<0.001$). Treatment with the standard drug (A-77636) (Fig. 3D, $p<0.001$) and the test compound (**16**) (Fig. 3D, $p<0.001$) significantly increased brain catalase levels compared to the corresponding 6-OHDA-treated group. These results clearly revealed antioxidant property of compound (**16**).

4.5. Test compound (16) increased DA levels in striatum of 6-OHDA lesioned rats

The unilateral 6-OHDA model has the benefit of giving side-biased motor impairments. The 6-OHDA lesion model can be used in both rats and mice. Unilateral 6-OHDA model is the traditional model for assessing Parkinson's treatments, particularly those proposed to enhance DA levels in the striatum. The main positive point of this model is that it is particularly sensitive to DA receptor agonists. The toxin 6-OHDA is injected unilaterally, while the inverse half serves as an intra-animal control. This injection produces loss of dopaminergic neurons on the 6-

OHDA-injected side while saving the contralateral dopaminergic neurons. In line to the above note, 6-OHDA treatment significantly decreased the striatum DA level compared to the control group (Fig. 3E, $p<0.001$). Treatment with the standard drug (A-77636) (Fig. 3E, $p<0.001$) and the test compound (**16**) (Fig. 3E, $p<0.001$) at 0.1 mg/ kg and 5 mg/kg respectively, significantly increased striatum DA levels compared to the corresponding 6-OHDA-treated group. Previously, Chan *et al.* [39] reported that DBZIM (an imidazolium compound) at 6 mg/kg significantly maintained brain DA levels in 6-OHDA-induced Parkinson's rat model. In the present study, compound (**16**) at 5 mg/kg significantly increased striatum DA levels. These results demonstrated the anti-Parkinsonian effect of compound (**16**).

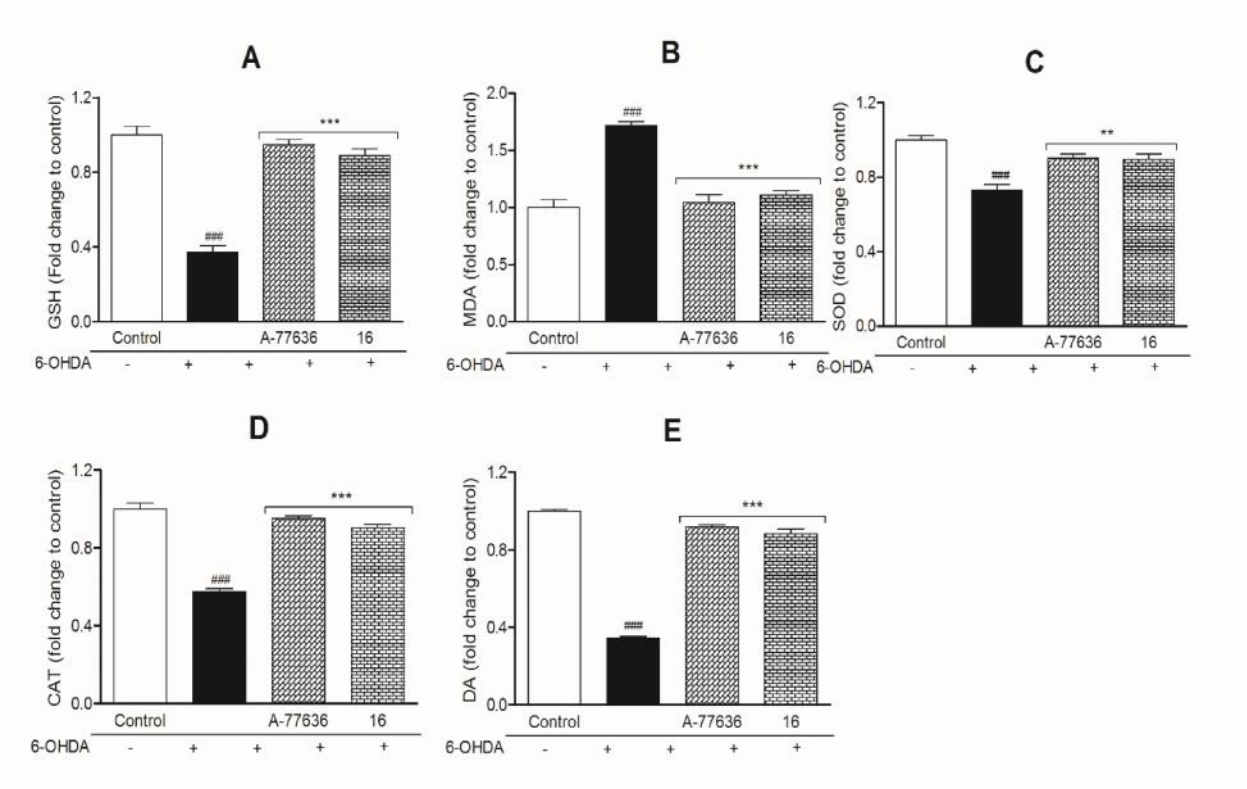

Fig. 3: Effect of compound (**16**) on the oxidative stress parameters and DA levels *ex vivo* in 6-OHDA-induced Parkinson's rat model. As compared to the vehicle-treated control group, GSH, SOD and catalase levels significantly decreased (A, C, D) and MDA level was significantly increased in 6-OHDA-treated group (B). Treatment with compound (**16**) significantly increased GSH, SOD and catalase levels (A, C, D) while decreased MDA levels as compared to 6-OHDA-treated group (B). As compared to the vehicle-treated control group, DA level significantly decreased in 6-OHDA-treated group (E). Treatment with compound (**16**) significantly increased DA level as compared to 6-OHDA-treated group (E). Values are expressed as mean ± SEM. (n=6) Significant values were compared with ***$p<0.001$ *vs* 6-OHDA-treated group & $^{###}p<0.001$ *vs* vehicle-treated control group.

4.6. Test compound (16) diminished cleaved caspase-3 and increased tyrosine hydroxylase (TH) expression in 6-OHDA-induced Parkinson's rat brain

In the current study, the expression of TH and cleaved caspase-3 proteins were determined to confirm the neuroprotective property of the compound (**16**). 6-OHDA treatment significantly increased the expression of cleaved capase-3 protein [Fig. 4A (*a*2)] and decreased TH expression [Fig. 4A (*b*2)] in ipsilateral SNpc region. However, following treatment with the compound (**16**)**,** the expression of cleaved caspase-3 was significantly decreased [Fig. 4A (a4)] while the TH expression was significantly increased [Fig. 4A (b4)] as compared to the 6-OHDA-treated group. Quantitative analysis revealed increased mean fluorescence intensity of cleaved caspase-3 (Fig. 4B, $p<0.001$) and reduced expression of TH (Fig. 4C, $p<0.001$) in the ipsilateral SNpc region of 6-OHDA-induced Parkinson's rat brain as compared to the vehicle-treated control group. Furthermore, treatment with the compound (**16**) significantly reduced the mean fluorescence intensity of cleaved caspase-3 (Fig. 4B, $p<0.001$) and increased the mean fluorescence intensity of TH expression (Fig. 4C, $p<0.001$) as compared to 6-OHDA group in the ipsilateral SNpc region of 6-OHDA-induced Parkinson's rat brain. These results demonstrated neuroprotective and antiapoptotic effects of the compound (**16**) against 6-OHDA-induced neurotoxicity.

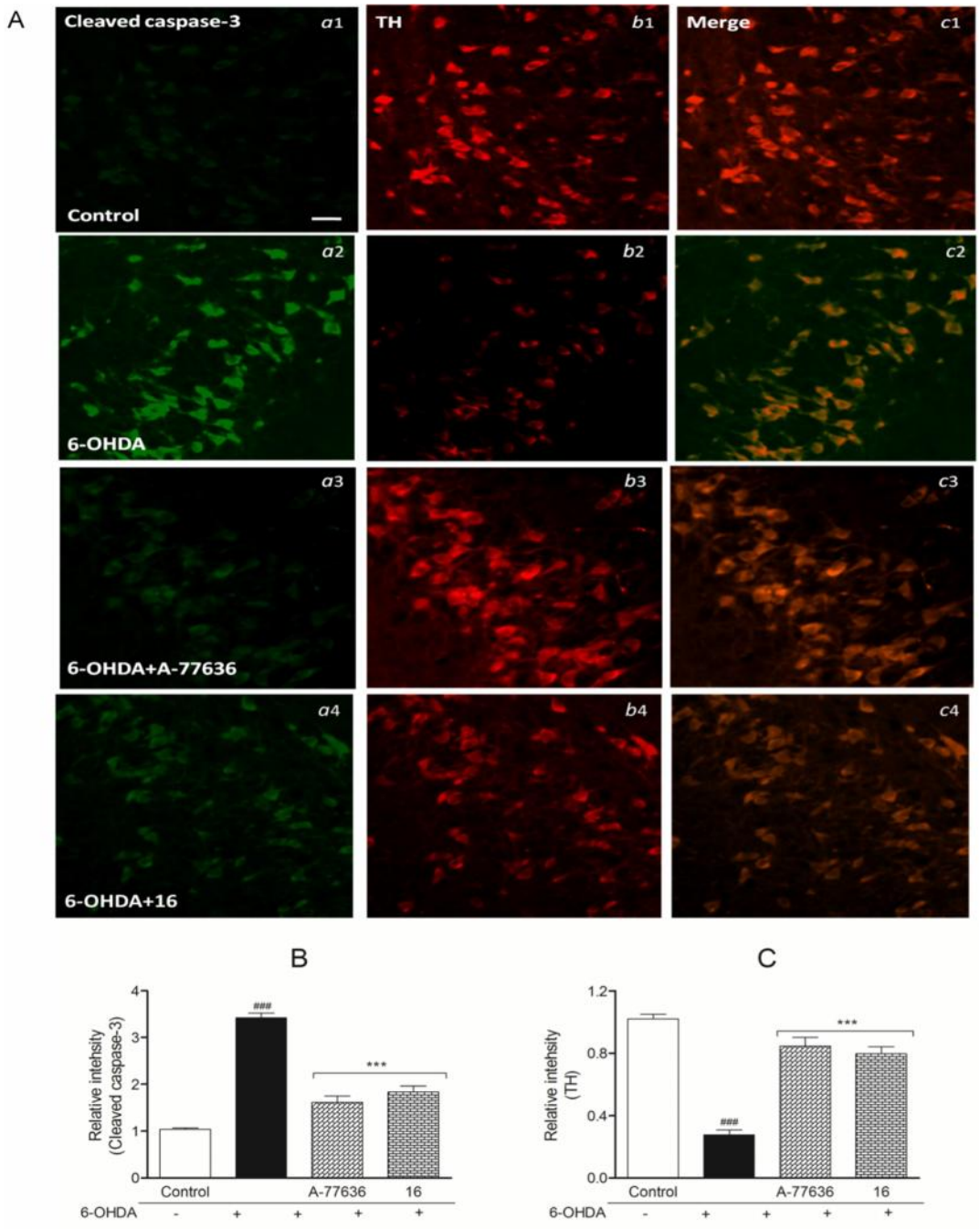

Fig. 4: Effect of compound (**16**) on the expression of cleaved caspase-3 and TH in 6-OHDA-induced Parkinson's rat brain. (A) Confocal microscopic images show the distribution of cleaved caspase-3 and TH in 6-OHDA-induced Parkinson's rat brain. 6-OHDA intoxication increased the expression of cleaved caspase-3 (*a*2) and reduced the level of TH (*b*2) proteins which were significantly reversed by compound (**16**) treatment (*a*2, *b*2). To determine the co-labelling of cleaved caspase-3 and TH proteins, individual images were merged (*c*1-*c*4). Quantitative analysis suggested that with treatment of compound (**16**)**,** there was significant decrease in relative intensity of cleaved caspase-3 (B) and increase in relative intensity of TH (C) proteins in the substantia nigra as compared to the 6-OHDA-treated group. Values are expressed as mean ± SEM (n=6). Significant values were compared with ***p<0.001 *vs* 6-OHDA-treated group and $^{###}p$<0.001 *vs* vehicle-treated control group. Scale bar = 100 µm.

4. RESULTS

4.1. D_3 Antagonist activity of test compounds on rat superior mesenteric artery strip

All the test compounds were evaluated for their DA receptor modulator activity as reported earlier. Amongst which compounds (**8**, **15** and **22**) showed potent D_3 antagonist activity while compound (**4**, **16** and **19**) showed preferential D_1 agonist activity. Compounds **(8, 15** and **22)** had no vasoconstrictor effect on arterial vessels on their own. **8, 15** and **22** significantly attenuated 8-OH-PBZI mediated relaxation with a pA_2 values of 7.68±0.15, 8.12 ± 0.34 and 7.48 ± 0.37 respectively (Table 1, Chapter 4). Compounds (**8**, **15** and **22**) showed the least effect on A-77636 and bromocriptine mediated relaxation which was evidenced by their pA_2 values. These results suggest that compounds (**8**, **15** and **22**) are potent and relatively selective D_3 antagonist which could be effective to treat neuropsychiatric conditions. Among the potent D_3 receptor antagonists, compounds (**8** and **15**) were chosen for further evaluation for antipsychotic activity using different *in vivo* experimental rodent models.

4.2. Compounds (8 and 15) attenuated apomorphine-induced stereotype behaviour

Apomorphine, a non-specific DA receptor agonist, produces stereotype behaviour. As shown in Fig. 1A, pre-treatment of the animals with compounds (**8** and **15**) (5, 10 and 20 mg/kg, p.o.) significantly abrogated apomorphine-induced stereotype behaviour ($p<0.001$). As expected, clozapine (5 and 10 mg/kg, p.o.) also significantly attenuated apomorphine-induced stereotype behaviour (Fig. 1A, $p<0.001$). The results supported DA receptor antagonist activity of compounds (**8** and **15**).

4.3. Compounds (8 and 15) attenuated spontaneous locomotor activity

Animals treated with compounds (**8** and **15**) (5, 10 and 20 mg/kg, p.o.) showed significantly reduced spontaneous locomotor activity as compared to the vehicle-treated control group (Fig. 1B, $p<0.001$). Clozapine (5 and 10 mg/kg, p.o.) as a standard drug also significantly attenuated spontaneous locomotor activity (Fig. 1B, $p<0.001$) as compared to the vehicle-treated control group. These results point out the antipsychotic potential of compounds (**8** and **15**).

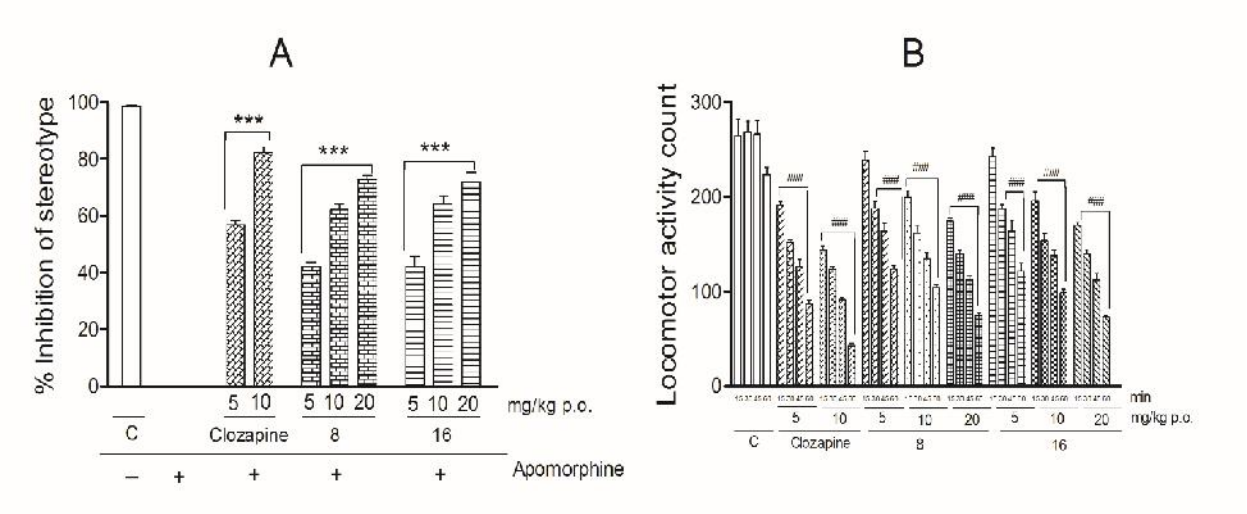

Fig. 1: Compounds (**8** and **15**) attenuated apomorphine-induced stereotype behaviour (A) and spontaneous locomotor activity (B). ### p<0.001, when compared to the vehicle-treated control group. *** p<0.001, when compared to the apomorphine-treated control group (n=6).

4.4. Compounds (8 and 15) attenuated 7-OH-DPAT-induced hypothermia

8-OH-DPAT, a selective D_3 agonist, elicited significant hypothermia (Fig. 2A, p<0.001) as compared to the vehicle-treated control group. Pre-treatment of the animals with compounds (**8** and **15**) significantly attenuated 8-OH-DPAT-induced hypothermia in a dose dependant manner (Fig. 2A, p<0.01). **8** and **15** did not produce hypothermia on its own. In contrast to this, clozapine (5 and 10mg/kg) by itself elicited significant hypothermia (Fig. 2A, p<0.01). Hence, treatment of clozapine potentiated 6-OH-DPAT-induced hypothermia (Fig. 2A, p<0.001). The results further supported selective D_3 antagonist activity of **8** and **15**.

4.5. Compounds (8 and 15) did not induce catalepsy at low doses

In neuropsychiatric conditions, the major drawback of targeting D_2 receptor is the development of motor alteration because of extrapyramidal side effects [6, 26]. As shown in Fig. 2B, compounds (**8** and **15**)-treated animals did not show any catalepsy response at moderate doses (5 and 10 mg/kg, p.o.) while at a relatively higher dose (20 mg/kg, p.o.), **8** and **15** induced significant level of catalepsy (Fig. 2B, p<0.001) as compared to the vehicle-treated control animals. Clozapine (5 and 10 mg/kg, p.o.), as expected, induced significant catalepsy (Fig. 2B, p<0.001), as compared to the vehicle-treated control group even at moderate doses (5 and 10 mg/kg, p.o.) which lasted up to 120 min.

4.6. Compounds (8 and 15) did not induce rota rod ataxia

Rota rod ataxia is another useful tool to evaluate motor alteration in test animals. Compounds (**8** and **15**), at moderate doses (5 and 10 mg/kg, p.o.), did not induce ataxia in rota rod test after 1 hr of post treatment period (Fig. 2C). However, at a relatively higher dose, **8** and **15** (20 mg/kg, p.o.) induced significant ataxia impairing rota rod performance as compared to the vehicle-treated control group (Fig. 2C, $p<0.001$). In contrast to this, clozapine induced significant alteration of rota rod performance in the animals even at lower doses (5 and 10 mg/kg) as compared to the vehicle-treated control animals (Fig. 2C, $p<0.001$). The results suggest that **8** and **15** have relatively lesser propensity to induce extrapyramidal side effects as compared to clozapine.

4.7. Compounds (8 and 15) attenuated apomorphine-induced striatal DA level

Administration of apomorphine significantly elevated the striatal DA level in rat brains as compared to the vehicle-treated control group (Fig. 2D, $p<0.001$). Compounds (**8** and **15**) showed promising antipsychotic effects in different behavioural rodent models. In support of this finding, **8** and **15** significantly attenuated apomorphine-induced striatal DA levels in a dose dependant manner (Fig. 2D, $p<0.01$). The results further confirmed DA receptor antagonist potential of **8** and **15**.

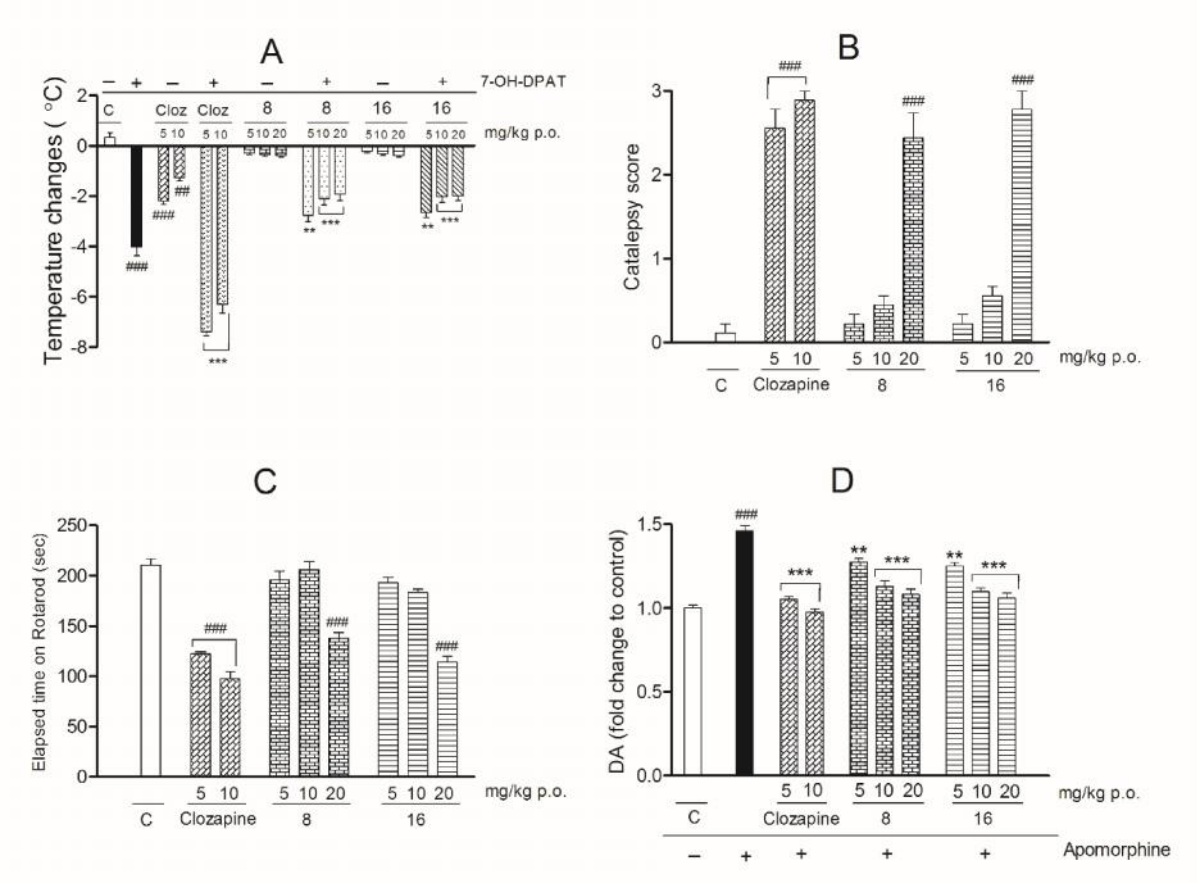

Fig. 2: Compounds (**8** and **15**) attenuated 7-OH-DPAT-induced hypothermia. In contrast to this, Clozapine potentiated 7-OH-DPAT-induced hypothermia (A). **8** and **15** did not induce catalepsy (B) or rota rod ataxia (C) at moderate doses. In difference, clozapine induced significant catalepsy (B) and rota rod ataxia (C) at the same dose levels. **8** and **15** attenuated apomorphine-induced striatal dopamine (DA) levels in rat brain (D). ## p<0.01, ### p<0.001, when compared to the vehicle-treated control group. ** p<0.01, *** p<0.001, when compared to the 7-OH-DPAT/apomorphine-treated control group (n=6).

4.8. Compounds (8 and 15) were found safe in acute lethality test

Treatment of compounds (**8** and **15**) up to 300 mg/kg, p.o. did not cause any mortality in the animals up to 14 days (LD_{50}≥300 mg/kg, p.o.). In contrast, all the mice treated with clozapine (100 mg/kg, p.o.) died within 48 hr of drug treatment. Thus, LD_{50} value of clozapine was found to be less than 100 mg/kg, p.o. while **8** and **15** were found to be safe up to 300 mg/kg, p.o. dose.